BIOMASS STRUCTURE AND ITS CONTRIBUTIONS TO RECALCITRANCE DURING CONSOLIDATED BIOPROCESSING WITH *CLOSTRIDIUM THERMOCELLUM*

A Dissertation
Presented to
The Academic Faculty

by

Hannah O. Akinosho

In Partial Fulfillment
of the Requirements for the Degree
Doctor of Philosophy in the
School of Chemistry and Biochemistry

Georgia Institute of Technology
August 2017

BIOMASS STRUCTURE AND ITS CONTRIBUTIONS TO RECALCITRANCE DURING CONSOLIDATED BIOPROCESSING WITH *CLOSTRIDIUM THERMOCELLUM*

Approved by:

Dr. Arthur Ragauskas, Advisor
School of Chemistry & Biochemistry
Georgia Institute of Technology

Dr. Pamela Peralta-Yahya
School of Chemistry & Biochemistry
Georgia Institute of Technology

Dr. Christopher Jones
School of Chemical and Biomolecular Engineering
Georgia Institute of Technology

Dr. Bridgette Barry
School of Chemistry & Biochemistry
Georgia Institute of Technology

Dr. Ronghu Wu
School of Chemistry & Biochemistry
Georgia Institute of Technology

Date Approved: [Month dd, yyyy]

ACKNOWLEDGEMENTS

I am very grateful to have encountered so many supportive individuals during my graduate school experience. Firstly, I would like to thank God for his oversight and direction throughout my studies at Georgia Tech; it is a truly blessing to graduate after all these years of school. I would like to acknowledge Dr. Arthur Ragauskas for giving me the opportunity to study biomass and bioethanol and guiding me in research at the PhD level. I am especially grateful that I was able to study under the supervision of such a knowledgeable individual. I also would like to acknowledge all of the post-docs (Dr. Garima Bali, Dr. Fang Huang, Dr. Doh-Yeon Park, Dr. Tyrone Wells, Dr. Qining Sun, Dr. Xianzhi Meng, Dr. Chang Geun Yoo, and Dr. Mi Li), graduate students (Allison Tolbert and Mark Cannatelli), and the visiting scholars that helped to address my wide range of needs and inquiries during all stages of my research. I am also appreciative of our research scientist (Dr. Yunqiao Pu) for his support and assistance throughout the past five years.

I would also like to recognize all of my family members (Tosin, Caleb, Abigail, Emerie, Samuel, and Tai) who have encouraged me and assisted me with my needs while in college.

Lastly, I would like to appreciate the financial support received from the Bioenergy Science Center (BESC) for the support of this research. BESC was established by U.S. Department of Energy in 2007 and is a multi-institutional and multidisciplinary research network that seeks to remove biomass recalcitrance as a barrier to ethanol production. I would also like to thank the Renewable BioProducts Institute for the Paper Science and Engineering fellowship.

TABLE OF CONTENTS

LIST OF TABLES

ed with S lignin (45). Similar to acetylation, lignin is believed to contain p-hydroxy benozate prior to radical polymerization (45, 46). Studies have suggest that increased p-hydroxy

benzoate concentrations improve enzymatic hydrolysis efficiencies with fungal cellulases (47, 48).

Radical polymerization of the coniferyl alcohol, sinapyl alcohol, and *p*-coumary

l alcohol monolignols generates ether and/or carbon-carbon bonds, which form guaiacyl (G), syringyl (S), and *p*-hydroxyphenyl (H) lignin. Additionally, the bond types generated during

the radical polymerizations vary widely (Table 5), but the β-O-4 linkage is most common. Figure 3 illustrates and further defines the several types of interunit linkages present in

lignin.

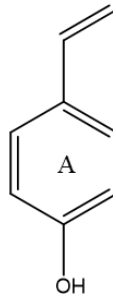

Figure 2 The three primary monolignol units of lignin (A) p-coumaryl alcohol (B) coniferyl alcohol and (C) sinapyl alcohol units

Table 5 – Select lignin interunit linkages and their relative abundances in various biomasses as

determined by HSQC 2D NMR

	β-C-4	β-β	β-5	β-1
Arabidopsis thaliana (49)	78.7	4.1	15.4	1.0
Forage sor	50	5	37	8

ghum (*Sorghum*, sp.) (50)				
Populus tremula × *alba*	86.7	7.9	2.0	2.1

(51)				
Bamboo (*Bambooo rigida*, sp.) (52)	49.01	7.07	2.17	NR
Miscanthu	42.1	3.8	9.9	NR

Secale cereale (53)				
Wheat straw (53)	45.3	5.6	8.3	NR
Poplar (53)	43.1	6.0	1.6	NR

NR: not reported in the original publication

Lignin's structure is highly heterogeneous, and its variability stems from a slew of factors including plant species and age. Lignin composition

varies between lignocellulose type (Table 6). For example, hardwoods contain both S and G lignin, whereas softwoods contain mostly G lignin and small amounts of H lignin.

G, S, and H lignin are all represented in herbaceous biomass.

Radical polymerization generates varied lignin molecular weights, which is partly attributed to its structural properti

es. For example, H-lignin participates in β-β and β-5 linkages that limit lignin polymerization, thereby reducing polymer length (54). The proportion of sinapyl alcohol that is incorpor

ated into lignin compared to coniferyl alcohol also appear to influence lignin molecular weight. More specifically, lower S/G ratio are associated with decreased molecular

weights (55).

Table 7 reports the molecular weights of lignin from diverse biomasses.

Table 6 – Lignin S, G, and H contents (%) of several biomasses determined by NMR

	S (%)	G (%)	H (%)
Wheat straw (56)	37	60	3
Olive tree pruning (56)	83	16	1
Miscanthus × *giganteus* (57)	52	44	4

Populus tremula × *Populus alba* (58)	69.2	30.8	NR
Typha capensis (57)	46	27	27
Sugarcane bagasse (59)	32.3	22.8	3.2

NR: not reported in the original publication

The phenolic groups present in lignin are important sites for the previously described

chemica
l
interacti
ons with
hemicell
ulose
and
cellulose
.
Addition
ally,
phenolic
groups
have
been
recogniz
ed as a
common
starting
point for
lignin
depolym
erization

or degradation with enzymes (60) or chemicals (61).

Table 7 – The molecular weights of MWL and CEL from hardwood, softwood, and herbaceous biomasses as determined by GPC

	Lignin: iso	Mn (g/mol)	Mw (g/mol)	PDI

	lation			
Beech (*Fagus sylvatica*) (62)	MVL	3690	5510	1.49
Sugarcane b	CEL	1673	3176	1.9

agasse (59)				
Populus albaglandulosa (63)	MVL	4176	13250	3.17
Populus	CEL	2959	9938	3.3

trichocarpa (64)				
Switchgrass (55)	CEL	3031	8856	NR
Alfalfa (*Med*	CEL	NR	6000	NR

icago satiiva) (65)				
Lobllolly pine (*Pinus taeda*)	NVL	9899	7790	7.9

(66)				

NR: not reported in the original publication

MWL, milled wood lignin; CEL, cellulolytic enzymatic lignin

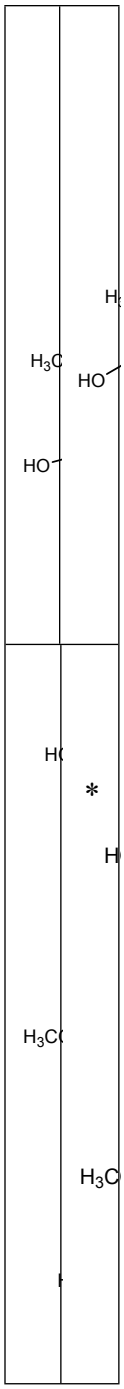

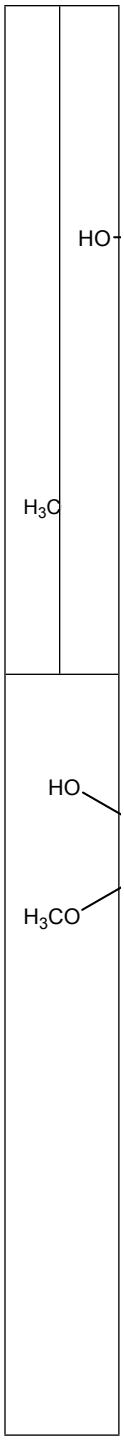

Figure 3 Select interunit linkages in lignin from left to right

LIST OF FIGURES

LIST OF SYMBOLS AND ABBREVIATIONS

BET	Brunauer Emmett Teller
CBP	Consolidated bioprocessing
CEL	Cellulolytic enzyme lignin
CELF	Co-solvent enhanced lignocellulosic fractionation
C. thermocellum	*Clostridium thermocellum*
DB 1	Direct blue 1
DO 15	Direct orange 15
GPC	Gel permeation chromatography
IBP	Integrated bioprocessing
KOH	Potassium hydroxide
LCC	Lignin carbohydrate complexes
Mn	Number average molecular weight
Mw	Weight average molecular weight
MWL	Milled wood lignin
NaOAc	Sodium acetate
NaOH	Sodium hydroxide
NMR	Nuclear magnetic resonance spectroscopy
NR	Not reported
P. trichocarpa	*Populus trichocarpa*
PDI	Polydispersity index
PTFE	Polytetrafluoroethylene
PVDF	polyvinyldifluoride

Ra	Average roughness
RFS	Renewable Fuel Standard
Rp	Mean peak roughness
Rv	Mean valley roughness
S/G	Syringyl to guiacyl lignin ratio
SHF	Separate hydrolysis and fermentation
SSCF	Simulatenous saccharication and co-fermentation
SSF	Simultaneous saccharification and fermentation
THF	Tetrahydrofuran
UV-Vis	Ultraviolet visible spectroscopy
WRV	Water retention value

SUMMARY

Although gasoline supplies a sizeable portion of the transportation industry's energy demand, renewable alternatives offer competitive environmental, economical, and innovative benefits. Biomass is a long-standing, renewable energy source that can potentially off-set the demand placed on corn ethanol. Cellulose and corn generate ethanol using similar production schemes; however, ethanol production from corn is much less labor intensive. As a result, cellulosic ethanol production requires a more rigorous four stage process that employs chemicals, enzymes, and microorganisms to convert cellulose into ethanol. Biomass structure limits the ease of cellulose conversion into ethanol. Numerous approaches have been explored to resolve this limitation, and their efficiencies are typically quantified by monitoring improvements in cellulose saccharification (1) with fungal enzymes. While these measurements hold great value, structural characterizations attempt to clarify structural reason(s) for the improved hydrolysis. The information gathered from characterization experiments will help to direct the selection of the most favorable features in biomass for ethanol production.

The three major polymers in biomass are cellulose, hemicellulose, and lignin, and each possesses structural properties that have been linked to recalcitrance through individual or combinatory effects (2, 3). Accordingly, various instruments and wet chemistry methods are available to measure these properties (4, 5). Recalcitrance is currently better understood in fungal cellulases than in an alternative, integrated scheme known as consolidated bioprocessing (CBP). Nonetheless, plant cell wall features that influence ethanol production during CBP can also be assessed with the same

methodology and instrumentation. Lignin, in particular, has been consistently identified as challenge to cellulose hydrolysis (6) and may pose similar issues in *C. thermocellum*. This work clarifies biomass features such as lignin content and structure that negatively influence the CBP microorganism *Clostridium thermocellum*.

To understand the structural properties that are altered by *C. thermocellum*, the initial investigation compared six *Populus trichocarpa* before and after CBP. Ethanol yields were recorded paired with characterization data to determine trends in CBP efficiencies. Several properties of cellulose, hemicellulose, and lignin in non-treated and CBP-treated *P. trichocarpa* were assessed. Gel permeation chromatography (GPC) was used for the molecular weight analysis of cellulose and hemicellulose, while nuclear magnetic resonance spectroscopy (NMR) detailed lignin structure in top, middle, and poor-performing *P. trichocarpa*. Lastly, total lignin contents were measured with pyrolysis molecular beam mass spectrometry in all natural variants to assess its contributions to recalcitrance. Overall, lignin structure and contents appeared to be related to ethanol yields.

Considering lignin's role in the initial findings, the second study attempted to detail the impact of lignin S/G ratio on ethanol yields. Two *P. trichocarpa* with S/G ratio extremes were selected to undergo CBP with *C. thermocellum* and yielded drastically different hydrolysis activities. Therefore, a series of experiments were conducted to account for the higher solids solubilization in the high S/G ratio *P. trichocarpa*. Potential inhibitors were identified with GC-MS and screened to measure their concentration differences between the two *P. trichocarpa*. Lignin S/G ratio was confirmed with NMR spectroscopy, and its molecular weight alongside cellulose molecular weights were also

obtained with GPC. Simon's staining, which requires UV-Visible spectroscopy, was also conducted to determine accessibility differences between samples. Lignin molecular weights and accessibilities pointed towards structural differences in lignin that were the most likely contributors to solubilization differences.

The third study examined the appropriateness of the Simons' stain in determining accessibility's role during CBP, as *C. thermocellum* is believed to carry out hydrolysis at the biomass surface. Simons' staining partially relies on biomass porosity to measure accessibility and may not be entirely transferable to CBP. Eight *P. trichocarpa* (four high density and four low density) and were subjected to separate hydrolysis and fermentation (SHF) and CBP. Klason lignin contents were assessed with wet chemistry, while cellulose molecular weights were measured with GPC. Surface roughness measurements were carried out to relate biomass porosity to the biomass surface. Simons' staining was applied to the control biomass and was paired with the ethanol yields from SHF and CBP data to correlate accessibility to CBP. Klason lignin contents and biomass accessibility appeared to be related to the extent of CBP.

The former three studies confirmed that recalcitrance persists during CBP, and lignin remains a barrier to ethanol production. To clarify, poorer performing biomass generally contained high lignin contents and/or feateures of lignin that had been previously associated with recalcitrance with fungal cellulases. In the final part of this work, an advanced NMR technique and ATR-FTIR were used to examine the structure of lignin before and after CBP to determine if lignin is altered during CBP. The analyses revealed that lignin structure experiences small, but discernable, changes following CBP, which suggest that *C. thermocellum* catalyzes changes to lignin.

Each study provided compelling reasoning to strongly consider lignin's part in limiting CBP efficiencies at the laboratory and eventually the industrial scale. To make cellulosic ethanol production feasible with CBP, lignin structure and content must be manipulated with genetic modifications or carefully selected in natural variants to combat these difficulties.

CHAPTER 1. INTRODUCTION

1.1 The Case for Cellulosic Ethanol

The development of the gasoline-powered internal combustion engine represented a major advancement in individual and industrial mobility. In 1875, the Congressional Horseless Carriage Committee, though weary of the adoption of gasoline, acknowledged the great potential of this fuel: "It [gasoline] may someday prove to be more revolutionary in the development of human society than the invention of the wheel, the use of metals, or the steam engine (7)." The impact of this resource was quickly realized upon the commercialization of the Model T in 1908 and the accompanying expansion of gasoline consumption (8). This demand has continued to surge over the past century to meet the world's ever-growing transportation energy needs. Even more recently, the number of gasoline barrels consumed is projected to steadily climb from 8.9 million per day in 2016 to 9.5 million per day in 2018 (9).

Gasoline is derived from petroleum, a naturally occurring mixture of gaseous, liquid, plastic, and solid hydrocarbons amongst other lesser constituents. Petroleum has remained a longstanding energy source for several reasons, as outlined in the National Petroleum Council's (NPC) report *Advancing Technologies for America's Transportation Future* (10). For example, petroleum is a relatively reliable energy source that seldom experiences shortages. Petroleum delivers high energy compared to many other fuel sources and is easily transported. Furthermore, petroleum contains a diverse group of hydrocarbon structures, thereby making it tunable and amenable to a variety of engines.

While gasoline can fuel an internal combustion engine alone, ethanol is often added, typically in percentages less than 15%, to attain a variety of benefits. Ethanol blending conserves gasoline, a nonrenewable resource, and improves octane content. Ethanol produced within the US also reduces the need for imported crude oil and encourages energy security. The 2014 Ethanol Industry Outlook documented the drastic reduction in oil imports from 60% in 2005 to 45% in 2011, which was partly attributed to expanded ethanol production (11). Domestic ethanol production supports job growth in rural areas. In 2015, the Renewable Fuels Association reported that ethanol production accounted for 86,000 jobs in the US (12). Additionally, ethanol generates reduced combustion deposits, promotes clean burning, and reduces the amount of greenhouse emissions produced. Typically, one gallon of gasoline produces 8.9 kg of carbon dioxide, whereas E10 blends (90% gasoline, 10 % ethanol) generate 8.02 kg of carbon dioxide (13). These benefits provide support for the continued use and expansion of ethanol.

Though ethanol demonstrates value in transportation, the key impediments to its widespread use are supply and cost. Corn, the primary feedstock for domestically produced ethanol, is not abundant enough to replace gasoline (14). Additionally, the *food vs. fuel debate* expresses concern that competition exists between corn or other foodstuffs for use as a fuel and food. Therefore, the demand for one industry may cut into the supply for another. Secondly, the costs for cellulosic ethanol production remain a major barrier to widespread commercialization. To address cost, significant governmental intervention has been required to encourage ethanol production and use. For example, the Energy Policy Act of 2005 established the Renewable Fuels Standard (RFS) program,

which was designed to increase the volume of renewable fuels added to gasoline by 7.5 billion gallons by 2012. The Energy Independence and Security Act of 2007 (EISA) later revised the RFS program to include 36 billion gallons of renewable fuels in the transportation fuel supply by 2022. Interestingly, the RFS restricts ethanol produced from corn to 15 billion gallons by 2015 in order to meet the demand of other industries (15). This cap provides an opportunity to explore nonfood feedstocks, such as cellulose more in depth.

Cellulosic biofuels encompass renewable fuels such as cellulosic ethanol or gasoline derived from the biopolymers hemicellulose, cellulose, and/or lignin (16). Lignocellulosic biomass, which describes plants or plant-based materials, is a typical source of hemicellulose, cellulose, and lignin (Figure 1). Cellulose is similar in composition to the plant polysaccharide starch, a common raw material for ethanol production. Both cellulose and starch can be converted to ethanol; however, ethanol derived from starch is currently produced at a cost that is 40% lower per liter than from cellulose (17). Stereochemical differences between these molecules partly account for this price discrepancy. In cellulose, glucose units are joined together by β(1→4) linkages as opposed to α(1→4) linkages in starch. Cellulose therefore adopts a linear structure, whereas starch assumes a helical conformation. Unlike starch, individual cellulose molecules can be packed more closely together and form a rigid, crystalline structure that is difficult to process during ethanol production (18). Cellulose's crystalline structure is one of several lignocellulosic structural impediments that have spurred ongoing research to enhance the cost-competitiveness of cellulosic ethanol.

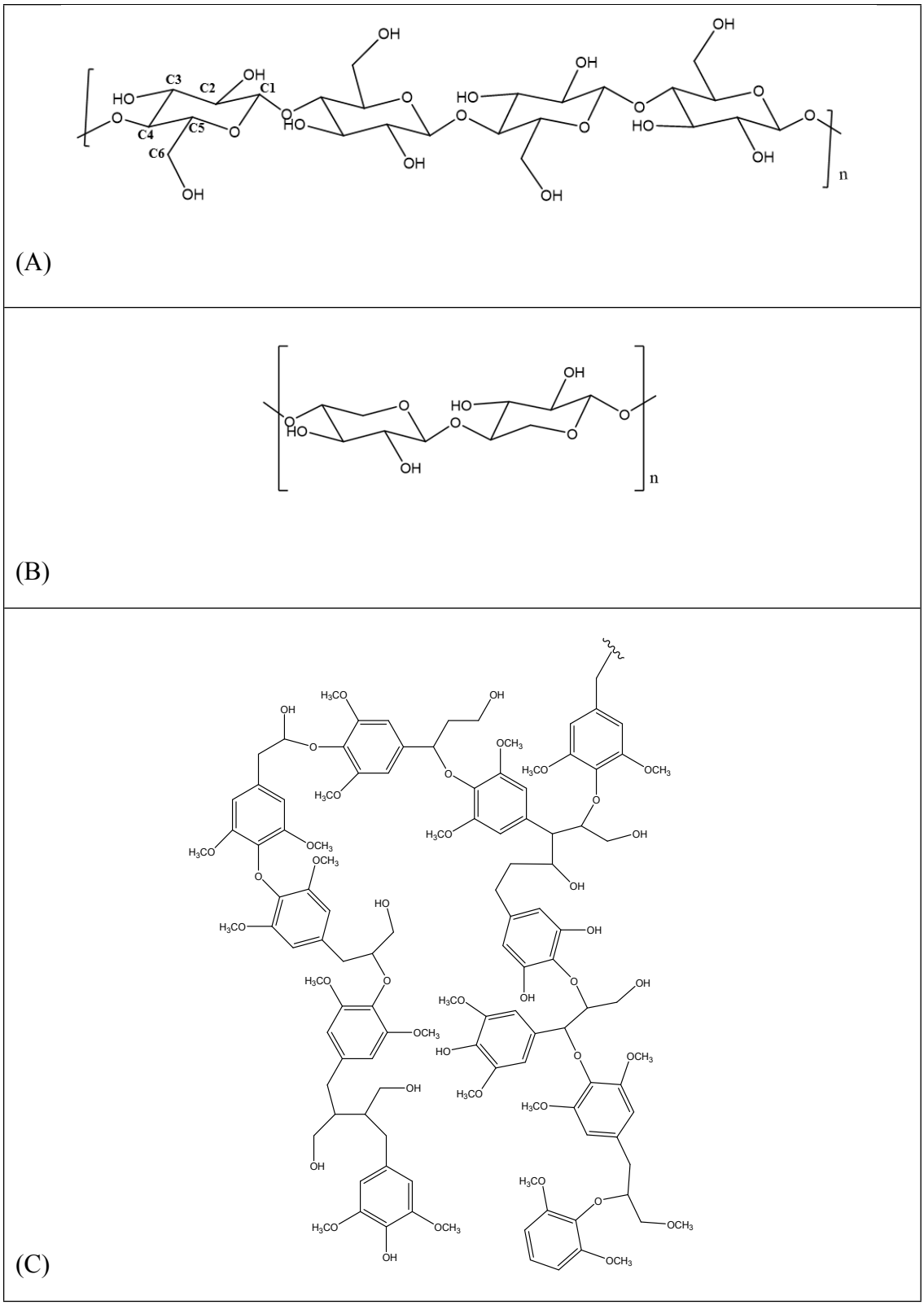

Figure 1 - The three primary cell wall polymers (A) cellulose, (B) [a representative] hemicellulose (xylan), and (C) lignin; n represents the number of repeat units

1.1.1 *Lignocellulosic Biomass*

Lignocellulosic biomass offers the transportation industry a geographically dispersed, renewable feedstock for ethanol production. Biomass encompasses several materials including but not limited to hardwoods, softwoods, and herbaceous plants. Each differs in cellulose, hemicellulose, and lignin composition (Table 1), which influences the ease, extent, and expenses associated with biomass processing. Typically, biomass is converted into ethanol in four steps: pretreatment, enzymatic hydrolysis, fermentation, and distillation. Due to its higher lignin content, softwoods generally require harsher pretreatments and higher enzyme loadings than herbaceous and hardwood biomass (19). The challenges presented during the processing of softwoods have shifted a great deal of interest into cellulosic ethanol production to the rapidly-growing hardwoods and the high-yielding herbaceous plants (20). It is worth noting that the three aforementioned polymers account for the majority of plant biomass; however, minor components such as structural proteins, ash, and extractives exist that constitute the remaining portion of plant biomass.

The genus *Populus* describes a collection of approximately 40 species of hardwoods (aspen, cottonwood, poplar, and their hybrids) located in Europe and North America that have emerged as a leading bioenergy crop. Poplars are short-rotation, genetically diverse crops that are well-characterized and are easily genetically manipulated. The US Department of Energy has embraced poplar for transportation fuels since the 1970s, and research for its use has continued into the present-day. The species *Populus trichocarpa* (black cottonwood) has attracted considerable interest for biofuel applications as it tolerates a range of climates and grows faster than any other hardwood

in the US. Its arguably most impressive trait is that its entire genome has been sequenced (21).

Table 1 - Representative cellulose, hemicellulose and lignin contents in various biomasses

	Cellulose (%)	**Hemicellulose (%)**	**Total Lignin (%)**
Hardwood			
Eastern cottonwood (*Populus deltoides*)	42.2	16.6	25.6
Yellow poplar	42.06	18.93	23.35
Black cotton wood (*Populus trichocarpa*) (22)	57.9	17.5	24.6*
Softwood			
Monterey pine (*Pinus radiata*)	41.7	20.5	25.9
Balsam fir (*Abies balsamea*) (23)	42	27	29
Herbaceous			
Switchgrass (Variety-Trailblazer)	34.44	25.46	19.96
Sweet sorghum (Variety-Cultivar M81E)	22.48	13.81	11.34

Source: http://www.afdc.energy.gov/biomass/progs/search1.cgi

*Klason lignin (%)

1.1.2 *Cellulose*

Cellulose, the most abundant macromolecule on Earth, is a linear chain of β-(1→4) linked D-glucose. Cellulose typically spans 10,000 units in length but varies depending on the source and contains between a highly variable cellulose content that commonly range between 25 and 90. Properties such as cellulose DP and crystallinity vary widely between biomass (Table 2). The fundamental repeat unit of cellulose is cellobiose, a disaccharide formed by a pair of β-D-glucose joined by acetyl linkages. Each glycosyl ring in cellulose contains three free hydroxyl groups at carbons 2, 3, and 6;

the hydroxyl group at C6 is the least sterically hindered and most accessible for chemical reactions. Accessibility to the hydroxyl groups influences cellulose's chemical interactions with other molecules. Within the plant cell wall, cellulose interacts with other cellulose chains, hemicellulose and lignin. Cellulose participates in intermolecular hydrogen bonding, which bundles individual cellulose chains into microfibrils, which contribute to cellulose's integrity and rigidity. These microfibrils also form multiple hydrogen bonds with hemicellulose to create a close association between the two (24). Under the appropriate reaction conditions, the hydroxyl groups participate in chemical reactions that add functional groups to the cellulose backbone and impart new chemical properties or interrupt bonds between cellulose and lignin or hemicellulose.

Table 2 – Cellulose crystallinities and degrees of polymerization (DP) from select biomass as determined by NMR and GPC

Source	Crystallinity	Cellulose DP
Aspen (*Populus tremula*)	48% (25)	4581 (26)
Sugarcane bagasse	58.9 % (27)	925 (26)
Balsam fir	NR	4400 (26)
Birch (*Betula pendula*)	41% (25)	5500 (26)
Scots pine (*Pinus sylvestris*)	~53% (28)	NR
Monterey pine (*Pinus radiata*)	~50% (29)	3063 (26)
Poplar	50 (30)	3500 (26, 30)
Populus trichocarpa x deltoides	~53% (3)	NR
Norway spruce (*Picea abies*)	54% (25)	NR

NR: not reported in the original publication

1.1.3 *Hemicellulose*

Hemicelluloses are linear or branched polysaccharides composed of five- and/or six- carbon sugars (Table 3). Hemicelluloses are either homo- (*i.e.* xylan, mannan, etc.) or heteropolymers (*i.e.* glucomannans, xyloglucans, etc.) and are soluble in alkali or water. Hemicelluloses are commonly linked by β-(1→4) acetal linkages; however, β-(1→3,1→4) linkages also occur between glucans. Furthermore, hemicelluloses typically span less than 200 units in length (31); typical hemicellulose molecular weights are listed in Table 4. As in celluloses, the monosaccharides in hemicelluloses contain hydroxyl groups that differ in reactivity and participate in various chemical interactions. For example, hemicellulose forms hydrogen bonds with water, making them easily hydrolyzable. As previously described, cellulose microfibrils form hydrogen bonds with hemicellulose. Hydrogen bonding occurs more extensively in unsubstituted hemicellulose rather than in substituted hemicellulose, as the side chains prevent close packing. Hemicelluloses are commonly covalently bound to lignin to form LCCs and also form crosslinks with structural proteins in plants (32).

Table 3 – Carbohydrate compositional analysis of several bioresources

	Glucan (%)	Xylan (%)	Mannan (%)	Arabinan (%)	Galactan (%)
Aspen (33)	44.5	17.7	1.7	0.5	1.3
Alfalfa (33)	30.2	9.7	1.5	3.8	3.0
Corn stover (34)	36.4	30.8	NR	1.8	NR
Douglas fir (35)	40.0	14.3	2.2	3.2	2.2
Eucalyptus grandis (36)	48.6	11.5	0.9	0.2	0.9
Populus deltoides × *Populus nigra* (37)	43.05	17.90	2.60	0.75	1.35
Rice straw (38)	36.32	19.45	NR	NR	NR
Switchgrass (39)	45.6	26.1	0.5	3.1	0.2

NR: not reported in the original publication

Table 4 – The molecular weights of hemicellulose isolated from various biomasses as determined by GPC

	Mn (g/mol)	Mw (g/mol)	PDI
Birch (40)	15,000	16,900	1.11
Larch (40)	14,000	17,400	1.23
Pine (40)	15,700	19,900	1.24
Populus trichocarpa (22)	25,000	33,500	1.3
Spruce (40)	14,600	18,400	1.22
Switchgrass (41)	10,800	18,700	7.3

1.1.4 *Lignin*

Lignin drastically differs from cellulose and hemicellulose in that it is a structurally complex polymer derived from phenylpropanoid units. Coniferyl alcohol, *p*-coumaryl alcohol, and sinapyl alcohol are the three monomeric units of lignin (Figure 2), which undergo radical coupling reactions to form this network polymer. Each monolignol contains a phenolic ring but differs in the number and position of methoxyl groups on its aromatic ring. Substitution on lignin is not limited to methoxylation on the aromatic ring; certain lignins have confirmed acetyl groups at their γ position. The acetyl groups are generally associated with S lignin but also occur on G lignin as well (42). Acetyl groups occur in a number of biomasses (42), but remain many biomasses that require similar confirmation. Acetylation quantification has been slightly challenging due to the removal of acetyl groups during samples preparation; however, the Derivatization Followed by Reductive Cleavage (DFRC) method has successfully identified acetylation in several hardwoods (42) and herbaceous plants (43). It appears that acetylation occurs prior to radical polymerization and functions in mechanical strength and resistance towards biological stressors (44).

In many plants, lignin's γ position can also house an aromatic moiety known as *p*-hydroxybenzoate. In poplars, p-hydroxybenzoate is almost exclusively associated with S lignin (45). Similar to acetylation, lignin is believed to contain p-hydroxybenozate prior to radical polymerization (45, 46). Studies have suggest that increased p-hydroxybenzoate concentrations improve enzymatic hydrolysis efficiencies with fungal cellulases (47, 48).

Radical polymerization of the coniferyl alcohol, sinapyl alcohol, and *p*-coumaryl alcohol monolignols generates ether and/or carbon-carbon bonds, which form guaiacyl (G), syringyl (S), and *p*-hydroxyphenyl (H) lignin. Additionally, the bond types generated during the radical polymerizations vary widely (Table 5), but the β-O-4 linkage is most common. Figure 3 illustrates and further defines the several types of interunit linkages present in lignin.

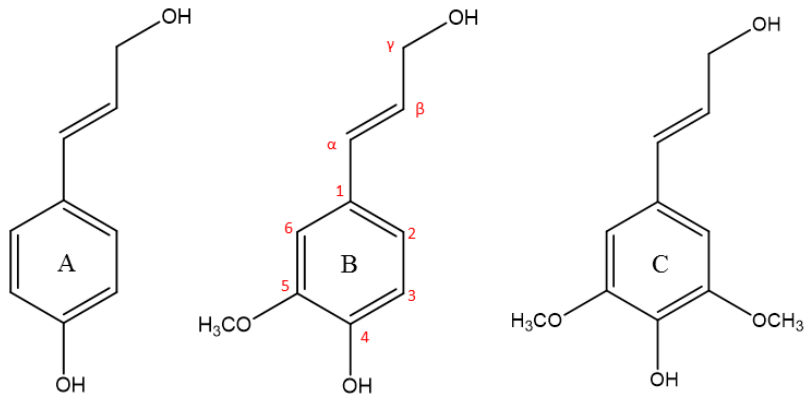

Figure 2 The three primary monolignol units of lignin (A) p-coumaryl alcohol (B) coniferyl alcohol and (C) sinapyl alcohol units

Table 5 – Select lignin interunit linkages and their relative abundances in various biomasses as determined by HSQC 2D NMR

	β-O-4	β-β	β-5	β-1
Arabidopsis thaliana (49)	78.7	4.1	15.4	1.0
Forage sorghum (*Sorghum*, sp.) (50)	50	5	37	8

Populus tremula × *alba* (51)	86.7	7.9	2.0	2.1
Bamboo (*Bamboo rigida*, sp.) (52)	49.01	7.07	2.17	NR
Miscanthus × *giganteus* (53)	42.1	3.8	9.9	NR
Wheat straw (53)	45.3	5.6	8.3	NR
Poplar (53)	43.1	6.0	1.6	NR

NR: not reported in the original publication

Lignin's structure is highly heterogeneous, and its variability stems from a slew of factors including plant species and age. Lignin composition varies between lignocellulose type (Table 6). For example, hardwoods contain both S and G lignin, whereas softwoods contain mostly G lignin and small amounts of H lignin. G, S, and H lignin are all represented in herbaceous biomass.

Radical polymerization generates varied lignin molecular weights, which is partly attributed to its structural properties. For example, H-lignin participates in β-β and β-5 linkages that limit lignin polymerization, thereby reducing polymer length (54). The proportion of sinapyl alcohol that is incorporated into lignin compared to coniferyl alcohol also appear to influence lignin molecular weight. More specifically, lower S/G ratio are associated with decreased molecular weights (55). Table 7 reports the molecular weights of lignin from diverse biomasses.

Table 6 – Lignin S, G, and H contents (%) of several biomasses determined by NMR

	S (%)	G (%)	H (%)
Wheat straw (56)	37	60	3
Olive tree pruning (56)	83	16	1
Miscanthus × *giganteus* (57)	52	44	4
Populus tremula × *Populus alba* (58)	69.2	30.8	NR

Typha capensis (57)	46	27	27
Sugarcane bagasse (59)	32.3	22.8	3.2

NR: not reported in the original publication

The phenolic groups present in lignin are important sites for the previously described chemical interactions with hemicellulose and cellulose. Additionally, phenolic groups have been recognized as a common starting point for lignin depolymerization or degradation with enzymes (60) or chemicals (61).

Table 7 – The molecular weights of MWL and CEL from hardwood, softwood, and herbaceous biomasses as determined by GPC

	Lignin isolation	Mn (g/mol)	Mw (g/mol)	PDI
Beech (*Fagus sylvatica*) (62)	MWL	3690	5510	1.49
Sugarcane bagasse (59)	CEL	1673	3176	1.9
Populus albaglandulosa (63)	MWL	4176	13250	3.17
Populus trichocarpa (64)	CEL	2959	9938	3.3
Switchgrass (55)	CEL	3031	8856	NR
Alfalfa (*Medicago sativa*) (65)	CEL	NR	6000	NR
Loblolly pine (*Pinus taeda*) (66)	MWL	989	7790	7.9

NR: not reported in the original publication

MWL, milled wood lignin; CEL, cellulolytic enzymatic lignin

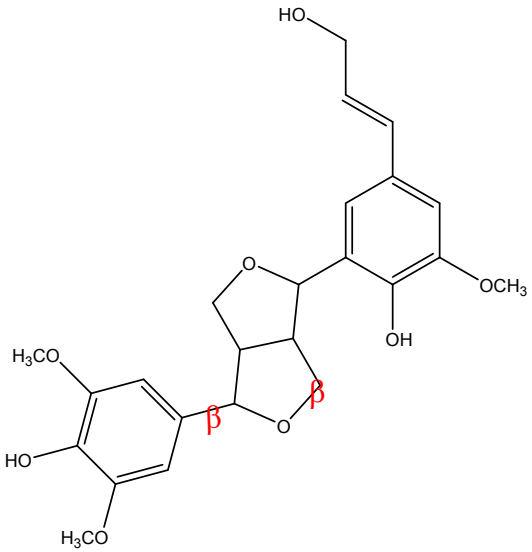
HO
O
OCH3
OH
H3CO
β
β
O
HO
H3CO

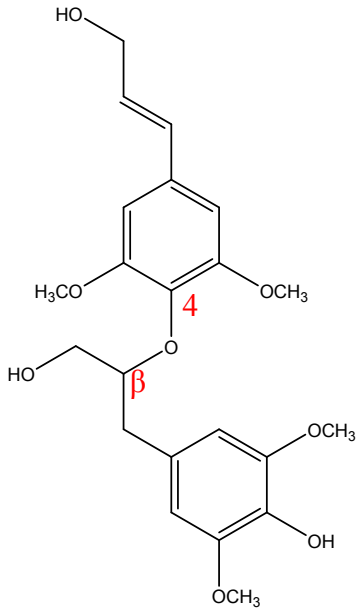
HO
H3CO
OCH3
4
O
HO
β
OCH3
OH
OCH3

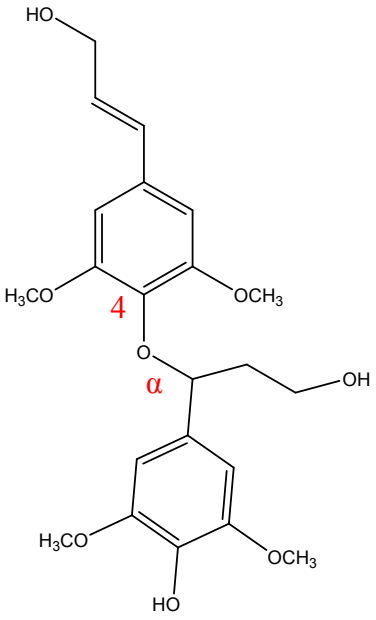
HO
H3CO
OCH3
4
O
α
OH
H3CO
OCH3
HO

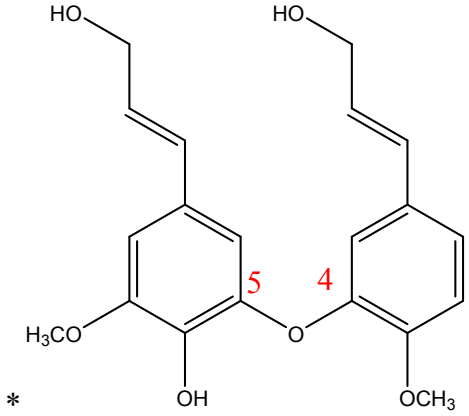
HO
HO
5
4
H3CO
O
OH
OCH3

*

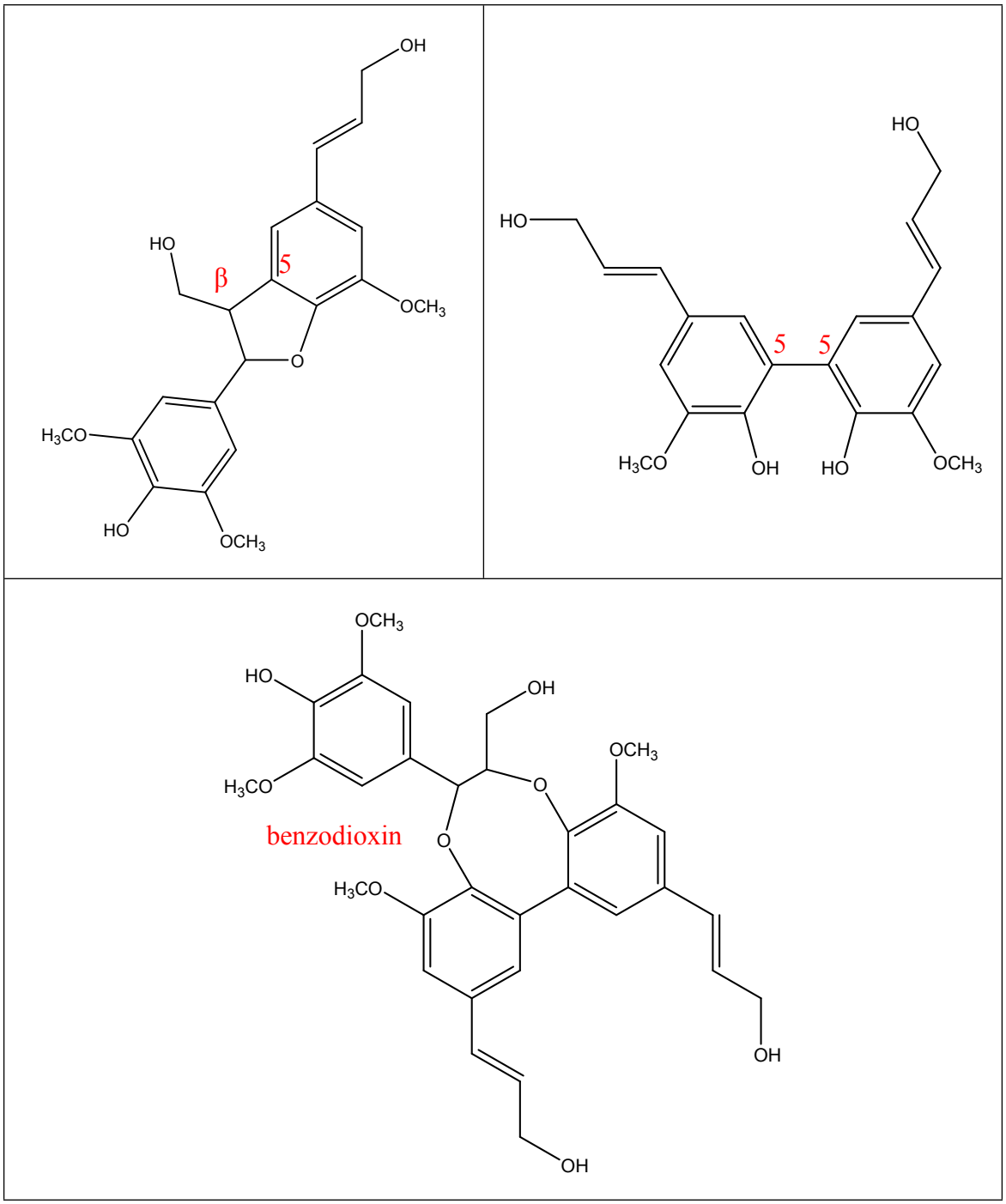

Figure 3 Select interunit linkages in lignin from left to right (β-β, β-O-4, α-O-4, 4-O-5, β-5 5-5, and benzodioxin)

1.2 Addressing Recalcitrance during Cellulosic Ethanol Production

Although compelling reasons exist to produce cellulosic ethanol, high production costs have stifled its broad commercialization. The plant cell wall's architecture, which is designed to promote plant survival, presents extensive challenges to cellulose conversion to ethanol. Cellulosic ethanol production typically involves four stages: pretreatment, enzymatic hydrolysis, fermentation, and distillation. Pretreatments are biological, chemical, and/or physical processes that induce structural alterations to biomass to facilitate the subsequent enzymatic hydrolysis. Fungal cellulases, which cleave cellulose chains into smaller fragments such as glucose, carry out cellulose hydrolysis. Yeast such as *Saccharomyces cerevisiae* uptake glucose and carry out fermentation to produce ethanol amongst other fermentation byproducts. Finally, distillation separates ethanol from the other fermentation products. Pretreatment, enzymatic hydrolysis, fermentation, and feedstock optimization either collectively or individually influence the feasibility and economics of ethanol production from lignocellulosic biomass.

Overcoming biomass recalcitrance, or resistance to enzymatic hydrolysis, has spurred several areas of technological interest. Plant genetics have become increasingly important as this area can be used to manipulate the lignin biosynthetic pathway and reduce recalcitrance (67). Plant genetics also reveal the inherent traits of natural variants that reduce recalcitrance (68), which demonstrate the relevance of genetics even in the absence of engineering.

While the acid-based approach offers lower costs, shorter processing times and greater resistance to product inhibition than hydrolytic enzyme-based approaches, cellulases remain the preferred tools for carrying out hydrolysis. This is because, unlike acid hydrolysis, cellulase-based enzymatic hydrolysis employs milder conditions, reduces capital costs, produces higher yields, and does not generate inhibitory byproducts that can disrupt downstream fermentation by microorganisms (69). In addition, the acid-catalyzed hydrolysis of cellulose generates carbohydrate-derived dehydration products, which are undesirable for the cellulase-based deconstruction of cellulose (70). Recently, studies have been conducted to improve the efficiency and decrease the cost of the enzymatic hydrolysis process using recombinant technologies (71), ionic liquids (72), accessory enzymes (73), and alterations of plant cell wall structure focused on modification to their lignin content (74-77), however, this stage still remains as the main bottleneck preventing cost efficiency. Therefore, as an alternative, the direct saccharification of lignocellulosic biomass has similarly been investigated, but has been shown to negatively impact the efficiency of enzymatic hydrolysis when compared to the saccharification of pretreated substrates in a variety of biomass sources (78-80).

Enzymes as well as pretreatments represent two costly processes in the cellulosic ethanol production scheme, and both are often targeted to combat recalcitrance (81). Pretreatments are an especially diverse approach to overcoming recalcitrance as a multitude of approaches (ionic liquids, dilute acid, hydrothermal, etc.) have been taken to achieve improvements in enzymatic hydrolysis (82). Recalcitrance can also be combatted by addressing the low activity of fungal cellulases and improving enzymatic hydrolysis efficiencies. In several cases, investigations have shifted towards employing systems that deconstruct biomass more efficiently than the traditional fungal cellulases.

For instance, certain microorganisms such as *Clostridium thermocellum* possess a multi-enzyme complex that promotes synergy between enzymes, thereby facilitating hydrolysis (83).

Though it was found to be industrially relevant since the late 1970s, *C. thermocellum* has presented a ground breaking approach to biomass deconstruction. Its multi-enzyme complex, known as its cellulosome, mobilizes several types of enzymes that break down not only cellulose but also other plant cell wall components. *C. thermocellum*'s cellulosome has demonstrated remarkable enzyme hydrolysis properties compared to fungal cellulases (83). Ongoing research aspires to solidify its significance and competitive edge in the biofuel industry.

CHAPTER 2. LITERATURE REVIEW

During the 1970s, the world oil crisis prompted intensive research into cellulosic ethanol as a gasoline substitute. Over the following decade, the scientific community intensely searched for biomass (84), microorganisms (85), and biochemical (86) and processing variables (87, 88) that could further the feasibility of cellulosic ethanol. Almost 50 years have elapsed since the oil crisis, and the scientific community remains baffled by fundamentally similar topics (89) and the central issue, how can cellulosic ethanol be produced in a large scale manner cost-effectively? Its solution is likely multifaceted, as several factors influence cellulosic ethanol production costs.

2.1 Cost Reduction through Integration

Condensing the ethanol production scheme towards the direct conversion of biomass into ethanol has consistently demonstrated desirable properties for ethanol production (90-92). While there are many approaches for ethanol production, there are five schemes that are excellent examples of process condensation: separate hydrolysis and fermentation (SHF), simultaneous saccharification and fermentation (SSF), simultaneous saccharification and co-fermentation (SSCF), consolidated bioprocessing (CBP), and integrated bioprocessing (IBP). Figure 4 illustrates how each subsequent scheme integrates steps in the former scheme.

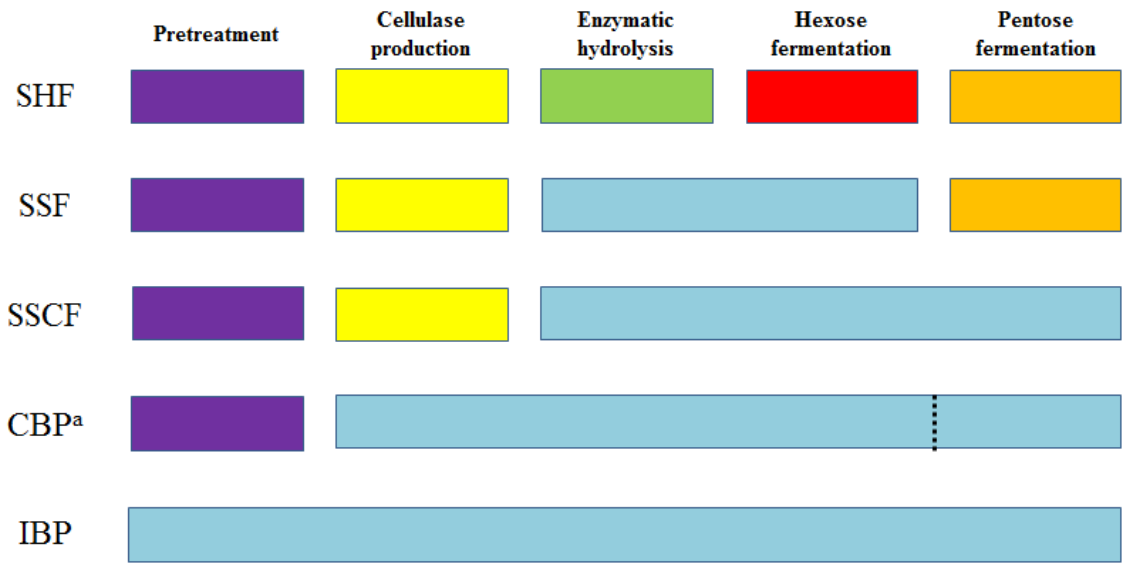

Figure 4 Process integration for ethanol production reduces the number of stages required to convert lignocellulosic biomass into ethanol. (purple – pretreatment, cellulose production – yellow, enzymatic hydrolysis-green, hexose fermentation-red, pentose fermentation-orange, condensation of stages - blue)

[a]All CBP microorganisms do not carry out hexose and pentose fermentation.

2.1.1 *Using Pretreatments to Facilitate Biomass Solubilization*

The minimum requirements for ethanol production are a pretreatment, cellulase production, the enzymatic hydrolysis of cellulose chains, and fermentation of five- and/or six-carbon sugars. Four of the five above schemes use a pretreatment, which employs biological, chemical, and/or physical means under a wide range of conditions to induce structural changes in biomass. These changes include but are not limited to the removal of hemicellulose, the redistribution of lignin, and the creation of larger pores. Hydrothermal pretreatments, for instance, use high-temperature water to remove hemicellulose and partially remove and redistribute lignin. These changes have been

linked to increased surface area and porosity in pretreated beech wood and a 63% improvement in enzymatic hydrolysis (93). Unlike the other systems, IBP emphasizes the use of microorganisms to carry out pretreatments (94) in an integrated scheme.

Pretreatments are believed to exert a significant impact on cost reduction in cellulosic ethanol production (95). Though pretreatments vary in type (Table 8), several considerations influence their efficacy and suitability. Firstly, the pretreatment should maximize cellulose recovery as sugar yields vary between pretreatments (96). Co-solvent enhanced lignocellulosic fractionation, or CELF, is an innovative pretreatment that uses a combination of water and tetrahydrofuran at 150°C to remove impressive amounts of hemicellulose and lignin. Furthermore, CELF achieves high theoretical yields (>80%) in the presence of modest enzyme (2 mg enzyme/g glucan) concentrations (97, 98). Under similar time and temperature combinations for example, CELF removed 57.4% more lignin than the dilute acid in pretreated corn stover and conserved approximately 30% more glucan (98).

Table 8 – Various pretreatments, their classification, and typical processing conditions for cellulosic ethanol production

Pretreatment	Classification	Typical conditions		
		Means	Duration	Temperature
Alkali (5)	Chemical	Base (NaOH, $Ca(OH)_2$, etc.)	1-30 h	25-85°C
Dilute acid (5)		Acid (H_2SO_4, HCl, etc.) at 0.3-2% w/w)	1 min – 2 h	120-180°C
CELF (97, 99)		THF and dilute (e.g. 0.5%) acid	15-45 min	110-170°C
Organosolv (5)		35-70% w/w ethanol	30-90 min	185-195°C
Ammonia fiber explosion (5)	Physicochemical	Liquid NH_3, > 3 MPa	10-60 min	60-100°C
Wet oxidation (5)		Water, 1.2 MPa	10-20 min	195°C
Comminution (100)	Physical	Chipping, milling, or grinding	-	-
White-rot fungi (5, 100)	Biological	*Pleurotus ostreatus*, *Phanerochaete sordida*, *Ceriporiopsis subvermispora*	Days to months	15-35°C

Secondly, the pretreatment should minimize inhibitor generation, which potentially restricts the subsequent hydrolysis and/or fermentation stages. In a comparative study, Qing et al. (2010) found that xylooligomers, which can be derived from pretreatments (101, 102), reduced the initial rate of hydrolysis of Avicel by as much as 81.9%, which was significantly more than xylose- or xylan-induced inhibition (103). Fermentation inhibition post-pretreatment also suppresses ethanol productivity but can potentially be mitigated with activated carbon or polymeric materials (104, 105).

Lastly, chemical costs and energy demands should be reasonably curtailed during the pretreatment (106) to avoid additional exorbitant costs to ethanol production. To meet this need, recent studies have focused on limiting energy-intensive process parameters (107), selecting less energy demanding pretreatments (e.g. steam explosion rather than conventional milling) (108), and using the hydrothermal pretreatment, which uses minimal, or if any, added chemicals (109).

2.1.2 *Managing the Costliness of Cellulase Production*

Cellulase production is expensive but essential to the enzymatic hydrolysis stage that proceeds pretreatment. Fungal cellulases isolated from *Trichoderma sp*. hold the greatest industrial relevance for cellulose hydrolysis, but cellulases may come from other fungi, bacteria, animals, plants, and microorganisms. Cellulase activities of 15 FPU are generally required to achieve the sugar yields necessary for cellulosic ethanol production from pretreated biomass (110). Cellulase isolation is carried out via submerged or solid state fermentation; submerged fermentations, though energy intensive, are favored as they provide a highly-controlled environment. The costs associated with enzyme production are proposed to range between $3.80 and $6.75 per kg enzyme and $4.00 to $8.80 per kg enzyme for on-site and off-site production, respectively (111). Cellulase production accounts for an estimated 25 to 50 percent of the total ethanol production costs (112) and potentially contributes between $0.10/gal to $0.32/gal to the total ethanol. Though estimates vary considerably, Klein-Marcuschamer et al. (2007) reported that the former approximations are underestimates and more reasonable values, as determined by modeling, range between $0.60 and $1.30/gal ethanol in poplar (113). Hence, original

but practical solutions that are desperately required to reduce these costs. The proposed solutions take the form of improved growth media for cellulase-producing organisms (114), optimized culture conditions (115, 116), or improved strains through genetic manipulations (117).

Cellulase production produces the enzymes that carry out cellulose hydrolysis. Cellulases are typically added at 15 FPU per g biomass (118) but can be added as low as 1 FPU per g biomass (118) or as high as 45 FPU per g biomass (119). Enzymatic hydrolysis converts cellulose chains into smaller units such as cellooligosaccharides, cellobiose, and glucose. Three categories of cellulases accomplish this conversion: endoglucanses, exoglucanases, and β-glucosidases. During this multi-step process, endoglucanases randomly cleave β-(1→4) linkages within cellulose chains to yield smaller fragments. Exoglucanases carry out hydrolysis on the resulting fragments at the nonreducing end to yield cellobiose. Exoglucanases and endoglucanases cleave cellulose differently due to structural differences in their active sites. Endoglucanases accommodate cellulose in a cleft-shaped active site, whereas exoglucanases accommodate cellulose fragments in a tunnel-shaped active site (120). Finally, β-glucosidases locate the disaccharide cellobiose and hydrolyze it into the monomer glucose.

While these enzymes can break down cellulose, their activity is low —100 times less than the amylases used to break down starch. The low activity translates into lengthy processing times and contributes to higher operating costs (121). The enzyme cocktail applied during biomass deconstruction generally contains additional enzymes such as

pectinases and hemicellulases to remove any barriers these materials present to hydrolysis.

2.1.3 *Recalcitrance Limits Enzymatic Hydrolysis*

The enzymatic hydrolysis stage is central to *recalcitrance* – the resistance of biomass to enzymatic (or microbial) degradation. Several features of biomass influence the ease of deconstruction, including but not limited to lignin composition, cellulose crystallinity, and extractive content. Many, if not all, of the plant attributes linked to recalcitrance hold value in plant integrity and survival. Cellulose crystallinity confers strength to the plant, while lignin assists in structural support (122). Enzymatic hydrolysis rates and the factors that drive their efficiencies are integral in understanding, approaching, and ultimately overcoming recalcitrance.

2.1.4 *Fermentation*

The glucose liberated during enzymatic hydrolysis is taken up by bacteria or yeast, most commonly *Saccharomyces cerevisiae*, to yield ethanol. *S. cerevisiae* incorporates glucose into the Embden-Meyerhoff pathway, where it undergoes several reactions to become the three-carbon intermediate pyruvate. Under anaerobic conditions, pyruvate is further converted into ethanol through fermentation (123). While glucose fermentation is well-established on a commercial scale, the fermentation of hemicellulose-derived C5 and C6 sugars is not. Utilization of these sugars adds additional starting materials for ethanol production and reduces waste. The fermentation of hemicellulose-derived sugars would require the incorporation of a hemicellulose hydrolysis step, but the sugars released could be fermented with a native (124) or

engineered *S. cerevisiae* (124) or another microorganism that utilizes both sugar types (125). Finally, distillation separates ethanol from other fermentation products.

2.1.5 *Integration: A Promising Route to Lowering Ethanol Production Costs*

Integration of the different steps of ethanol production represents a powerful step towards managing costs. For instance, enzymatic hydrolysis occurs between 45-50°C, while fermentation occurs between 30-32°C. Systems that carry out both processes simultaneously mitigate the temperature difference between stages and reduce the associated heating and cooling energy costs. Furthermore, practices that enable onsite cellulase production help to lower added costs associated with offsite production and capital investments (126). A process cost reduction analysis for biofuels identified CBP as the leading tool for cost management during ethanol production. Of the eight areas considered, CBP's potential stood at 41%, while pretreatment elimination had the next highest cost reduction potential at 22% (127).

2.1.6 *Consolidated Bioprocessing Microorganisms*

Currently, several microorganisms have attracted considerable interest in combining the steps used during ethanol production in a process termed consolidated bioprocessing (CBP). Select microorganisms that carry out CBP are listed in Table 9 in addition to their benefits and limitations. Table 9 highlights the many considerations for a CBP matrix such as ethanol tolerance, hydrolysis rate, and ethanol titer. Although there is no known perfect candidate, *Clostridium thermocellum* is a frontrunner.

Table 9 – Select CBP microorganisms and their associated benefits and limitations

	Benefits	**Limitations**
Zymomonas mobilis (128, 129)	• Relatively high ethanol productivity, titers, and yields (min. 12% w/v) • Tolerant to low pH and high ethanol concentrations (max. 16% w/v)	• Cannot ferment C5 sugars • Inhibited by lignocellulosic hydrosylates
Clostridium thermocellum (130)	• Hydrolyzes C5 and C6 sugars amongst several other cell wall components • Contains a multi-enzyme unit that promotes synergism between enzymes • Achieves cellulose hydrolysis rates of 2.5 $g \cdot L^{-1} \cdot h^{-1}$	• Ferments cellulose-derived sugars • Does not undergo genetic manipulations easily • Low ethanol tolerance
Caldicellusiruptor bescii (131)	• Utilizes a wide range of plant-derived substrates	• Low ethanol tolerance (20.7 $g \cdot L^{-1}$)
Escherichia coli (132, 133)	• Easily amenable to genetic manipulation • Well understood microorganism for recombinant technologies	• May require the addition of enzymes • Low ethanol production
Clostridium phytofermentans (134, 135)	• Converts a wide array of biomass components and	• Low ethanol yields (2.8 $g \cdot L^{-1}$)

substrates to ethanol

2.2 *Clostridium thermocellum* and its Relevancy to the Cellulosic Ethanol Industry

Fossil fuels raise significant concerns related to supply longevity, sustainability, energy security, and environmental impact. For these reasons, renewable energy sources are attracting considerable attention as alternatives to their nonrenewable counterparts. However, in the search for an alternative replacement, any new fuel compound must first meet three primary considerations in order to be regarded as a viable candidate: it must have the potential to supply the world's energy demands, it must be able to reduce negative environmental effects relative to current fossil fuels, and it must be cost-competitive. With the current state of the art, ethanol derived from lignocellulosic biomass addresses two of these considerations, however, its production in a cost-effective manner is currently lacking due to the difficulties in breaking down and converting the sugars locked within the lignocellulosic feedstocks.

Currently, most industrial lignocellulosic bioprocessing applications utilize *Escherichia coli*, *Zymomonas mobilis*, *Saccharomyces cerevisiae*, or a handful of other yeast strains in conjunction with exogenous hydrolytic enzymes to release fermentable sugars from the biomass substrate (136). These organisms, however, are utilized primarily because of their thoroughly developed and studied genetic engineering toolkits, physiology, and metabolic pathways. As a possible exception, *S. cerevisiae* does have several advantageous traits such as its natural ethanol tolerance and ability to grow at acidic pH, however, it remains incapable of surviving at the optimal temperatures of

exogenous hydrolytic enzymes and, in its wild type form, is unable to ferment pentose sugars (137, 138).

One promising approach to circumventing the cost and restriction of this conventional workflow is the use of consolidated bioprocessing (CBP). CBP technologies combine the enzyme production, hydrolysis, and fermentation stages into a single step, improving processing efficiencies, eliminating the need for added exogenous hydrolytic enzymes, and reducing the sugar inhibition of cellulases ride(132, 139, 140). This approach reduces the number of unit operations, and lowers the overall capital cost of the process (132, 141).

However, for this approach to be economically feasible, an industrially relevant consolidated bioprocessing microorganism is required that produces a hydrolytic enzyme system capable of solubilizing a realistic biomass substrate and fermenting both hexose and pentose sugars to ethanol at > 90% of its theoretical yield, a titer of at least 40 g/L, and a fermentation rate of > 1 g/L/hr (142, 143). Unfortunately, no microorganisms with these characteristics have yet been discovered, and therefore genetic engineering strategies will be required to develop such a strain. In this regard, two strategies have been developed to engineer an appropriate organism. The first approach seeks to engineer a naturally highly efficient cellulolytic microbe to produce the desired product. The second approach applies a recombinant cellulolytic strategy, and strives to engineer a microbe with naturally high product titer, rate, and yield to express a hydrolytic enzyme system that efficiently solubilizes biomass substrates (132, 139, 144, 145).

While there are myriad gene sets available that encode enzymes capable of degrading plant biomass, heterologously expressing these suites of enzymes in a non-natively cellulolytic host microorganism requires the transfer, optimization, expression, and coordination of many genes. This potentially represents a more difficult barrier to

overcome than engineering a naturally cellulolytic microorganism to produce ethanol. Therefore, thermophilic cellulolytic microorganisms have become attractive targets for this approach, as their growth at high temperatures reduces the risk of contamination, integrates well with existing processing streams, and increases the solubility and digestibility of their required substrates (145-147). However, regardless of which strategy is realized, each has the potential to unlock an efficient method for the production of ethanol from lignocellulosic biomass (132, 139, 142, 148, 149). To date, a wide variety of microorganisms have been investigated for this process (150, 151), however, *Clostridium thermocellum* has emerged as a particularly attractive high utility candidate because its use of a cellulosome has demonstrated remarkable enzymatic hydrolysis efficiency compared to free cellulases (152, 153). This review will therefore focus specifically on *C. thermocellum*'s role as a candidate for CBP and how it can be utilized to improve the suitability of this process towards the production of ethanol as a realistic replacement for existing liquid transportation fuel sources.

2.2.1 *Clostridium thermocellum*

2.2.1.1 Isolation and Initial Characterization

C. thermocellum is an anaerobic, rod shaped, Gram positive thermophile that is capable of producing ethanol directly from cellulose. Despite its relatively recent rise to popularity in the literature, it was first isolated in 1926 by Viljoen et al. in an attempt to identify novel organisms capable of degrading cellulose (154). This initial characterization by Viljoen, while basic, provided the framework required for future investigators to work with and develop this unique organism, but proved unreliable due to potential contamination of the culture with additional organisms (154). The first robust description, therefore, was not available until almost 30 years later. This characterization

was the first to report that *C. thermocellum* could grow at temperatures between 50 – 68°C, and demonstrated this growth on cellulose, cellobiose, xylose, and hemicelluloses. It also detailed the major fermentation products, consisting primarily of carbon dioxide and hydrogen gases, formic, acetic, lactic, and succinic acids, and ethanol (155). It is important to note, however, that significant discrepancies in the list of fermentable carbon sources have been shown to exist among alternate characterized *C. thermocellum* strains, so caution must be taken when comparing the growth conditions in the early literature (156).

Following these initial characterizations, there were still many setbacks in the initial attempts at culturing *C. thermocellum* and isolating pure stocks (157). Fortuitously, these have largely been overcome with the development of defined mediums that allow for routine growth and maintenance of *C. thermocellum* cultures (158, 159), significantly improving the ease of subculturing and providing an ideal environment for defined selection and genetic modification. As these media were developed, they determined a requirement for several essential vitamins, including biotin, pyridoxamine, B_{12}, and *p*-aminobenzoic acid (159) and demonstrated a requirement for pH maintenance between 6.2 - 7.7. It is now known, however, that the optimal pH for growth occurs between 6.7 - 7.0 (160) and that the optimal growth temperature is 55°C.

Employing these defined growth techniques, *C. thermocellum* can be cultured using either batch or continuous flow approaches, with growth rates of 0.10/h and 0.16/h, respectively (161). However, in the presence of cellulosic material *C. thermocellum* has been observed to form biofilms, which may more closely resemble its growth under

environmental conditions. Upon biofilm formation, *C. thermocellum* will orient itself parallel to the carbon fibers of its substrate, forming a single monolayer of cells that will gradually spread outward from the initial site of colonization. These cells will closely mimic the topography of the substrate, with each cell maintaining direct contact if possible (162). This orientation may be maintained in order to facilitate the extracellular hydrolysis of the substrate, which is then incorporated into the cell directly as soluble oligosaccharides and used for fermentative catabolism (163). Throughout this process, cells are constantly attaching and detaching from the carbon source, with no apparent correlation to cellular life cycling, and relatively similar percentages of cells involved in division or sporulation in either their attached (11 ± 3%) or detached (5 ± 3%) states (162).

One of the main products of this fermentation activity, and indeed the reason that *C. thermocellum* has enjoyed increased attention in the recent past, is ethyl alcohol. However, despite the production of this fermentation end product, wild type *C. thermocellum* can only tolerate ethanol up to 5 g/L before it is significantly inhibited (164). A contributing factor towards this sensitivity has been determined to be the endogenous membrane structure. The predominant lipids that make up *C. thermocellum*'s cell wall are branched and straight chain 16 carbon fatty acids, and 16 carbon plasmalogens that, along with the other components, display a total lipid content of ~82 μg/mg dry cell weight, with roughly 28% of that weight comprised of plasmogens (165). This membrane orientation leads to a high degree of fluidity that is compounded by the presence of moderate levels of ethanol. As the fluidity increases, the membrane begins to lose its integrity and the health of the cell is negatively impacted. Therefore, to

tolerate increased levels of ethanol *C. thermocellum* must alter its membrane composition to decrease fluidity and compensate for the artificial fluidity imparted by its own fermentation products.

2.2.1.2 Amenability to Consolidated Bioprocessing

Despite its endogenous disadvantage of ethanol inhibition, *C. thermocellum* retains many qualities that position it well for use as a consolidated bioprocessing organism, including its fast rate of digestion of cellulose from plant biomass and its ability to hydrolyze both hemicellulose and cellulose. In addition, it is capable of naturally producing ethanol, albeit at low concentrations (< 3 g/L), and one strain, DSM 1313, has both a finished genome sequence and a developed genetic transformation system that allows for the construction of mutant strains (166-170). Although it does suffer from a detriment in that it can only utilize C_6 sugars, it has been demonstrated to perform efficiently in co-culture with C_6 and C_5 utilizing thermophilic anaerobic bacteria, making it an excellent springboard for development into a CBP host.

2.2.1.3 Structure, Function, and Fermentative Characteristics of the *C. thermocellum* cellulosome

The distinguishing feature of *C. thermocellum*, and indeed its most attractive feature as a platform for development into a CBP host, is its cellulosome. The cellulosome is an extracellular multi-enzyme complex 18 nm in diameter with a molecular weight greater than 2×10^6 Da (171) that is central to *C. thermocellum*'s ability to reduce lignocellulosic biomass recalcitrance (Figure 5) (172). This multi-enzyme complex consists of over 20 distinct enzymes (173), housing cellulases,

hemicellulases, pectinases, chitinases, glycosidases, and esterases for the breakdown of lignocellulose (174, 175).

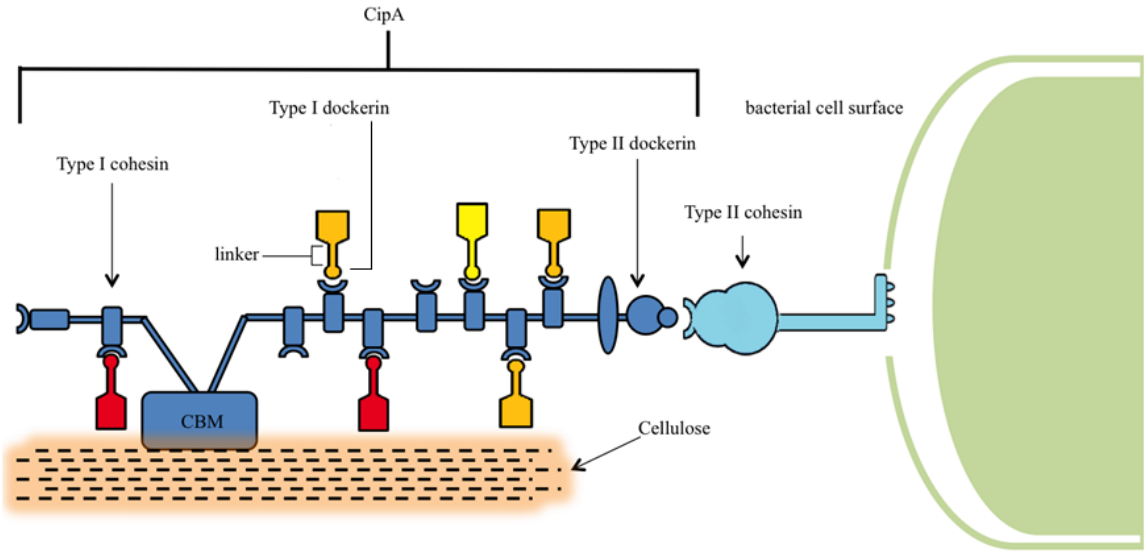

Figure 5 Illustration of *C. thermocellum*'s cellulosome (not drawn to scale) (130)

Characterization of the cellulosome began in the 1980s, and since that time a stream of discoveries have elucidated its role in cellulose binding (176, 177), its position on the bacterial cell wall surface (178), its structure during cellulose degradation (179), and its diversity of associated cellulases (180). Central to the assembly of this complex is a macromolecular non-catalytic scaffoldin protein known as CipA. This CipA scaffoldin contains nine type I cohesin domains that bind to type I dockerin domains, which are in turn connected to the catalytic domains of their enzymes through a linker (181) in a calcium dependent fashion (182). CipA is itself anchored to the bacterial cell surface by way of a type II dockerin and mediated by the LpB, Orf2p, and SdbA anchoring proteins (181) and, in addition, also contains a carbohydrate binding module that attaches the cellulosome to its carbohydrate substrate (183).

Crystallographic interrogation has suggested that these integral cohesin-dockerin complexes are primarily mediated by hydrophobic interactions (184), and these results have been supported via subsequent molecular dynamics simulations as well (185). As such, it has been presumed that the cellulosome assembles in a nonselective or mildly selective manner due to the inability to assign each dockerin to a single cohesin and the relative similarities in affinity between several dockerins and cohesins (182). However, evidence has recently surfaced that suggests some degree of selectivity. Sakka et al. observed the binding of the CelJ dockerin only to selected cohesin modules, indicating a degree of specificity during cohesin-dockerin recognition that was not previously detected (186). Similarly, Borne et al. have studied the role of randomness during the binding of an alternative *Clostridium cellulolyticum* dockerin to a chimeric scaffoldin containing one *C. cellulolyticum* cohesin and one *C. thermocellum* cohesin. In this case, binding occurred successively in a manner dependent on linker length, reinforcing the notion of order during cellulosomal assembly (187).

Findings that support selectivity surrounding enzyme recruitment and/or synergistic effects present during the digestion of biomass point towards major advancements in the production of cellulosic ethanol via the optimization of enzyme combinations. For example, opportunities for synergy between cellulases in *C. thermocellum*'s cellulosome during the degradation of crystalline cellulose increase statistically as the number of cohesins present on the scaffoldin increases. In one study, the inclusion of two cohesins instead of one on the cellulosome increased synergism by a factor of 1.7 (188).

To take advantage of this fact, and leverage the utility of the cellulosome itself, an artificial cellulosome, termed the rosettasome has been genetically engineered to

incorporate the dockerin domains of cellulases from *C. thermocellum*. Just as with the native cellulosome, this rosettasome has demonstrated enhanced cellulolytic activities as additional cellulases have been attached (189). Building upon these efforts, Gefen et al. have developed a chimeric cellulosome, BglA-CohII, that was designed to manage cellobiose inhibition by affixing a β-glucosidase (BGL) to one of the open binding domains. This attachment of BGL lessened cellobiose inhibition in the presence of Avicel and pretreated switchgrass relative to the native cellulosome with or without BGL present (190).

These findings have led to the development of the plasticity theory, which rationalizes this synergistic behavior. This theory contends that the flexibility of a linker within the cellulosome directly leads to its enhanced adaptability towards utilization of different substrates. Coarse-grain models have investigated this theory by monitoring plasticity and uncovering the preferential scaffoldin binding of dockerins from CbhA, a large endoglucanase, over those from the smaller CelS exoglucanase and Cel5B endoglucanase, even though each had the potential to bind to any cohesin. In these models, the large structure of the CbhA exoglucanase appeared to influence key parameters such as its extended scaffoldin residence time and its prolonged diffusion rate, both of which improved its likelihood of binding (191).

Regardless of the components employed, the cellulosome breaks down its lignocellulosic substrate into cellodextrins, which are brought into the cell via one of at least five identified ATP binding cassette transporter proteins (192) in order to support a modified form of glycolysis (190). Once within the cell, cellobiose phosphorylase or cellodextrin phosphorylase phosphorylates the cellobiose or cellodextrin, respectively, to

yield glucose-1-phosphate and glucose. These compounds are then shunted to the Embden-Meyerhof pathway, and glycolysis takes place to yield pyruvate, GTP, and ATP. Thereafter, a series of phosphorylation reactions follow, although the exact nature and flux of these reactions has not yet been fully elucidated (193). Under our current understanding, both ATP and GTP-linked glucokinases have been identified in *C. thermocellum*, as well as phosphoenolpyruvate carboxykinase, which may be responsible for the conversion of phosphoenolpyruvate to oxaloacetic acid. This has led to the assumption that both of these compounds undergo glycolysis to produce ethanol during fermentation (193). Pyruvate is similarly converted into several fermentation products depending on the enzyme that catalyzes the reaction, with lactate dehydrogenase forming lactate and pyruvate formate-lyase forming formate (194). These products are then available for use just as with traditional processing strategies, completing the CBP process.

The cellulosome is one of the fastest hydrolyzers of microcrystalline cellulose; however, there are many other hydrolytic enzymes associated with the cellulosome, including pectinases and hemicellulases, which are also essential for the digestion of biomass feedstocks. While relatively fewer studies have been undertaken to explore these components, when *C. thermocellum*'s draft genome sequence was screened for open reading frames related to cellulosomal components, it was discovered that only one third of these were related to cellulases and the rest were related to hemicellulases, pectinases, chitinases, glycosidases and esterases (175). Of particular interest from these groups of enzymes are the hemicellulases, which can degrade the hemicellulose matrix through the random cleavage of carbohydrates. Zverlov et al. characterized the structure and activity

of two hemicellulytic cellulosome components consisting of xyloglucanase Xgh74A and endoxylanase Xyn10D, demonstrating that when their lysis events occurred in close enough proximity, short oligosaccharides were formed that assisted in exposing the underlying cellulose (195). Moreover, it has been demonstrated that *C. thermocellum* JW20 (ATCC 31549) preferentially digests high degree of polymerization xylan, a hemicellulose common to birch wood, with degradation becoming increasingly efficient as the number of monomer units in xylan exceeds six. In contrast, degradation of lower, 2 - 5 unit, degree of polymerization xylan did not occur until 240 h later and, after 300 h, only xylose remained, as these monomers are not imported by the cell (196). Taken together, these findings support the hypothesis that *C. thermocellum*'s hemicellulases target higher molecular weight hemicelluloses.

Current studies evaluating the interaction of the cellulosome relative to free cellulases for the digestion of either crystalline cellulose or plant biomass have provided additional insights into their mechanisms of hydrolysis, potentially leading to improvements in the deconstruction step through enzyme engineering and optimization of biomass pretreatment conditions. For instance, the cell free cellulosome of *C. thermocellum* can process roughly 40% of high degree of polymerization cellulose (presented as Whatman filter paper) in 120 h, compared with free *T. reesei* cellulases that can only achieve less than 20% conversion in the same time frame (83). However, in contrast, the *T. reesei* free enzyme system was more active on plant biomass than the cell free cellulosome extract. Moreover, post enzymatic hydrolysis images of the crystalline cellulose substrate determined that the mechanisms were vastly different between the free enzyme cocktail, which used a fibril sharpening method, and the cellulosome, which

splayed open and separated the individual microfibrils (83). Most importantly, however, has been the demonstration of synergistic effects when these two approaches are combined. Ding et al. revealed that this is likely due to a difference in mechanisms between the free enzyme systems and the cellulosome. Using real-time imaging to show the production of solubilization pits in the surface of the delignified plant biomass treated with free enzyme systems and the splaying of individual microfibrils in cellulosome-treated biomass, they concluded that biomass pretreatments which remove the highest amount of lignin and leave the largest amount of carbohydrates improve hydrolysis regardless of whether a free enzyme system or cellulosome is employed (197). The supplementation of free enzymes with cellulosomes aligns well with other technologies that aim to improve enzymes used in biomass deconstruction (2).

2.2.1.4 Biomass Utilization

The high degree of biomass recalcitrance is one of the major factors limiting the cost-effective production of lignocellulosic ethanol. Therefore, the ability of *C. thermocellum* to efficiently digest a range of biomass structures is an important consideration for its practicality as a CBP host. To investigate its fermentative abilities, Puls et al. compiled one of the earliest characterization studies relating to the solid residuals remaining after cellulosomal processing of steam pretreated, sodium chlorite delignified Birchwood by *C. thermocellum*. It was discovered that, following treatment, the solid residuals contained an unchanged crystallinity content (52%) that was attributed to the simultaneous hydrolysis of amorphous and crystalline cellulose. Cellulose experienced an increase in its weight-average degree of polymerization, while the polydispersity remained the same following microbial treatment, indicating the

preferential consumption of low degree of polymerization cellulose. These findings ran contrary to those obtained using free cellulases from *Neocallimastix frontalis*, *Trichoderma koningii*, and *Penicillium pinophilum*, providing one of the first indications that the organization and ultrastructure of *C. thermocellum's* cellulosome contained unusual properties (198).

Since that time, many additional studies have been performed to elucidate the function of *C. thermocellum*'s cellulosome on a variety of substrates. One of the main focal points of these studies has been to determine how *C. thermocellum*'s cellulosome circumvents the inhibition of activity and adsorption that cellulose crystallinity has imparted on many previously characterized fungal cellulases (199, 200). In this regard, it has been determined that *C. thermocellum* approaches deconstruction atypically, in that it displays a remarkable propensity towards the hydrolysis of microcrystalline cellulose. For instance, *C. thermocellum* is capable of converting 100% of Avicel, which is 74% crystalline, in 100 hr, compared to free cellulases isolated from *T. reesei*, which were only able to consume 50% of Avicel in the same time frame (83). While this is encouraging, it should be noted that, in general, Avicel demonstrates excellent conversion properties in comparison to pretreated biomass. Therefore, to expand the scope of this evaluation, Shao et al. further identified differences in *C. thermocellum*'s efficiency during the consolidated bioprocessing of Avicel and ammonia fiber expansion pretreated (AFEX) corn stover. While Avicel displayed high conversion rates (> 95%) after 24 hr when treated with *C. thermocellum*, AFEX pretreated corn stover glucan experienced lower conversion rates (60 - 70%), even after extended incubation times of 4 days. While the reason for this discrepancy in efficiencies was not elucidated during this study, initial

enzyme concentrations and restricted cell growth on AFEX pretreated corn stover were ruled out as possibilities (201).

Along with differences in biomass structure, the employment of differing pretreatment methods has also been shown to influence *C. thermocellum*'s digestion and fermentation efficiency. Hörmeyer et al. investigated the treatment of Avicel, poplar (*Populous tremuloides*), and wheat straw (*Triticum vulgare*) with *C. thermocellum* strain NCIB 10682 using either unpretreated, organosolv (methanol/water), or hydrothermolysis pretreated biomass, and used pH to indicate the extent of cellulose metabolism via acetic acid production. Under this experimental design, hydrothermally-treated poplar produced lower pHs (~6.0 - 7.0) than unpretreated poplar (~7.4) after 150 min of processing, signifying an increased efficiency in the presence of the hydrothermal substrate (202). Likely, this increase in efficiency can be attributed to the structural changes incurred by the biomass during pretreatment, which led to an increased accessibility of the sugars during digestion while maintaining favorable conditions for growth and enzymatic function (83). Alternate strategies for overcoming the recalcitrance barrier, such as altering the plant cell wall structure to be more easily digested by reducing lignin content or altering lignin composition, have also been employed (74, 76). Fu et al. and Yee et al. demonstrated the feasibility of this approach, showing that a transgenic switchgrass with reduced lignin content and syringyl/guaiacyl (S/G) ratios had improved fermentation yield and required a lower severity pretreatment and less enzyme loading to obtain equivalent yields to their control switchgrass when employing a yeast-based fermentation with exogenous hydrolytic enzymes in a simultaneous saccharification and fermentation (SSF) format. More importantly, they observed that *C.*

thermocellum exhibited equivalent or higher fermentation yields than the yeast-based SSF approach, which lead to the hypothesis that the cellulosome is more reactive in a CBP format than a cell-free extract configuration (75, 203). In an alternate approach, Bothun et al. subjected *C. thermocellum* to elevated hydrostatic pressures (7.0 and 17.3 MPa) in a high-pressure bioreactor, resulting in a ~100-fold rise in the ethanol:acetate ratio compared to batch cultures at atmospheric pressure. These results were attributed to the enhanced solubility of gaseous fermentation products under their reaction conditions (204), further demonstrating the importance of pretreatment conditions on hydrolysis and fermentation efficiency.

2.2.1.5 Genomic, Transcriptomic, Proteomic, and Metabolic Responses to Ethanol production

Due to its high amenability towards use as a CBP microorganism, *C. thermocellum* has attracted significant interest in its genomic, transcriptomic, proteomic, and metabolomic profiles and their respective dynamics throughout the CBP process. These evaluations have been performed across a variety of different strains and, taken together, provide crucial insight into how it can perform the complex reactions necessary to break down and utilize cellulosic material.

At its most basic level, the genome of the type strain, *C. thermocellum* ATCC 27405, consists of 3.8 Mb of DNA arranged as a single chromosome. The average guanine/cytosine (GC) content of the genome is a moderate 38.9%, and 3,173 candidate protein encoding genes have been identified via automated analysis (205). In addition to the type strain, sequences for several additional strains have also been elucidated and

yielded similar characteristics (166, 206, 207). Genomic analysis following adaptation to increased ethanol tolerance has indicated several conserved genetic alterations, including changes to glucokinases, aminotransferases, transcriptional regulators, aldehyde/alcohol dehydrogenases, and aspartate carbamoyltransferases. In addition, non-conserved changes have been identified in a variety of membrane proteins as well. Taken together, these genetic changes significantly improved *C. thermocellum*'s ethanol tolerance from ~15 g/L to 50 g/L and improved its utility as a CBP host (208).

While relatively few genetic changes were discovered related to enhanced ethanol tolerance, significantly more transcriptomic alterations have been observed that can provide insight into how *C. thermocellum* responds to changes in substrate availability and ethanol production. Transcriptomic analysis revealed a set of 348 genes that displayed significant variation in their expression levels in response to utilization of either cellulose or cellobiose as a carbon source, or concurrent with changes in growth rate resulting from nutrient availability and population density. Of these 348 genes, 78 demonstrated a significant decrease in expression when cellobiose was provided as a carbon source and 95 were up regulated. Of note is that the majority of these genes contained signal peptides, or were transcriptional regulators, indicating that they are likely involved in the extracellular recruitment and uptake of metabolites, demonstrating *C. thermocellum*'s ability to sense and respond to external cues regarding nutrient availability (209). Similarly, switching from cellobiose to cellulose fermentation elicited changes in the expression of roughly 40% of all genes, with expression profiles generally indicating increased transcription levels for those genes related to energy production, translation, glycolysis, and amino acid, nucleotide, and coenzyme metabolism.

Expression of these genes under cellulose utilization was shown to be growth stage dependent, with transcription decreasing as the available cellulose is consumed and transcription of genes encoding for cellular structure and motility, chemotaxis, signal transduction, transcription, and cellulosomal proteins becoming increased, presumably due to an increased necessity to discover alternative carbon sources in accordance with the classic feast-or-famine survival strategy (210). When pretreated biomass was supplied in place of cellulose or cellobiose, an even larger number of genes displayed differential regulation. Using pretreated yellow poplar as a model carbon source, 1,211 genes were up regulated, and 314 were down regulated compared to growth on cellobiose. Of particular note is that 47 of the 81 recognized cellulosome genes (58%) were up regulated upon yellow poplar-mediated biomass growth, compared with only 4 that showed lower expression levels relative to cellobiose fermentation. In addition to these cellulosome genes, significant up regulation was also observed for genes involved in inorganic ion transport and metabolism, signal transduction, and amino acid transport (211). Similar regulation profiles were found, albeit with up regulation of phosphate transport and Resistance-Nodulation-Division (RND) transporters, when pretreated switchgrass was substituted for poplar (212). Together, these results demonstrate the significant differences that can be imparted when *C. thermocellum* transitions between prepared sugars and raw biomass as carbon sources.

In general, the results obtained from these transcriptomic studies are supported by similar proteomic studies that have directly interrogated protein levels under similar growth conditions. Expression of the core metabolic proteins, as predicted, reveals that they are primarily growth-phase dependent to position *C. thermocellum* for the most

efficient use of the nutrients on hand under growth and stationary phases, leading to much more consistent expression levels relative to specialized proteins such as those found in the cellulosome. Approximately a quarter of the 144 core metabolic proteins demonstrate only a moderate change in expression as the cells transition from exponential to stationary phase, with several notable exceptions including decreases in the presence of pyruvate synthesis machinery and increases in the prevalence of glycogen metabolism, pyruvate catabolism, and end product synthesis pathway proteins (213). Much more expression variability has been detected, and indeed much more research has been focused, on the proteins comprising the cellulosome. Unlike the relatively consistent expression of core metabolic proteins, cellulosome proteins demonstrate expression variability in response to changes in carbon source availability. When presented with cellobiose, hemicellulases are the most abundant cellulosome components, with XynA, XynC, XynZ and XghA up regulated alongside of the endoglucanase CelA and GH5 endoglucanases CelB, CelE, and CelG. Conversely, when presented with cellulose as a carbon source, the GH9 cellulases represented the most abundant group, along with the cell surface anchor protein OlpB and the exoglucanases CelS and CelK (214). These same trends continue to manifest when pretreated switchgrass is used as a feedstock, with the exoglucanase CelK and the GH9 cellulases further increasing in abundance relative to cellulose fermentation. Notably, under switchgrass utilization the xylanases decrease in prevalence, possibly due to removal of the majority of hemicellulose and reduction of xylan content in the switchgrass following dilute acid pretreatment (215). Importantly, it has also been noted that expression of many of the cellulosome proteins is decreased following adaption to increased ethanol tolerance. Indeed, while ethanol tolerant strains

can still degrade cellulose, both the rate and extent of this degradation is impaired due to this down regulated expression (216).

Compared to the genetic, transcriptomic, and proteomic studies that have been performed, there have been relatively few investigations regarding *C. thermocellum*'s metabolomics under laboratory or natural growth conditions. It is known, however, that, relative to cellobiose, growth on cellulose results in diversion of carbon flow into a transhydrogenase-malate pathway, resulting in increases to available NADPH and GTP supplies. Assimilation of ammonia is also up regulated under these growth conditions, resulting from an increase in the production of glutamate dehydrogenase as *C. thermocellum* repositions itself to produce the biosynthetic intermediates necessary to respond to cellulose utilization (217). Additional evidence suggests that the end products of this fermentative process can similarly alter metabolic activity as well. As ethanol and lactate collect, H_2 and acetate yields coordinately increase, while ethanol yields themselves are shown to increase upon accumulation of H_2, acetate, and lactate (194). In an effort to improve our knowledge regarding *C. thermocellum* metabolism, and to aid in the development of engineered strains, a flux balance model of *C. thermocellum* metabolism has recently been developed (218) that will hopefully aid in developing this nascent field.

2.2.2 Efforts to Enhance Ethanol Production from *C. thermocellum*

2.2.2.1 Development of engineered strains

In nature, *C. thermocellum's* main ecological function is to degrade cellulose, and in this regard, it is one of the fastest microcrystalline cellulose utilizers. This

characteristic has led to a series of studies that have robustly characterized its function in regards to the digestion of plant biomass (75, 161, 201, 203, 212, 215, 219), however, until recently there has been a deficit in our understanding of *C. thermocellum*'s genetic and proteomic functions that have hindered its development as an ideal CBP host. The recent attainment of a finished, annotated genome sequence and an enhanced understanding of its gene and protein expression, in combination with metabolic pathway models, has filled this gap and become essential for the development of targeted genetic engineering strategies and optimization of fermentation conditions that are needed to move forward in strain development. In a wider sense, these aspects have also been crucial for improving the feasibility of consolidated bioprocessing as a platform for production of biofuels as well (152, 194, 208, 210, 212, 213, 215, 218, 220-225).

To this end, several engineered strains have been developed using adapted or directed evolution to improve ethanol or inhibitor tolerance, as these traits have been deemed the most important for industrial applications (Table 10). Linville et al. reported the development of a mutant strain through direct evolution of *C. thermocellum* ATCC 27405 that displayed an enhanced growth rate and tolerance up to 17.5% vol/vol dilute acid pretreated poplar hydrolysate (226). Resequencing of the wild type and mutant strains indicated that multiple mutations were responsible for this phenotype, including genes related to cell repair and energy metabolism. Similarly, a wild type *C. thermocellum* culture was adapted through sequential passaging to tolerate 8% wt/vol (80 g/L) ethanol and several analysis were performed to determine the basis of this increased tolerance in the mutant strain, which was designated strain *C. thermocellum* EA. Proteomic analysis of this strain by Williams et al. showed changes in membrane-

associated proteins, leading them to hypothesize that the increased tolerance was the result of lower quantities and/or lower incorporation rates of proteins into the membrane, preventing increased fluidity upon ethanol exposure (216). Further analysis by Timmons et al. corroborated this hypothesis by observing changes in the fatty acid membrane composition that endowed the mutant strain with increased membrane rigidity, reducing the fluidizing effect of ethanol (165). Recently, Brown et al. resequenced the genome of the mutant strain and, in comparison to the wild type, identified the genetic basis of this tolerance as a mutation in the bifunctional *adhE* gene. This was then confirmed by recreating the mutation in the more genetically tractable DSM 1313 strain (227).

Table 10 – Natural and engineered *C. thermocellum* stains used for consolidated bioprocessing.

	Growth Conditions				Products					Efficiency			
Strain	Substrate	Medium	Temp (°C)	pH	Ethanol (g/L)	Acetate (g/L)	Lactate (g/L)	CO_2 (g/L)	H_2 (g/L)	Carbon Recovery	Yield (g/g)	Economic Feasibility	Reference
27405	0.3 % wt/vol Milled Filter Paper	EM	60	7.0	0.80	0.54	ND	ND	ND	ND	ND	Low	Lv and Yu et al., 2013
	Microcrystalline Cellulose (1% wt/vol)	BM7	60	6.0 - 7.5	1.09	1.49	2.43	ND	ND	ND	ND	Low	Tachaapaikoon et al., 2012
	^{15}N Cellulose (5 g/L)	MTC	58	6.8	1.34	1.17	ND	ND	ND	ND	0.50	Low	Raman et al., 2009
	^{14}N Cellulose (5 g/L)				1.27	1.16					0.49		
	Cellobiose (5 g/L)				1.02	1.43					0.49		
	Z-Trim® (5 g/L)				0.54	0.81					0.45		
	Cellulose-Xylan (5 g/L)				0.62	0.71					0.44		
	Cellulose-Pectin (5 g/L)				0.49	0.69					0.39		
	Celluose-Pectin-Xylan (5 g/L)				0.54	0.60					0.38		
	Pretreated Switchgrass (5 g/L)				0.32	0.60					0.37		
	Pretreated Switchgrass (5 g/L)	MTC	58	6.8	0.20	0.50	ND	ND	ND	ND	ND	Low	Wilson et al., 2013a
	Pretreated *Populus* (5 g/L)				0.30	0.80						Low	
	Avicel (5 g/L)	MTC	58	7.0	0.83	0.83	ND	ND	ND	ND	ND	Low	Raman et al., 2011
DSM 1313	Cellulose	CM3	60	7.8	0.96	0.75	0.38	1.20	0.04	0.88	ND	Low	Weimer and Zeikus et al., 1977
	Avicel (19.5 g/L)	MTC	55	7.0	1.32	2.74	2.49	ND	ND	0.72	ND	Low	Argyros et al., 2011
	Cellobiose (5 g/L)	Rich media	55	7.0	0.68	1.10	0.25	ND	ND	ND	ND	Low	Tripathi et al., 2010
	Avicel (5 g/L)				0.70	1.10	0.05						
CS7	0.3 % wt/vol Milled Filter Paper	EM	60	7.0	0.79	0.32	ND	ND	ND	ND	ND	Low	Lv and Yu et al., 2013
CS8	0.3 % wt/vol Milled Filter Paper				0.83	0.43	ND	ND	ND	ND	ND	Low	Lv and Yu et al., 2013
S14	Microcrystalline Cellulose (1% wt/vol)	BM7	60	6.5 - 7.0	1.90	3.72	0.74	ND	ND	ND	ND	Low	Tachaapaikoon et al., 2012
YS	Cellulose	CM3	60	7.3	1.40	1.90	ND	ND	0.10	ND	ND	Low	Lamed et al., 1988
	Cellobiose				1.20	1.80			0.10				
LQRI	0.4% wt/vol Cellulose	GS	60	7.0	0.71	0.96	0.31	1.33	0.05	≥ 0.80	ND	Low	Ng et al., 1981
	0.4% wt/vol Glucose				0.75	0.89	0.22	1.21	0.04				
	0.4% wt/vol Cellobiose				0.72	0.74	0.21	1.52	0.06				
	Cellulose	CM3	60	7.3	0.90	2.90	ND	ND	0.20	ND	ND	Low	Lamed et al., 1988
	Cellobiose				0.90	3.00			0.20				
JW20	1% (wt/vol) Cellulose	Minimal Media	58 - 61	6.1 - 7.5	0.61	1.21	0.43	2.38	0.14	0.87	ND	Low	Freier et al., 1988
BC1	Cellulose, glucose, sorbitol	ND	67	ND	ND	ND	ND	ND	ND	ND	ND	Low	Koeck et al., 2013
M1570	Avicel (19.5 g/L)	MTC	55	7.0	5.61	0.16	0.11	ND	ND	0.61	ND	Low	Argyros et al., 2011

NR: Not reported in the original publication.

Isolation of additional *C. thermocellum* strains is also ongoing, with the novel CS7, CS8, and S14 strains being isolated from compost and bagasse paper sludge, respectively (228, 229). Interestingly, when the CS7 and CS8 strains were characterized for growth on crystalline cellulose and cellobiose, in contrast to many *C. thermocellum* strains, neither exhibited any xylanase activity. However, both of these strains demonstrated increased ethanol:acetate ratios and enhanced cellulase activity in comparison to the wild type strain. Strain S14 also proved to be notable, as its cellulosomal glycoside hydrolases provided increased crystalline cellulose degradation rates relative to both the wild type and to strain JW20. In addition, strain S14 was found to tolerate both a higher temperature (70°C) and pH (9.0) than the wild type while consuming a broader range of substrates including sorbitol. However, as of yet, CS7, CS8, and S14 do not have draft genome sequences, which will be crucial for the development of genetic or metabolic engineering approaches in these strains.

Draft or finished genome sequences are, however, currently available for six *C. thermocellum* strains including the wild type (ATCC 27405), YS, LQRI, JW20, BC1, and DSM 1313 (166, 206, 207, 212). *C. thermocellum* YS was isolated from hot springs at Yellow Stone national park and has been characterized as a highly efficient cellulose utilizer. Notably, it is this strain, in tandem with the adherence-defective mutant *C. thermocellum* AD2 strain, that was used in the studies that reported the initial description of the adherence of *C. thermocellum* to insoluble cellulose substrate and paved the way for the discovery of the cellulosome (176, 177). Strain YS has since been leveraged for multiple studies reporting on the digestion of lignocellulosic feedstocks, cell surface interactions, the structure and function of the cellulosome, and transcriptomic evaluations

in response to plant biomass hydrolysis (178, 230-234). *C. thermocellum* JW20 was isolated from a cotton bale in Louisiana and LQRI was isolated from a contaminated culture of strain DSM 1313, which at the time was referred to as LQ8 (207, 235, 236). The growth and physiological properties for each of these strains have since been characterized (235, 237), with strain JW20 demonstrating the ability to utilize a spectrum of growth substrates ranging from crystalline cellulose to lignocellulosic feedstocks, including pretreated hardwood, straw, and hay (160). Most recently, *C. thermocellum* BC1 was isolated from a compost treatment site in Germany, and a draft genome sequence has been established (238). This strain has exhibited improved cellulose hydrolysis and utilization of a wider range of substrates, including glucose and sorbitol, at a higher temperature (67°C) than the wild type strain. The diversity of unique characteristics demonstrated by these strains, and the important contributions they have made towards improving *C. thermocellum*'s position as a relevant CBP host, highlight the importance of continuing to isolate, characterize, and compare new strains that may have advantageous characteristics for CBP applications.

C. thermocellum DSM 1313, previously known as *C. thermocellum* LQ8, represents arguably the most important of the strains discovered to date. First isolated in 1926 by Viljoen et al. from manure or soil (154), it has been widely studied for its cellulolytic and physiological properties, and has been characterized on cellobiose, microcrystalline cellulose, and lignocellulosic feedstocks (239, 240). However, DSM 1313's high utility comes from the establishment of its draft genome sequence in 2011 and the subsequent development of a genetic system for its transformation that has allowed for the construction of mutant strains (166-170). This ability has allowed

investigators to target specific genetic changes within the DSM 1313 background, leading to an unparalleled ability to interrogate the genetic basis for observed phenotypes and to develop strains endowed with specific, engineered functions.

In one such study, comparisons were drawn to previous investigations focusing on the use of proteomic analysis and global gene expression data to enhance understanding of *C. thermocellum's* highly efficient cellulosomal hydrolysis of cellulose and hemicellulose. These initial investigations demonstrated that the catalytic sub-units of the cellulosome were assembled based on their substrate and growth rate (212, 215), allowing researchers to create mutant strains of DSM 1313 with knockouts of the *cel48S* gene, that encode an abundant and up regulated cellulase during growth on microcrystalline cellulose, in order to investigate its role in hydrolysis (141). Using this targeted approach, they determined that the deletion of *cel48S* reduced growth rate and specific activity by 2-fold, however, also discovered that it was still able to completely solubilize a 10 g/L loading of Avicel. Without the ability to establish this targeted mutation, it would be difficult, if not impossible, to hypothesize this retention of biomass utilization efficiently in light of such a deleterious mutation. Furthermore, these studies are also important in advancing the creation of designer multi-enzyme complexes for industrial applications (141, 214, 215, 241), as was highlighted by the recent improvement in hydrolysis performance achieved by Gefen et al. through targeted cellulosome engineering, resulting in a three-fold increase in microcrystalline cellulose hydrolysis and a two-fold improvement for switchgrass hydrolysis (190).

Mutational strain development has also been leveraged to increase ethanol titer and tolerance towards the minimum value of 40 g/L that is required for the economic viability

of cellulosic ethanol production (142, 143). While wild type *C. thermocellum* strains only produce < 3 g/L and are tolerant to < 16 g/L of ethanol (145, 242), mutant strains constructed through adapted evolution have shown ethanol tolerance up to 80 g/L, albeit with inconsistent and slow growth, and up to 50 g/L with stable growth (216, 227). To achieve these results, mutant strains of DSM 1313 were constructed with disrupted end product fermentation pathways that altered their natural carbon flow and, conversely, increased their ethanol yield (167, 243-245). These strains were established through mutations in their acetate and lactate pathways (Δ*hpt* Δ*ldh* Δ*pta*), however, once subsequently evolved, they produced contrasting results in their effect on ethanol yield. In one case, no increase in ethanol yield was observed following mutation (245), while in a separate report a 4-fold increase was detected (243). However, in both cases it was hypothesized that the mutations led to a redox imbalance because of the secretion of pyruvate and amino acids into the fermentation broth, low product yields, unsubstantial increases in ethanol, and resulting open carbon balances. In an attempt to reconcile these reports, Mohr et al. used a thermotargetron approach to disrupt the acetate and lactate pathways in place of the homologous recombination approach used by Arygros and van der Veen, resulting in a decrease to lactate and acetate production, a slight increase in ethanol production and a 6-fold increase in pyruvate production (167).

Building upon these studies, Deng et al. noted that pyruvate kinase had not been annotated in the DSM 1313 genome sequence and did not register during enzymatic assays. This led them to the hypothesis that a malate shunt was being used to convert phosphoenol pyruvate to pyruvate (244). Leveraging the genetic tractability of DSM 1313, they improved ethanol yield by expressing an exogenous pyruvate kinase and

deleting the malic enzyme gene in the lactate and acetate pathway deficient strain. As a result, their novel mutant strain achieved an approximately 3-fold higher ethanol yield, increased carbon recovery, increased formate production, increased ethanol tolerance, and decreased amino acid secretion relative to the parent strain. The sheer number of mutations and genetic knowledge required to achieve this goal perfectly demonstrates the necessity of obtaining a fundamental understanding of gene expression, regulation, redox state, carbon catabolism, and metabolic modeling, and the prerequisite of establishing a functional genetic manipulation system that must be obtained prior to the development of mutant strains for use in CBP settings (145, 218).

2.2.2.2 Co-culture of *C. thermocellum* with other microorganisms

In addition, to the development and isolation of additional *C. thermocellum* strains, it is worth noting that there are naturally highly efficient cellulolytic consortia and mixed cultures of *C. thermocellum* that can be employed as well. However, significant difficulties exist in engineering these populations towards the production of their desired fermentation products at high yields for industrial applications. Nonetheless, these populations still pose a high value in that they can be mined for novel cellulolytic microorganisms (223, 246-250). While consortia and mixed-cultures will not be covered in depth in this review, defined co-cultures containing *C. thermocellum* have previously been studied for the digestion of lignocellulosic biomass (223, 235, 251-255) and have recently been reviewed elsewhere (145). In general, these co-cultures are utilized due to *C. thermocellum*'s unique ability to hydrolyze hemicellulose and cellulose utilizing only the cellodextrin breakdown products and forgoing the consumption of C_5 sugars (163, 256), making it amenable to co-culture with pentose utilizing thermophiles. Notably, the

highest ethanol titer yet reported for the fermentation of microcrystalline cellulose has been obtained under these conditions, with the co-culture of a metabolically engineered *C. thermocellum* and *Thermoanaerobacterium saccharolyticum*. This fermentation achieved approximately 80% of theoretical ethanol yield at 38 g/L, and was able to keep organic acid concentrations below their detection limits (243), demonstrating the utility of this type of approach.

2.2.3 Tools for Genetic Manipulation

The evolution and selection of naturally occurring *C. thermocellum* strains has provided an initial springboard for development of more industrially relevant organisms, however, the full realization of this effort requires targeted development and optimization of specific characteristics that will enable *C. thermocellum* to function synergistically towards the production of fuels and chemicals from cellulosic biomass. While development of the tools required for the genetic manipulation of *C. thermocellum* is still in its infancy, significant strides have already been made to enable the introduction of exogenous DNA (257) and selection of successfully modified strains (258). The utilization and expansion of these efforts will be key to achieving *C. thermocellum*'s full potential as a CBP host (259).

2.2.3.1 Methods for introducing foreign DNA

The primary method for introducing DNA into *C. thermocellum* has been through electroporation. This method, which transiently applies an electrical field to generate openings on the cell surface for the introduction of DNA, has been successfully demonstrated for several available strains (ATCC 27405, DSM 1313, and DSM 4150)

and has been optimized specifically for strain DSM 1313 (170). Particularly of note for the application of this technique to *C. thermocellum* transformation is the relationship between current oscillation and transfection efficiency. Tyurin et al. have demonstrated a one-to-one correspondence between the presence of 24 MHz oscillations and successful transformations, noting that the proper oscillations can be achieved by using a > 12 kV/cm field strength during transformation. This field strength was itself noted to contribute significantly to transformation optimization as well, with increasing field strengths up to 25 kV/cm producing higher efficiencies (260). Using this technique, it has been possible both to present exogenous genes for expression and to introduce genetic modification systems capable of altering the native *C. thermocellum* genome and knocking out endogenous loci (168).

2.2.3.2 Genetic Delivery systems

Three basic strategies exist for the genetic modification of *C. thermocellum*. The first of these simply places additional genetic material into the organism for expression, ideally adding functionality or complimenting a deficiency in order to better prepare the organism for its intended task. Under this strategy, plasmid DNA is introduced using the electroporation approach discussed above. Depending upon the design of the introduced vector, the gene of interest is then either expressed directly from the plasmid or incorporated into the host genome and replicated along with the endogenous DNA during routine cell maintenance. For plasmid-based expression, in addition to the gene of interest, the plasmid must also contain an origin of replication and a selectable marker. There are several selection markers available (discussed below) but, in general, the thermophilic RepB origin of replication is the most prevalent for use in *C. thermocellum*.

This origin, which works via rolling circle replication, has also been synthetically modified to generate a temperature sensitive variant that cannot function above 55°C. This provides an additional layer of flexibility that can be utilized for controllable expression of the novel DNA sequence being added (261). It is also possible to integrate the target DNA sequence directly into the genome through the incorporation of homologous loci up- and downstream of the gene of interest. Under this design, once the construct is successfully introduced the homologous regions can permit recombination for the gene of interest into the *C. thermocellum* genome. This forgoes the need to maintain an additional plasmid within the host, but requires the remaining plasmid DNA to be cured following genetic introduction. Either of these two approaches is equally acceptable, and their utilization is usually made on a case-by-case basis following careful assessment of the experimental design.

The second system performs the opposite function by permitting the removal of endogenous genes from the *C. thermocellum* genome. This plasmid-based strategy can be performed either by replacing the targeted deletion gene with a selectable marker, or by a multi-step process that allows for gene removal followed by marker removal. While the former is a much quicker process, the latter allows for the recycling of selectable markers and therefore permits additional downstream modifications to occur (Figure 6). For retention of the selective maker, 5′ and 3′ flanking regions that match 500 – 100 bp of the 5′ and 3′ flanking regions of the deletion target are designed and placed up- and downstream of the marker. The 5′ flanking region/selective maker/3′ flanking region cassette is then introduced into the cell where the selective maker is homologously recombined in place of the target gene (168). For marker free gene removal, the 5′ and 3′

flanking regions are both placed upstream of the *cat* and *hpt* selection makers (described in detail below) and a third region, which is referred to as the "int region" and is homologous to a 500 – 1000 bp region of the gene of interest, is placed downstream of the selection markers. In this multi-step process, an initial selection is performed to isolate strains that have achieved homologous recombination at the 5′ flanking and int regions, which successfully replaces a portion of the gene of interest with the remaining 3′ flanking region and *cat* and *hpt* selection markers. A second selection is then made to remove these markers (and the remaining portion of the gene of interest) and isolate the subset of strains that have performed a second homologous recombination event between the two 3′ flaking regions that are now present on the chromosome. This second recombination will successfully remove all exogenous material, leaving only the 5′ and 3′ flanking regions on the chromosome, with no genetic material between them (243). Because this method allows the selective makers to be reused, it is often utilized over the alternative method, despite its additional investment in time and resources.

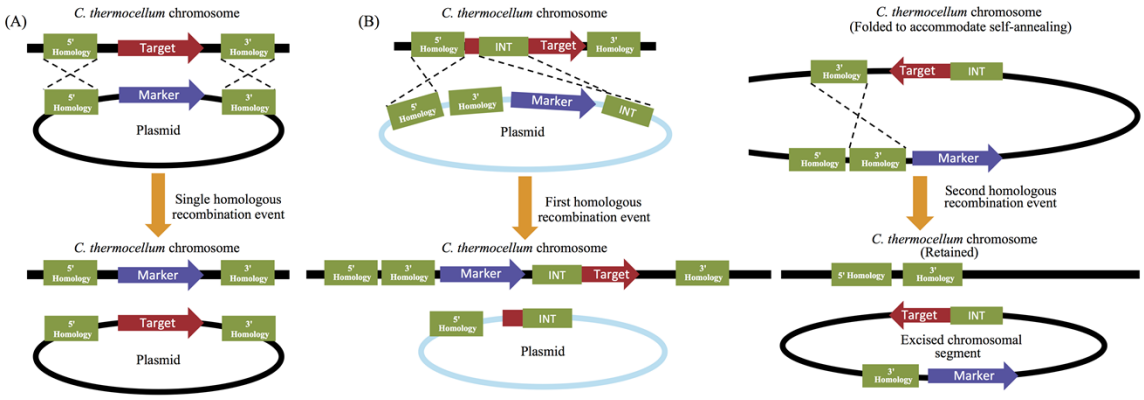

Figure 6 Targeted gene deletions that (A) retain their selection markers can be performed quickly using only a single homologous recombination step, while strategies that (B) remove the marker and allow it to be reused for subsequent genetic manipulations require multiple rounds of homologous recombination and selection.

The third, and newest of the approaches, leverages the function of a mobile group II intron, often referred to as a "targetron," from *Thermosynechococcus elongatus* to knock out expression of an endogenous gene via the insertion of a non-coding intron into the native sequence. The advantage of this strategy is that the intron can be engineered by the researcher to insert at any desired location within the genome by including short, homologous sequences flanking the intron that will be used to direct it to its intended location within the genome. In addition to these regions of homology, an intron encoded reverse transcriptase protein is required that aids in locally melting the target region of the chromosome and facilitating the insertion of the intron sequence. Fortuitously, because of the thermophilic temperatures present during the culture of *C. thermocellum*, the function of this secondary protein product is minimized and the homology of the targeting regions becomes the most important factor regulating insertion efficiency. The plasmid containing these required sequences is incorporated into the organism using standard electroporation techniques, but then does not require any additional cofactors in order to function. When deployed in *C. thermocellum*, this approach was able to knock out six chromosomal genes with efficiencies ranging from 67 – 100%, resulting in the development of a lactate dehydrogenase deficient strain with increased ethanol production (167). The development of this system to function in thermophilic bacteria, and *C. thermocellum* in particular, is a promising development that will hopefully significantly improve the ease with which mutant strains can be developed.

2.2.3.3 Selection of Modified Strains

A key component of any genetic modification strategy is the ability to select for the resulting altered strain at the conclusion of the procedure. Although not nearly as

many markers are available as are for mesophilic bacteria such as *E. coli*, a host of selection markers are available and have been validated in *C. thermocellum*. For negative selection, expression of the Thymidine kinase (*tdk*) or Hygromycin phospotransferase (*hpt*) markers may be used to provide resistance against 5-fluorodeoxyuridine and hygromycin, respectively. Of these, *tkd* is often preferred since *C. thermocellum* has an endogenous *hpt* homolog, and thus requires an *hpt* deficient genetic background for proper function(168). The chloramphenicol acetyltransferase (*cat*) and aminoglycoside phosphotransferase (*neo*) markers can be similarly employed for positive selection, however, the former is preferred as the latter has been demonstrated to inhibit growth at the expression levels required for selection (141). An additional maker, orotidine 5-phosphate decarboxylase (*pyrF*) can also act as either a positive or negative selection maker. On the one hand, expressing the *pyrF* gene in a *pyrF* deficient host makes it possible to compliment a uracil auxotroph and select only for strains actively expressing the maker. On the other hand, treatment of *pyrF*-expressing strains with 5-fluoroorotic acid will lead to cellular death as those harboring the gene will incorporate it as a toxic uracil analog(169). Used together, these markers allow researchers to select and modify strains in efforts to further engineer *C. thermocellum* for the optimized production of high value products.

2.2.4 Future Directions

Although ethanol has been the focus of this review, *C. thermocellum* produces several additional fermentation products that may have value in a variety of industries. The production optimization of these pathways can serve to position *C. thermocellum* as a key industrial organism on par with existing models such as *S. cerevisiae*. One

potential route for initial optimization is the production of hydrogen, which can serve as a potential energy source for combustion engines or fuel cells when produced in sufficient quantities. Five strains of *C. thermocellum* (1237, 1313, 2360, 4150, and 7072) have already been evaluated to assess their efficiencies in hydrogen production after using microcrystalline cellulose as a feedstock. Under these conditions, yields ranged between 0.7 - 1.2 mol of hydrogen per mol of glucose (262). Acknowledging this potential for hydrogen generation, additional recent studies have investigated the steps involved in *C. thermocellum*'s hydrogen synthesis pathways (263) and evaluated inclusion of an electrohydrogenesis stage (264) to boost hydrogen production.

In addition to hydrogen, lignocellulosic biomass remains an attractive starting material for the production of lactic acid, formic acid, and acetic acid using *C. thermocellum*'s natural fermentation pathways. By mimicking the action of existing lactic acid bacteria or the fungus *Rhizopus oryzae*, which have previously been demonstrated to produce lactate using corn starch biomass (265), it would be possible to assemble the basic units for a variety of high value bio-based polymers. Similarly, while methanol carbonylation is currently used to synthesize the majority of acetic acid (266), this process could also be offloaded to *C. thermocellum* under the appropriate CBP conditions. Regardless, the success of these processes will rely heavily on several factors, such as the existing limitation regarding lactic acid (262) and formic acid (267) yields, which are currently inversely related to hydrogen production.

Similarly, the production of butanol from lignocellulosic biomass using a CBP platform is another attractive option because butanol, which is more similar to gasoline than ethanol, has a higher energy density, and can be mixed with gasoline at higher ratios.

Unfortunately, all *Clostridium* spp that naturally produce butanol are non-cellulolytic, and only two, *Clostridium acetobutylicum* and *Clostridium beijerinckii*, have been studied in detail (268). Moving towards this goal of butanol production, there have been a series of studies utilizing co-cultures of *C. thermocellum*, and it has recently been reported that a co-culture of *C. thermocellum* and *Clostridium saccharoperbutylacetonicum* N1-4 can produce up to 7.9 g/L butanol in 9 days using microcrystalline cellulose as a carbon source (269). Moreover, the recent development of a transformation system for *C. thermocellum* has led to research efforts aimed at engineering *C. thermocellum* with new pathways to produce butanol as well (270). Through these, and other related pathway studies, it may one day be possible to shift all of *C. thermocellum's* natural array of products towards industrial scale production.

2.3 The Cellulosome

The cellulosome introduces a distinguishing level of synergism between enzymes in *C. thermocellum* as compared to other CBP microorganisms; however, the enzymes used are nonetheless similar to those that have presented difficulties in the conversion of biomass to ethanol but are fashioned in an unusual manner. Although CBP is a promising, alternative route to ethanol production, the same features that have been linked to recalcitrance in the former technologies will remain problematic. To confirm the role of recalcitrance in limiting CBP, structural differences between the solid residuals that remain following CBP and the original structural features of biomass will be evaluated.

2.4 Plant Cell Wall Architecture and Its Influence on CBP

Cellulose, hemicellulose, and lignin are among several components of biomass that contribute to the many layers of complexity during biomass deconstruction. Each polymer possesses its own set of attributes that may hinder the progression of enzymatic hydrolysis, depending on how the traits are organized. These attributes are often confounded and present difficulties in pinpointing, and therefore addressing a single cause of recalcitrance. Nonetheless, analyzing these features offers useful guidance in the development of feasible strategies to overcome recalcitrance.

2.4.1 *Cellulose and CBP*

Cellulose contains three possible contributors to recalcitrance: its degree of polymerization (DP), crystallinity, and accessibility. Cellulose DP indicates cellulose chain length and may influence enzymatic actions. During enzymatic hydrolysis with fungal cellulases, endoglucanases randomly hydrolyze cellulose and are largely responsible for the drop in DP (271). The newly created reducing ends are starting points for hydrolysis with exoglucanases, which typically cleave cellulose to a DP of six or seven (272). β-glucosidases carry out the last stage of hydrolysis to form glucose from the insoluble exoglucanase hydrolysis products.

Generally, shorter chain cellulose is hypothesized to be less recalcitrant than longer chain cellulose for fungal enzyme cocktails as longer cellulose chains contain more hydrogen bonds and fewer reducing ends. Yet, studies report varied relationships (272, 273). The relationship between recalcitrance and cellulose DP during CBP with *C. thermocellum* remains even more obscure as only two known studies suggest the utilization of short chain cellulose before longer chain cellulose (274, 275).

Amorphous and crystalline regions in cellulose microfibrils arise from the number of hydrogen bonds between individual cellulose molecules (Figure 7). Fewer intrachain hydrogen bonds result in amorphous regions of cellulose, while larger numbers of intrachain hydrogen bonds result in crystalline areas. Accordingly, amorphous cellulose is more hydrophilic than crystalline cellulose as there are more hydroxyl groups available to participate in hydrogen bonding. Lower cellulose crystallinities are generally viewed as favorable and may be related to better cellulase adsorption abilities, enhanced moisture uptake, increased surface areas, and better accessibilities to facilitate hydrolysis (276). A number of reports argue that cellulose crystallinity is strongly associated with recalcitrance (200, 277, 278). Sathitsuksano et al. altered the crystallinity of switchgrass with a solvent-based pretreatment and achieved an 89% increase in digestibility (277). In a separate study, an ionic liquid pretreatment decreased cellulose crystallinity from 26.2% to 2.6%, resulting in 96% cellulose solubilization in 24 hrs (279). Nonetheless, a few studies regard cellulose crystallinity as negligible (273).

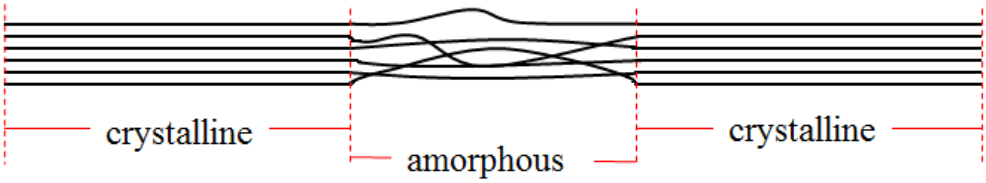

Figure 7 Illustration of the crystalline (ordered) and amorphous (disordered) regions of cellulose

During CBP, it is widely accepted that *C. thermocellum* rapidly converts microcrystalline cellulose (Avicel) (83, 201); however, no known research has identified the driving force for this occurrence as Avicel has a low DP (~250) in conjunction with high crystallinity (~65%) [data not shown]. Nonetheless, cellulose crystallinities that are

close to 100% negatively influence *C. thermocellum*. Cellulosomes isolated from *C. thermocellum* degraded bacterial cellulose ribbons, which were 75% crystalline, in 24 hrs. Conversely, *Valonia* cellulose, which is almost 100% crystalline, required 16 days to attain 95% solubilization (280).

Lastly, cellulose accessibility describes the cellulose surface area that is available for enzymatic hydrolysis and may play a large role during enzymatic hydrolysis. For example, fully hornified cellulose experienced 94% reduction in enzymatic hydrolysis compared to its never dried counterpart (281). Pretreatments often alter cellulose accessibilities by removing or restructuring hemicellulose and/or lignin and changing the cellulose structure (i.e. crystallinity, DP, etc.). Accordingly, accessibility studies are commonly conducted with pretreated substrates (282-284). The accessible surface area is predominantly rooted in the cellulose fiber dimensions and porosity. Porosity, in particular, promotes or restricts synergy between enzymes; however, *C. thermocellum* carries out deconstruction at the surface of biomass (285), which may negate the relevancy of accessibility. Dumitrache et al. hasdefined accessibility for *C. thermocellum* in terms of the surface area available for microbial colonization and found that the most accessible biomass was associated with the best hydrolysis properties (285). It is unclear which structural properties contributed to this occurrence, though.

2.4.2 *Hemicellulose and CBP*

Hemicelluloses can be structurally complex carbohydrates that possess several attributes that may be linked to recalcitrance. For instance, the hemicellulose xylan participates in unproductive enzyme binding with approximately one quarter of added

cellulases (286), which may explain xylan's inhibitory effect towards cellulases (287, 288). Hemicellulose substitution, particularly acetylation and methyl esterification, (289, 290), DP (103), composition (291) and content (292, 293) have also been recognized as contributors to recalcitrance. There are minimal known studies surrounding *C. thermocellum* and difficulties in hydrolysis due to hemicellulose. Though little is known, it appears that *C. thermocellum* degrades high DP (15 to 40 units) xylan first during hydrolysis (196) and converts ~10% more glucan in the absence of hemicellulose (201).

2.4.3 *Lignin, Recalcitrance, and CBP*

Lignin's role in recalcitrance (294-296) is relatively well-characterized compared to cellulose and hemicellulose. Lignin adsorbs to enzymes and engages in nonproductive enzyme binding, thereby reducing the available cellulase concentrations. Binding interactions are influenced by lignin structure. For example, G lignin binds more strongly to cellulases than S lignin (297). Additionally, lignin's adsorption capacity towards cellulases have been enhanced following the liquid hot water pretreatment as its surface charge was more negative (298). Lignin may also serve as a physical barrier to enzymes by reducing the available surface area. Studies have acknowledged that lignin S/G ratio (299) and content (299-302) shape progression of enzymatic hydrolysis. As lignin-related obstacles are identified, countless technologies are introduced to combat them. Surfactants have been introduced to alleviate lignin adsorption onto cellulases (303, 304), while modified pretreatments have been used to lower the concentration of lignin-derived inhibitors present in pretreated materials (305). Others carry out genetic manipulations to alter the lignin structure or content to facilitate enzymatic hydrolysis

(295, 306, 307). In *C. thermocellum*, at least two studies suggest that high lignin contents (308, 309) and low S/G ratios (275) appear to be detrimental to CBP.

2.4.4 *Structural Analysis to Identify Recalcitrant Features of Biomass*

While a number of assays can be run to assess these polymers and their structures, tests in this particular setting must rapidly and precisely analyze high sample volumes with mg sample quantities. Typically, these analyses characterize one or more structural features of biomass and pair the results with enzymatic hydrolysis data to identify how structure influences the rate of hydrolysis. Structural features that cause depressions in enzymatic hydrolysis rates likely contribute to recalcitrance. Ideally, these studies should pinpoint one structural feature in whole biomass that contributes to recalcitrance; however, it is difficult to separate the many contributors to recalcitrance from one another without isolation. Nonetheless, there are several chromatographic and spectroscopic tools that are used to assess the structure of biomass and relate the findings to the progression of enzymatic hydrolysis and CBP.

2.4.4.1 Isolation for Characterization using Wet Chemistry

Prior to analysis, wet chemistry is regularly required to isolate lignin, cellulose, and hemicellulose to expedite their subsequent characterizations. Following isolation, these polymers can be further treated (i.e. derivatized, dissolved, etc.) to prepare them for instrumental analysis. In certain circumstances, wet chemistry is also used quantify biomass components as in the determination of Klason lignin contents (310). In brief, these wet chemistry methods utilize processes such as delignification and carbohydrate removal with enzymes.

2.4.4.2 Molecular Weight Analysis by Gel Permeation Chromatography

Following cellulose, hemicellulose, or lignin isolation, these polymers are analyzed to establish their role in recalcitrance. Lignin, cellulose, and hemicellulose use a host of instrumentation (5, 40, 311) that can provide molecular weights; however, gel permeation chromatography (GPC) remains an attractive tool as it offers a relatively rapid assessment of a wide range of molecular weights with mg quantities of starting material (5). GPC, which uses a column filled with a porous packing material, separates polymers based on their hydrodynamic radii. Larger polymers are excluded from smaller pores and travel through the column quickly, whereas smaller polymers travel through more pores and experience extended travel times. In order to convert the elution time into molecular weights, the operator must construct a calibration curve that correlates known molecular weights with elution time. For biomass-derived polymers, the calibration curve uses either polystyrene or pullulan standards, depending on the mobile phase.

Polymers may require derivatization prior to dissolution in the mobile phase. Hemicellulose does not require derivatization in aqueous solvents, whereas lignin and cellulose may or may not. Derivatization offers benefits such as reduced association effects, which are often observed in underivatized lignins (312, 313), and improved solubility. Nonetheless, studies have been conducted that eliminate the need for cellulose and lignin derivatization, which may have advantages over the traditional methods. Cellulose dissolution, for example, in dimethylformamide and the ionic liquid 1-ethyl-3-methylimidazolium acetate reduced typical sample preparation times for a GPC from days to a few h (314). Acetobromination has also been found to improve lignin solubility

for GPC (313). Acetylated Norway spruce milled wood lignin (MWL) required six days to achieve 60% dissolution in THF; however, acetobromination achieved complete dissolution in glacial acetic acid in the same time frame (313). Ultimately, the decision to derivatize the polymers depends on each individual study's needs.

After sample preparation methods and the appropriate testing parameters have been selected, molecular weight data can be obtained. Molecular weight data is described in terms of the number-average molecular weight (Mn), the weight average molecular weight (Mw), and the polydispersity index (PDI). Mn describes the average molecular weights of the polymer chains. Mw provides a similar estimation of the average molecular weight, except the average is skewed towards heavier chain polymers. PDI is a measure of the range of molecular weights. Each parameter is calculated according to equations 1, 2, and 3, respectively.

$$\overline{Mn} = \frac{\sum M_i \times n_i}{\sum n_i} \tag{1}$$

$$\overline{Mw} = \frac{\sum M_i^2 \times n_i}{\sum M_i \times n_i} \tag{2}$$

$$PDI = \frac{M_w}{M_n} \tag{3}$$

2.4.4.3 Attenuated Total Reflectance-Fourier Transform Infrared Spectroscopy (ATR-FTIR) and Solid-State Nuclear Magnetic Resonance Spectroscopy (NMR) to Assess Cellulose Crystallinity

Unlike molecular weight analysis which is applicable to all three polymers, crystallinity measurements pertain to cellulose alone. Similar to molecular weight analysis, there are several instrumentation available to quantify crystallinity (315). Attenuated total reflectance Fourier-transform infrared spectroscopy (ATR-FTIR) and solid-state nuclear magnetic resonance spectroscopy (NMR) are two types of instrumentation available to characterize crystallinity and offer numerous advantages for cellulose crystallinity estimations.

ATR-FTIR identifies particular bonds that are present within cellulose to calculate the lateral order index (LOI), an estimate of cellulose crystallinity. ATR-FTIR minimizes sample preparation and can provide results within minutes, depending in the number of scans, with high reproducibility. During analysis, an infrared beam is directed towards the crystal accessory such as a diamond or germanium at an angle. The beam is totally reflected and generates an evanescent wave that penetrates the material of interest and subsequently becomes weakened. The evanescent wave then returns this energy to the infrared beam, which travels to the detector to form the infrared spectrum. A representative cellulose spectrum is presented in Figure 8, and Table 11 outlines select peaks in the cellulose structure located in the ATR-FTIR spectrum (316). The peaks at 1430 and 898 cm^{-1}, which are sensitive to crystallinity changes, are used to calculate the LOI (317).

Table 11 – Select functional groups in cellulose, hemicellulose, or lignin and their bond assignments

Wavenumber (cm^{-1})	Functional group
3570-3200 (broad)	H-bonded O-H
2970-2950 and/or 2880-2860	Methyl C-H asymmetric/symmetric bend
2850-2815	Methoxy, C-H stretch
1615-1580	Aromatic ring stretch
1510-1450	Aromatic ring stretch
1470-1430 and 1380-1370	Methyl C-H asymmetric/symmetric bend
~1200	Phenol, C-O
~1100	Secondary alcohol, C-O
~1050	Primary alcohol, C-O
900-670 (multiple)	Aromatic C-H out-of-plane bend

Coates, J. (2006). Interpretation of Infrared Spectra, A Practical Approach. Encyclopedia of Analytical Chemistry, John Wiley & Sons, Ltd.

Solid-state NMR generates a ^{13}C NMR spectrum that quantifies cellulose crystallinity with the cellulose crystallinity index, or CrI (%). While the sample preparation efforts are similar to those needed for ATR-FTIR, solid-state NMR requires lengthier times for data acquisition. Solid-state NMR has been recognized as a highly accurate measure for cellulose crystallinity relative to other methods (315, 318) and can provide more complex information than about crystalline structure than ATR-FTIR, if desired. Solid-state NMR differs from solution-state NMR in that anisotropic interactions

between nuclei broaden peaks; however, rapid spinning at the magic angle 54.74° helps to relieve the broadening. Additionally, spectral quality is improved with increases in the signal-to-noise ratio with cross-polarization, where polarization from abundant nuclei such as ^{1}H can be transferred to less abundant nuclei like ^{13}C.

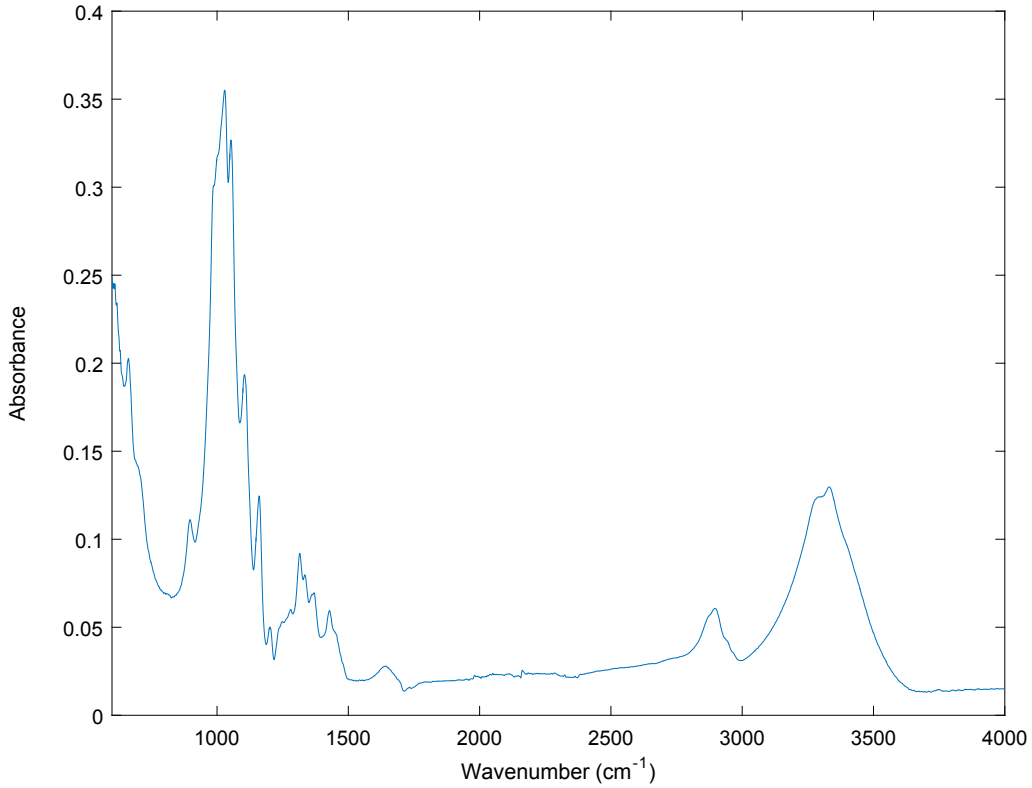

Figure 8 A representative cellulose ATR-FTIR spectrum of Avicel pH 101

The ^{13}C CP/MAS spectrum of cellulose contains seven peaks; however, the calculation of CrI (%) requires the area attributed to C4 in the glucose monomer, which yields two peaks during analysis (Figure 9). These peaks occur at $A_{79\text{-}86\ ppm}$ and $A_{86\text{-}92\ ppm}$, which represent amorphous and crystalline cellulose, respectively. CrI (%) is

determined from the below equation, which computes a percentage from the total amorphous and crystalline character of cellulose:

$$CrI(\%) = \frac{A_{86-92\,ppm}}{A_{79-86\,ppm} + A_{86-92\,ppm}} \times 100 \quad (4)$$

In sum, both ATR-FTIR and ^{13}C CP/MAS are effective methods for characterizing cellulose structure (273, 319-324).

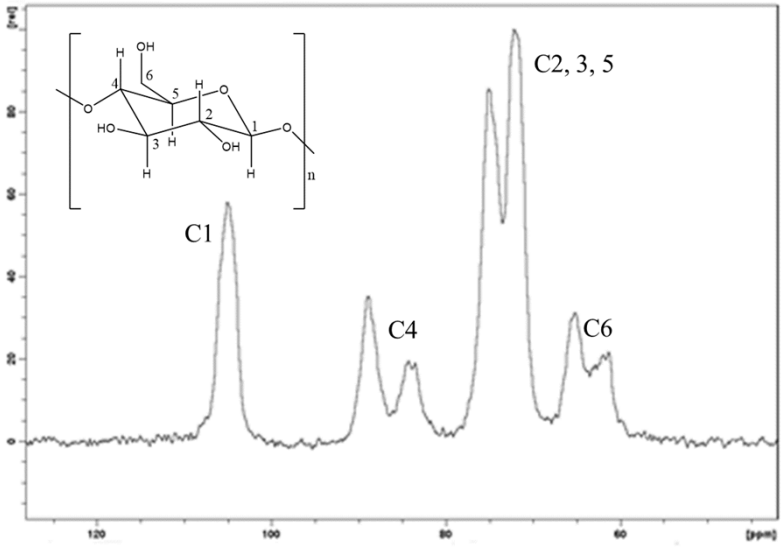

Figure 9 ^{13}C NMR spectrum of cellulose with hemicellulose removed by acid hydrolysis

2.4.4.4 Accessibility Assessment with the Simons' stain technique

Common ways to asses cellulose accessibility include water retention values (WRV) (325), the Brunauer-Emmett-Teller method (BET) (326), the Simons' stain (327), and other methods (328). Recent advances have even led to the use of the TGC protein, which contains a cellulose-binding module and a green fluorescence protein, to determine accessibility via its binding capability to cellulose (281, 282, 329). The Simons' stain is a

simplistic semi-quantitative assessment of accessibility that uses two aqueous dyes and an ultraviolet spectrophotometer, or UV-Vis. Simons' stain has several advantages over other test methods. Unlike a number of other methods that measure accessibility, Simons' stain works on both wet and dry samples. Additionally, methods such as BET and WRV risk overestimating accessibility as the sizes of nitrogen and water are much smaller than cellulases (281).

Direct Orange 15 (DO 15) and Direct Blue 1 (DB 1), the two dyes used during the Simons' stain (Figure 10), bind to cellulose based on their affinities to cellulose and their sizes. DO 15 has a higher affinity to cellulose than DB 1. Additionally, DO 15 (molecular weight>100,000 kDa) generally binds to larger pore sizes (5-36 nm) than DB 1 (1 nm). These two variables become especially relevant to describing a cellulose fiber's specific surface area available to cellulases and the pore sizes that cellulases can pass through to carry out hydrolysis.

Direct Blue 1

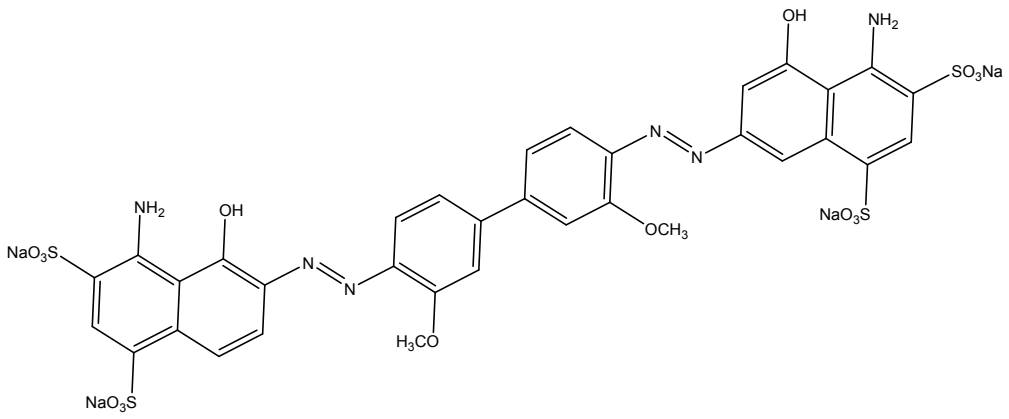

Direct Orange 15

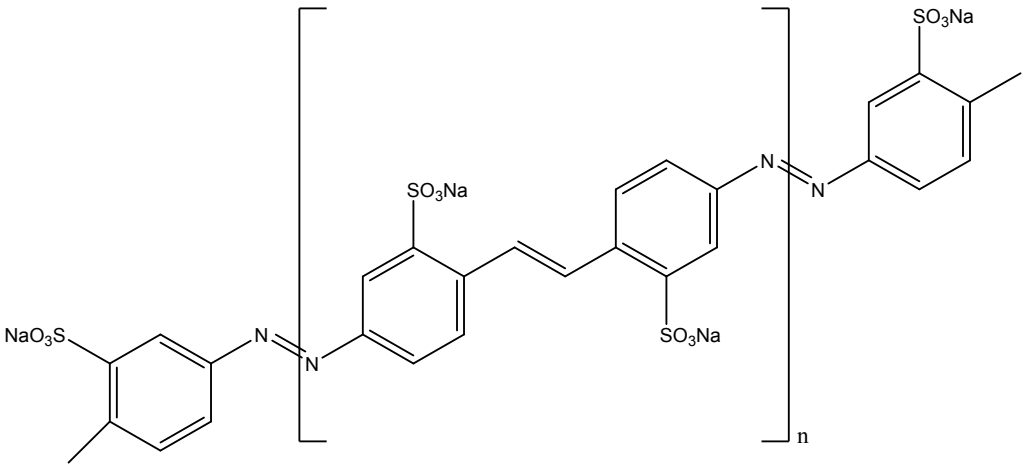

Figure 10 Chemical structures of DB1 and DO15 (330)

During the Simons' stain, DO 15 and DB 1 are incubated with milled biomass, and the unbound dyes are removed and measured with UV-Vis to quantify changes in dye between molar concentration and dye absorbances with Beer-Lambert's law (Equation 5). Prior to analysis, Simons' staining requires the construction of a standard curve to

calculate ε, molar absorptivity, at wavelengths 455 and 624 nm. These wavelengths represent the maximum absorbances for the blue and orange dyes respectively. Because pathlength (l) and ε are constants and known, the absorbance (A) of the spent dyes can be measured and used to calculate c, the dye concentrations with Beer-Lambert's law for a binary mixture (Equation 6). The dyes' absorbances are then obtained to quantify changes in dye concentrations due to interactions with cellulose. Finally, the maximum dye absorbance can be calculated with the Langmuir isotherm (Equation 7) by linearly plotting the concentrations of the adsorbed and free dyes.

$$A = \varepsilon \times c \times l \tag{5}$$

$$\begin{aligned} A_{455\ nm} &= \varepsilon_{O\ at\ 455\ nm} \times l \times C_O + \varepsilon_{B\ at\ 455\ nm} \times l \times C_B \\ A_{624\ nm} &= \varepsilon_{B\ at\ 624\ nm} \times l \times C_B + \varepsilon_{O\ at\ 624\ nm} \times l \times C_B \end{aligned} \tag{6}$$

A: absorbance, ε: molar absorptivity, c: concentration (mol/L), and l: pathlength (cm)

Subscripts B and O denote blue and orange dyes, respectively

$$\frac{1}{[A]} = \frac{1}{[A]_{max}} + \frac{1}{K_{ads}} \times [A]_{max} \times [C] \tag{7}$$

[A]: amount of adsorbed dye, [C]: amount of free dye, $[A]_{max}$: maximum adsorbed dye, K_{ads}: adsorption constant

2.4.4.5 Two-Dimensional NMR for Detailed Plant Cell Wall Analysis

Heteronuclear single quantum coherence (HSQC) solution-state NMR spectroscopy represents one of the most powerful tools for biomass characterization. NMR

spectroscopy provides detailed information about lignins, LCCs, and/or the whole cell wall that allows for semi-quantitative measurements and structural comparisons using the ^{1}H and ^{13}C spectra. Although NMR spectroscopy and mass spectrometry (MS) generate similar structural information such as lignin S/G ratio (331) and interunit linkages (332), MS is a destructive technique and structural information may be lost during analysis. NMR spectroscopy's primary drawback, however, is its reduced ability test a high number of samples in comparison to the previously mentioned techniques (i.e. GPC, solid-state NMR, FTIR). Nonetheless, supporting data from other instrumentation can identify a "strong lead" to narrow down samples of interest for 2D NMR.

Multidimensional NMR experiments like HSQC interpret structurally complex molecules by correlating the chemical shifts (Table 12) of ^{1}H and ^{13}C that are directly bonded to one another. HSQC contains spectral cross peaks that are used to measure interunit linkages and structural properties such as the relative proportions of S, G, and H lignin. HSQC has captured lignin restructuring following the ethanol organosolv (333), hydrothermal (334), and dilute acid (335) pretreatments as well as in transgenic plants (55, 58, 336). Certain well-resolved peaks in the HSQC spectra are integrated (Figure 11), and their proportions are expressed as a fraction of the total aromatics or aliphatics.

Table 12 – Peak chemical shifts and assignments in the 2D HSQC NMR spectrum of lignin

δ_C/δ_H (ppm) (334)	Assignment
53.2/3.5	C_β/H_β phenyl coumaran substructure
55.7/3.8	C/H in methoxyl groups
60.2/3.6	C_γ/H_γ in β-O-4 substructures
62.8/3.8	C_β/H_β in β-1
71.5/4.8	C_α/H_α in β-O-4 linkage
84.8/4.3	C_β/H_β in β-O-4 linkage
84.7/4.7	C_α/H_α in β-1
87.1/5.5	C_α/H_α in phenyl coumaran
104.3/6.7	$C_{2,6}/H_{2,6}$ in etherified syringyl units ($S_{2,6}$)
105.5/7.3	$C_{2,6}/H_{2,6}$ in oxidized syringyl units ($S'_{2,6}$)
111.4/7.0	C_2/H_2 in guaiacyl units (G_2)
115.4/6.77	C_5/H_5 in guaiacyl units (G_5)
119.3/6.82	C_6/H_6 in guaiacyl units (G_6)
130.0/7.5	$C_{2,6}/H_{2,6}$ in *p*-hydroxybenzoate units ($PB_{2,6}$)

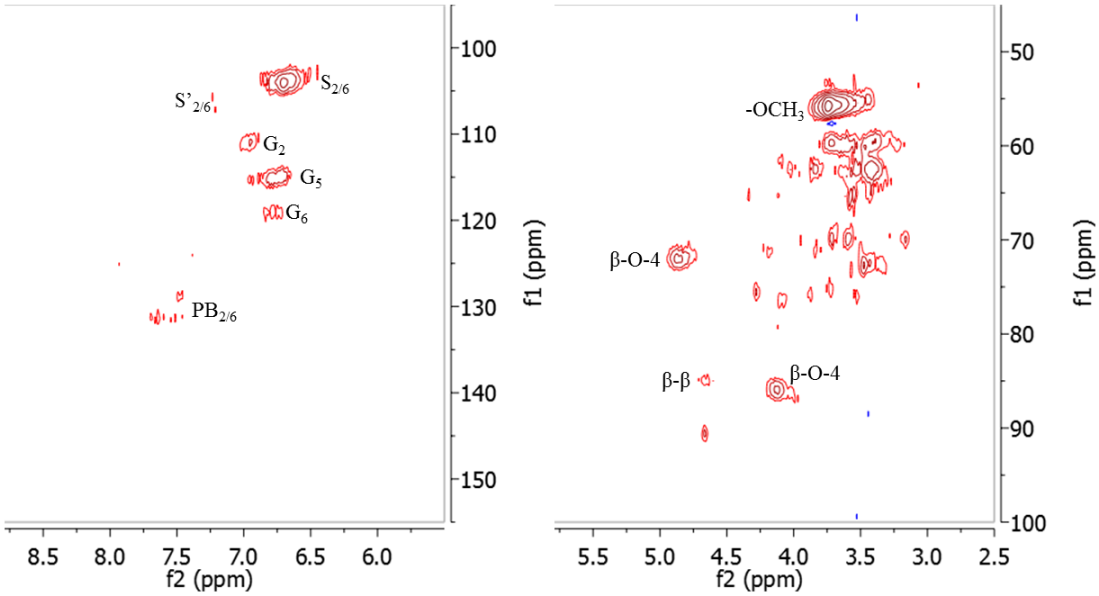

Figure 11 – A representative 2D HSQC NMR spectrum from *P. trichocarpa*

2.4.5 *Biomass Analysis Reveals Contributors to Recalcitrance*

Aside from these tools, there are an abundance of other tools such as glycome profiling (337) and Raman spectroscopy (338) that are available for biomass characterization. For simplicity purposes, the above-mentioned techniques and instrumentation will be the central focus of this work.

CHAPTER 3. MATERIALS AND METHODS

3.1 Chemical and Supplies

With few exceptions, laboratory reagents and supplies were purchased from VWR International (Radnor, PA) and/or Sigma Aldrich (St. Louis, MO). Pylam Products Co. (Garden City, NY) provided the orange and blue dyes, while Amicon, Inc. (Beverly, MA) provided the ultrafiltration apparatus. For Klason lignin analysis, the G8 glass fiber filters were purchased from Thermo Fisher Scientific (Madison, WI). The cellulases Ctec2 and Htec2 were obtained from Novozymes (Franklinton, NC).

3.2 Biomass: *Populus trichocarpa*

Four-year-old *Populus trichocarpa* was cultivated and harvested in Clatskanie, OR. The logs were sliced, debarked, air-dried and subsequently milled (Thomas Scientific, Swedesboro, NJ) through a 0.841 mm screen. The milled *P. trichocarpa* was stored at -20°C prior to use.

3.3 Fermentation Residues

Fermentation residues, or *P. trichocarpa* that had been treated with *C. thermocellum* (ATCC, Manassas, VA) were obtained from the BioSciences Division at ORNL. The fermentation residues were received frozen and were freeze dried (VirTis, SP Scientific, Warmister, PA) overnight prior to analysis.

3.4 Experimental Methods

3.4.1 *Consolidated Bioprocessing with C. thermocellum*

Consolidated bioprocessing (CBP) was carried out in batch bottle fermentations with *C. thermocellum* at 60°C at 150 rpm for 5 d. The biomass was autoclaved for sterilization purposes (121°C for 20 min) and washed prior to experimentation. The biomass loadings were calculated on a dry basis and were at least 5 g/L, depending on the starting amount of biomass. *C. thermocellum* was grown on media for thermophilic *Clostridia*. Fermentation yields were determined by HPLC quantification.

CBP was also conducted on fermentation media in the Satorius BIOSTAT QPlus bioreactors (Sartorius Stedium Biotech, Göttingen, Germany) at 60°C and pH 7 at 200 rpm under nitrogen. The pH was maintained though out the experiment with the addition of 3 N KOH. HPLC was also used to quantify fermentation products at specified intervals.

3.4.2 *Separate Hydrolysis and Fermentation*

The enzymes Cellic Ctec2 and Htec2 (Novozymes, Franklinton, NC) were used to hydrolyze cellulose in batch bottles at a 5% (w/v) loading. The hydrolysis took place at 50°C for 5 d in 50 mM citrate buffer. Fermentations were subsequently carried out with *Saccharomyces cerevisiae* D5A (ATCC 200062), which was grown on yeast extract peptone dextrose agar at 35°C for 3 d. Fermentation yields were determined by HPLC quantification.

3.4.3 *Soxhlet Extraction*

In order to remove extractives, *P. trichocarpa* underwent Soxhlet extraction with dichloromethane or 1:2 (v/v) ethanol:toluene. Milled biomass was dispersed into Whatman cellulose extraction thimbles (33 mm × 80 mm). The Soxhlet extraction apparatus was assembled, and the appropriate extraction solvent (or solvent mixture) was added. The extraction thimble was inserted into the extraction chamber, and the solvents were heated under reflux to achieve six cycles per h for 4.5 h with dichloromethane or 12 h with 1:2 (v/v) toluene:ethanol. Upon completion, the biomass was air-dried in the extraction thimble to evaporate residual solvent.

3.4.4 *Wet Chemistry for Biopolymer Isolation*

3.4.4.1 Delignification: Cellulose and Hemicellulose Isolation

Peracetic acid (32% w/w) was added to air-dried *P. trichocarpa* or the freeze-dried solid residuals (3.5 g/g biomass) to remove lignin (339). The delignified wood pulp, or holocellulose, was washed with water several times via filtration and air-dried.

3.4.4.2 Cellulose and Hemicellulose Isolation from Holocellulose for Molecular Weight Analysis

Cellulose and hemicellulose were isolated from holocellulose based on solubility differences in sodium hydroxide (NaOH). Holocellulose was weighed (0.1 g), added to 5 ml of 17.5% NaOH, and stirred for 2 h in 20 ml scintillation vials. Water was added to dilute the NaOH concentration to 8.75%, and the mixture stirred for an additional 2 h. The mixture was filtered through a 0.45 μm polyamide filter to separate the soluble

hemicellulose from the insoluble cellulose. The cellulose was washed with 1% acetic acid and rinsed several additional times with nanopure water. The cellulose was frozen for two h, freeze-dried overnight (Virtis, SP Scientific, Warmister, PA), and vacuum-dried for an additional 12 h.

Hemicellulose was recovered through precipitation in 7:3 v/v ethanol:acetic acid and subsequent centrifugation at 8228 g (Eppendorf Centrifuge 5804R, Eppendorf North America, Hauppauge, NY). The ethanol:acetic acid mixture was decanted, and the hemicellulose was washed with nanopure water two additional times via centrifugation and vacuum-dried.

3.4.4.3 Cellulose Isolation for Crystallinity Analysis

Hemicellulose was hydrolyzed from holocellulose (approx. 300 mg) with 2.5 M HCl under reflux for 1.5 h. The isolated cellulose was washed via filtration with Milli-Q water several times and remained damp (30-60% moisture) prior to analysis.

3.4.4.4 Lignin Isolation

Soxhlet-extracted *P. trichocarpa* (1-1.5 g) was pulverized with the PM100 planetary ball mill (Verder Scientific, Newtown, PA) at 580 rpm for 2 h 26 min. Ctec2 and Htec2 (Novozymes, Franklinton, NC) were added at 20 FPU/g biomass to remove cellulose and hemicellulose, respectively. C1730, β-glucosidase from almonds (Sigma Aldrich, St. Louis, MO), and cellulase (Sigma Aldrich, St. Louis, MO) were employed in some experiments to remove cellulose alone from the whole biomass. In either case, the enzymatic hydrolysis was carried out in pH 5, 20 mM sodium acetate (NaOAc) buffer for

two 48 h periods. After the first 48 h period, the spent enzyme broth was separated from the solid residuals via centrifugation (3889 g) and replaced with new enzymes, which carried out hydrolysis for an additional 48 h. Again, the spent hydrolysis broth was removed, and the lignin-enriched residuals were rinsed with the 20 mM NaOAc buffer and water. The lignin was placed in a freezer for two h, freeze-dried overnight, and vacuum-dried for 12 h at 40°C.

3.4.5 *Derivatization and Dissolution for Molecular Weight Analysis*

3.4.5.1 Lignin Derivatization and Dissolution

To remove additional carbohydrates, vacuum-dried lignin-enriched residues (100 mg) were mixed with 96% (v/v) *p*-dioxane for 48 h. The used 96% v/v *p*-dioxane was removed, and the procedure was repeated. The remaining solids were frozen, freeze-dried overnight, and vacuum-dried at 40°C. The isolated lignin was derivatized via acetylation with 4:1 v/v pyridine and acetic anhydride over 96 h. The derivatized lignin was precipitated in ethanol and was separated from the solvents through evaporation with a rotary evaporator. The resulting solids were air-dried and subsequently vacuum-dried. The resulting lignin was dissolved overnight in the mobile phase (tetrahydrofuran) at a final concentration of 1-2 mg/ml. Following dissolution, each sample was filtered through a 0.45 µm PTFE syringe filter into a 2 ml vial.

3.4.5.2 Cellulose Derivatization

Derivatization via tricarbanilation was accomplished by adding cellulose (15 mg) to phenyl isocyanate (0.5 ml) and anhydrous pyridine (4 ml) in 20 ml scintillation vials.

The derivatization reaction proceeded over 72 h at 70°C and was quenched with addition of methanol (1 ml). Cellulose was precipitated dropwise in 7:3 methanol:water and was centrifuged (8228 g) to separate the solvent from the solids. The derivatized cellulose was rinsed once with 7:3 methanol: water and two additional times with water. The derivatized cellulose was vacuum-dried prior to dissolution. The cellulose was added to THF to achieve a final concentration of 1-2 mg/ml and dissolved overnight. The solution was filtered through a 0.45 μm PTFE syringe filter and added to a 2 ml vial.

3.4.5.3 Hemicellulose Dissolution

Hemicellulose was dissolved directly in the mobile phase, 0.05 M NaOAc/0.1 M NaOH buffer at pH 11.80, to achieve a final concentration of 1 mg/ml. The samples were dissolved overnight and filtered through a 0.45 μm PVDF syringe filter.

3.5 Surface Roughness of *P. trichocarpa* logs

Logs from *Populus trichocarpa* were sliced with a band saw and sanded with 120 grit sandpaper to reduce irregularities at the wood surface. The slices cut to 100 mm thickness and were stored at room temperature at 65% relative humidity for two weeks to reach a moisture content of 12% (340). The moisture content was verified with a moisture balance (Sartorius MA35, Bohemia, NY).

3.6 Operational Procedures

3.6.1 *Gel Permeation Chromatography of Lignin, Cellulose, and Hemicellulose*

3.6.1.1 Organic Phase GPC

The organic phase GPC, SECurity Agilent 1200 series, used THF as its mobile phase. The injection volume was 25 µl, and the flow rate was 1 ml/min for 50 min. The GPC was equipped with four Waters Styragel columns (Waters, Corp., Boston, MA). Standard polystyrene (Polymer Standards Service, Amherst, MA), ranging in molecular weights from 1.5×10^3 to 3.6×10^6 g/mol, was used to construct the calibration curve for the extrapolation of the relative molecular weights. The resulting peaks were integrated with the UniChrom WinGPC7 software (Polymer Standards Service, Amherst, MA), and Mn, Mw, and PDI were recorded.

3.6.1.2 Aqueous Phase GPC

The aqueous GPC, SECurity Agilent 1200 series, used sodium acetate (0.1 M NaOH/0.05 M NaOAc buffer. The GPC contained three Ultrahydrogel columns (Waters, Corp., Boston, MA). The calibration curve was constructed with pullulan (3.42×10^2 – 7.08×10^5), which was supplied by Polymer Standards Service (Amherst, MA). The injection volume was 25 µl and the flow rate was 0.5 ml/min for 70 min.

3.6.2 *Log Surface Roughness*

Each log slice was cut to size (100 mm thickness) and analyzed with the Tencor P-6 stylus profiler (KLA-Tencor, Milpitas, CA). Each slice was scanned at a rate of 200 µm/s on a scan size of 500 µm. The stylus tip, which had a radius of 5 µm, was positioned at a 90° with an applied force 5 mg. The surface profiles were used to calculate Ra (average roughness), Rv (mean valley roughness), and Rp (mean peak roughness).

3.6.3 *Cellulose Crystallinity Analysis with Solid-State NMR*

^{13}C NMR spectra were acquired with a Bruker DSX-400 spectrometer, equipped with a double-resonance MAS probe head, at spin speeds of 8000 kHz and an operating frequency of 43.55 MHz. The ^{13}C CP/MAS experiments were carried out with a 1.5 ms contact pulse, 5 μs (90°) proton pulse, 4000 scans and a 4 s recycle delay. The spectra were integrated at the peaks representing carbon 4 in cellulose between 79-86 ppm and 86-92 ppm with the Topspin 2.1 software to calculate the crystallinity index (CrI).

3.6.4 *Cellulose Crystallinity Analysis with ATR-FTIR*

The cellulose, which was isolated from hemicellulose via acid hydrolysis, was analyzed on a 100 FTIR spectrometer (PerkinElmer, Waltham, MA) with 32 scans at a 4 cm^{-1} resolution. The data was collected with a universal ATR crystal accessory.

3.6.5 *Simons' Stain to Measure Accessibility*

3.6.5.1 Dye preparation

The blue and orange dyes were added to Millipore Milli-Q water to achieve a final concentration of 10 mg/ml. To remove components with molecular weights less than 100,000 kDa, the orange dye was filtered twice through 100K filter paper on an Amicon ultrafiltration apparatus. The remaining orange dye was recovered, and 1 ml was pipetted onto a petri dish. The petri dish was placed in the 105°C oven to dry for 3 days. After drying, the weight of the dye in 1 ml of solution was obtained, and the orange dye was diluted again to achieve a final concentration of 10 mg/ml.

3.6.5.2 Standard Curve, Sample Preparation and Analysis

The calibration curve was prepared with both the orange and blue dyes. The dyes were diluted and prepared in varying concentrations between 0.1 ml and 0.8 ml. The blank for the UV-Vis was water, and the instrument was zeroed with water prior to use. The dye absorbances were recorded at 455 and 624 nm, respectively, and water was maintained as a reference. The data from the standard curves were used to determine the molar absorptivities (ε) for the orange and blue dyes.

Phosphate buffered saline solution (0.3 M sodium phosphate, 1.4 M sodium chloride) was prepared in Millipore Milli-Q water.

The calibration curve was prepared with both the orange and blue dyes. The dyes were diluted, and their absorbances were measured. The blank for the UV-Vis was water, and the instrument was zeroed with water prior to use. The dye absorbances were recorded at 455 and 624 nm, respectively, and water was maintained as a reference. The data from the standard curves were used to determine the molar absorptivities (ε) for the orange and blue dyes.

Soxhlet-extracted poplar (100 mg) and phosphate buffered saline solution (0.1 ml) were added to seven test tubes. The DB 1 and DO 15 dyes were added in increasing volumes (0.1, 0.2, 0.3, 0.4, 0.6, and 0.8 ml) to each tube. Phosphate buffered saline was also added (0.1 ml), and the solution was made up to 1 ml with water. The mixture was incubated for 6 h at 150 rpm at 70°C. Following incubation, the mixture was centrifuged at 10,252 g to separate the biomass from the unbound dyes.

The mixture of dyes was diluted and the absorbances at 455 and 624 nm were measured with the Lambda 35 UV-Vis spectrophotometer (Perkin Elmer, Waltham, MA). The absorbances were used to calculate the concentration of free dye, which was used to determine the concentration of bound dye based on an initial concentration of 10 mg/ml. The maximum absorbance is also calculated from the previously mentioned data to compute the O:B ratio.

3.6.6 *Klason Lignin and Carbohydrate Compositional Analysis*

Dry, milled biomass was weighed (0.175 g) and hydrolysed with 1.5 ml 72% sulfuric acid. The acid hydrolysis was carried out in a Digiblock heater (Sigma Aldrich, St. Louis, MO) for 1 h while stirring every 3 to 5 min. The solution was diluted to 42 ml and autoclaved for 1 h at 121°C. After cooling, the mixture was diluted to volume (50 ml) and was filtered through G8 glass filters to separate the Klason lignin from the hydrolysed sugars. The Klason lignin was dried for 24 h at 105°C and weighed to determine its representation in the original biomass.

The filtrate was diluted accordingly and analysed on the Dionex-ICS 3000 with the Chromeleon 7.1 software (Thermofisher, Waltham, MA) and fucose (1 mg/ml) as the internal standard. The Dionex ICS-3000 contained a PC10 pneumatic controller, a conductivity meter, an AS40 autosampler, a CarboPac PA1 guard column (Dionex Corp., Sunnyvale, CA), and a CarboPac PA1 column (Dionex Corp., Sunnyvale, CA). Calibration curves were constructed individually for five common biomass-derived sugars: glucose, xylose, mannose, arabinose, and galactose. The carbohydrate

compositions were extrapolated from the calibration curves and adjusted for their respective dilutions to determine their concentrations in the original biomass.

3.7 Statistical Analysis

Except for 2D HSQC NMR, all analyses were conducted in triplicates. Outlier detection was carried out using a modified z-score (341). The modified z-score (M_i) was calculated using equation 8, which is calculated with the mean ($\overline{x}$), the modified absolute deviation (*MAD*), and each individual observation (x_i). The MAD was calculated using equation 9. Any data possessing a modified z-score of ±3.5 were considered an outlier.

$$M_i = \frac{0.6745(x_i - \overline{x})}{MAD} \tag{8}$$

$$MAD = median(|x_i - \overline{x}| \tag{9}$$

Statistically significant differences between means were determined with one-way analysis of variance (ANOVA) and Tukey's test at a 95% confidence level.

CHAPTER 4. LIGNIN EXHIBITS RECALCITRANCE ASSOCIATED FEATURES FOLLOWING THE CONSOLIDATED BIOPROCESSING OF NATURAL VARIANTS OF *POPULUS TRICHOCARPA*

4.1 Introduction

Industrially, starch has enjoyed much more attention and commercial success than cellulose for ethanol production. Starch is depolymerized into glucose more easily than cellulose, which renders it a more popular substrate. Difficulties in cellulose bioconversion are rooted in several inherent structural features of biomass that restrict fungal enzyme activities. Recalcitrance describes this resistance to enzymatic deconstruction and severely complicates the conversion of cellulose into ethanol. While pretreatments (342) and genetic modifications (343) have been investigated to minimize recalcitrance, consolidated bioprocessing (CBP) is an alternative approach to addressing difficulties in biomass deconstruction that have contributed to the high costs of ethanol production.

The common methodology for ethanol production from cellulose follows a four step process. Bioresources such as switchgrass or poplar are pretreated to enhance enzyme accessibility for the subsequent enzymatic hydrolysis. Fungal cellulases are

traditionally employed to depolymerize cellulose into glucose units, which are fermented by yeasts to yield ethanol. The final stage is distillation, where ethanol is separated from other fermentation products. Alternatively, CBP uses microorganism(s) to solubilize and ferment five- and/or six- carbon sugars in lignocellulosic biomass in one step and without added enzymes. While a number of microorganisms can carry out CBP (132), *Clostridium thermocellum*, a thermophilic anaerobic bacterium, has attracted considerable attention as a robust CBP microorganism (344).

C. thermocellum contains a cellulosome, a multi-enzyme assembly that is attributed to the efficient solubilization of biomass and saccharification of cellulose. The cellulosome promotes synergistic relationships between enzymes, which in turn may be associated with its impressive cellulose hydrolysis rates compared to that of fungal cellulases, particularly in the presence of Avicel (83, 345). It is worth considering whether the synergistic relationships between cellulosomal enzymes are subject to limitations imposed by recalcitrance during CBP. While *C. thermocellum* has been heavily investigated from a diverse group of perspectives (132, 344), the structural features of biomass that facilitate enzymatic activity remain relatively obscure. Previous studies suggest that short DP (or high crystallinity) cellulose (83, 346) and high S/G ratio lignin (346) affect CBP. This investigation aims to characterize cellulose, hemicellulose, and lignin structure before and after CBP in *Populus trichocarpa* to associate structural changes to the progression of CBP.

4.2 Experimental Method

4.2.1 *Biomass and Fermentation*

Four-year-old natural variants of *P. trichocarpa* were cultivated and harvested from a shared garden in Clatskanie, OR. The natural variants were sectioned into logs, dried, debarked, and milled through a 0.841 mm screen. Carbohydrate composition was determined using NREL's Determination of Structural Carbohydrates and Lignin in Biomass (347).

Autoclaved *P. trichocarpa* was hydrolyzed and fermented with *Clostridium thermocellum* (ATCC 27405) in no yeast extract media for thermophilic *Clostridia*. Consolidated bioprocessing was carried out in bottles at 1 g/L (dry basis) biomass loadings for five days at 58°C and 300 rpm. The fermentation broth was separated from the solid residuals via centrifugation, and the solid residuals were frozen prior to structural analysis.

4.2.2 *Lignin, Cellulose, and Hemicellulose Characterization*

4.2.2.1 α-Cellulose and Hemicellulose Isolation

Air-dried *P. trichocarpa* was dispersed into Whatman cellulose extraction thimbles and Soxhlet-extracted for 4.5 h in dichloromethane at 100°C to remove extractives. The Soxhlet-extracted biomass was air-dried overnight in a fume hood to evaporate residual solvent. Peracetic acid (5% w/w) was added to 0.6 g of the extractive-free biomass, and delignification proceeded at 22°C for 26 h. The delignified wood pulp (0.10 g) was treated with 17.5% w/w NaOH for two h and with 8.75% w/w NaOH for two additional h, a slight modification to TAPPI test method T 203 cm-99. The alkali extraction separated cellulose from hemicellulose based on solubility differences; the recovered cellulose was washed with 1% w/w acetic acid (5 ml) and with water twice (50

ml). α-Cellulose was frozen overnight and freeze-dried for 12 h. The soluble component, hemicellulose, was precipitated in 7:3 ethanol:acetic acid, washed with water (50 ml) via centrifugation, and dried in the vacuum oven for 24 h.

4.2.2.2 Molecular Weight of α-Cellulose

Freeze-dried α-cellulose was vacuum-dried at 40°C and weighed (15 mg) into an oven-dried scintillation vial. Anhydrous pyridine (4 ml) and phenyl isocyanate (0.5 ml) were added to each vial, which was capped and sealed with parafilm. The samples were stirred at 60°C for 3 d, and the reaction was quenched with methanol (1 ml). The solution was precipitated in 7:3 methanol:water (25 ml) and washed with water twice (50 ml) via centrifugation. The tricarbanilated α-cellulose was dried overnight at 40°C in the vacuum oven and dissolved for 12 h in tetrahydrofuran (1 mg/ml). The dissolved samples were filtered through 0.45 μm polytetrafluoroethylene membrane syringe filters prior to analysis. Each sample was analyzed using an Agilent 1200 series GPC-SEC System (Polymer Standard Service, Waltham, MA, USA), equipped with four Waters Styragel columns (HR1, HR2, HR4, and HR6). The mobile phase was tetrahydrofuran with a flow rate of 1 ml/min, and the instrument was calibrated using narrow polystyrene standards.

4.2.2.3 Molecular Weight of Hemicellulose

Dried hemicellulose (1 mg) was dissolved overnight in 0.05 M NaOH/0.1 M NaOAc buffer (1 ml) and subsequently filtered through 0.2 μm polyvinylidene fluoride membrane syringe filters. The molecular weight analysis was conducted on an Agilent 1200 series SECurity System (Polymer Standards Service, MA, USA) with Ultrahydrogel columns with a flow rate of 0.5 ml/min, using the NaOH/NaOAc buffer

(pH 11.80) as the mobile phase.

4.2.2.4 Cellulose Crystallinity and Solid-state NMR Analysis

The delignified wood pulp was refluxed in 2.5 M HCl at 40°C for 1.5 h to hydrolyze hemicellulose. The mixture was cooled to room temperature and filtered to recover cellulose. The retentate was washed with water (100 ml), and the moist cellulose was packed into 4 mm cylindrical ceramic MAS rotors. A Bruker DSX-400 spectrometer, containing a double-resonance MAS probe head, was used to collect the ^{13}C spectra at spinning speeds of 8 kHz. The CP/MAS experimental parameters were 4000 scans, 1.5 ms contact pulse, 4 s recycle delay, and a 5 ms (90°) pulse. Peak integration was carried out with the TopSpin software (Bruker, Billerica, MA) at 79-86 ppm to represent the amorphous cellulose and 86-92 ppm to represent the crystalline cellulose. The crystallinity index (CrI) was determined by calculating the fraction of crystalline cellulose as a fraction of the total crystalline and amorphous cellulose.

4.2.2.5 Lignin Isolation and Preparation for HSQC

Untreated *P. trichocarpa* was Soxhlet-extracted for 12 h with toluene:ethanol (2:1 v/v) and air-dried overnight. The dry biomass was ball-milled with the PM 100 planetary ball mill (Verder Scientific, Inc., Newton, PA, USA) at 580 rpm for 2 h 26 min. The ball-milled biomass was treated over 48 h with Ctec2 and Htec2 (Novozymes, Bagsværd, Denmark) in 20 mM sodium acetate buffer to remove cellulose and hemicellulose, respectively. The enzymatic hydrolysis broth and solids were separated from one another through centrifugation, and the enzymatic hydrolysis was recommenced with new enzymes and buffer for 48 h. The mixture was centrifuged, and the solids were washed

with water, frozen, and freeze-dried. The isolated lignin was vacuum-dried at 40°C and dissolved in d_6-DMSO.

4.2.2.6 HSQC Parameters

2D HSQC NMR experiments were carried out on the Bruker Avance III 400 MHz NMR (298 K) using a 5 mm Broadband Observe probe (5 mm BBO 400MHz W1 with Z-gradient probe, Bruker). The spectra were acquired with the pulse sequence, hsqcetgpsi2, with spectral widths of 11 ppm with 2048 data points for the proton experiment and 190 ppm with 256 data points for the carbon experiment. Furthermore, the SN was 64, and D1 was 1 s. Chemical shift calibration was achieved with DMSO at solvent peaks δ H/δ C=2.49/39.5 ppm.

4.3 Statistical Analysis

Statistical analyses were conducted on the DP of cellulose, molecular weight of hemicellulose, and cellulose crystallinity data to determine outliers using the modified z-score proposed by Ingclewicz and Hoaglin. The modified z-score was calculated, as described in a previous study (275). Any datum possessing a modified z-score 3.5 was considered an outlier and discarded from the data set. Statistically significant differences between means were determined with one-way analysis of variance (ANOVA) testing at a 95% confidence level. Tukey's test was used to compare means in the data set to further assess significant differences between means at 95% confidence

4.4 Results

4.4.1 *Carbohydrate compositions and fermentation yields*

Carbohydrate compositions for six *Populus trichocarpa* were obtained prior to microbial treatment. Glucose concentrations ranged from 455.2 mg/g dry biomass in BESC-316 to 498.9 mg/g dry biomass in GW-9947. The remaining sugars (xylose, galactose, arabinose, and mannose) exhibited minor variations in their concentrations between samples. Xylose, specifically, demonstrated the greatest difference in concentration between samples at 13.9 mg/g dry biomass. Acetate was the dominate fermentation product followed by ethanol and then lactate (Table 13). Ethanol yields ranged from 7.62 mg/g in BESC-316 to 32.22 mg/g cellulose in GW-9947. Accordingly, GW-9947 produced the greatest concentrations of lactate (2.43 mg/g cellulose) and acetate (123 mg/g cellulose), while BESC-316 produced the least concentrations (0.34 mg/g and 68.44 mg/g cellulose, respectively).

Table 13 – Fermentation product yields from the six natural variants of *P. trichocarpa*

	mg/g cellulose					
	EtOH	SD	Lactate	SD	Acetate	SD
BESC-876	18.00	0.34	0.67	0.33	94.39	0.81
GW-9920	29.29	0.75	1.43	0.13	114.42	1.42
GW-9947	32.22	0.73	2.43	0.26	123.31	0.11
BESC-292	24.50	0.37	1.09	0.07	104.62	0.87
BESC-316	7.62	0.32	0.34	0.09	68.44	1.93
GW-9762	22.63	1.24	1.09	0.02	99.33	1.70

EtOH: ethanol; SD: standard deviation

4.4.2 *Carbohydrate structure*

4.4.2.1 Cellulose DP and crystallinity

Cellulose weight-average degrees of polymerization, or DP, from untreated poplar (TAPPI test method T203 cm-09) ranged between roughly 2000 and 3000 units in

length and did not demonstrate statistically significant differences (P>0.05). Following CBP, cellulose degrees of polymerization increased in all of the samples (Figure 12), which is consistent with other observations (346, 348). Cellulose degrees of polymerization in the solid residuals were generally two or more times greater than the initial degree of polymerization. Crystallinity indices (CrIs) for cellulose isolated from the untreated biomass ranged between 54.1 and 61.4%, and only GW-9920 was significantly different from the others (P<0.05). Following CBP, the CrIs of the solid residuals ranged between 54.7 and 57.7%, and significant differences were negligible (P>0.05). Though these variations were observed, there was no trend in cellulose degree of polymerization or crystallinity that aligned well with fermentation yields.

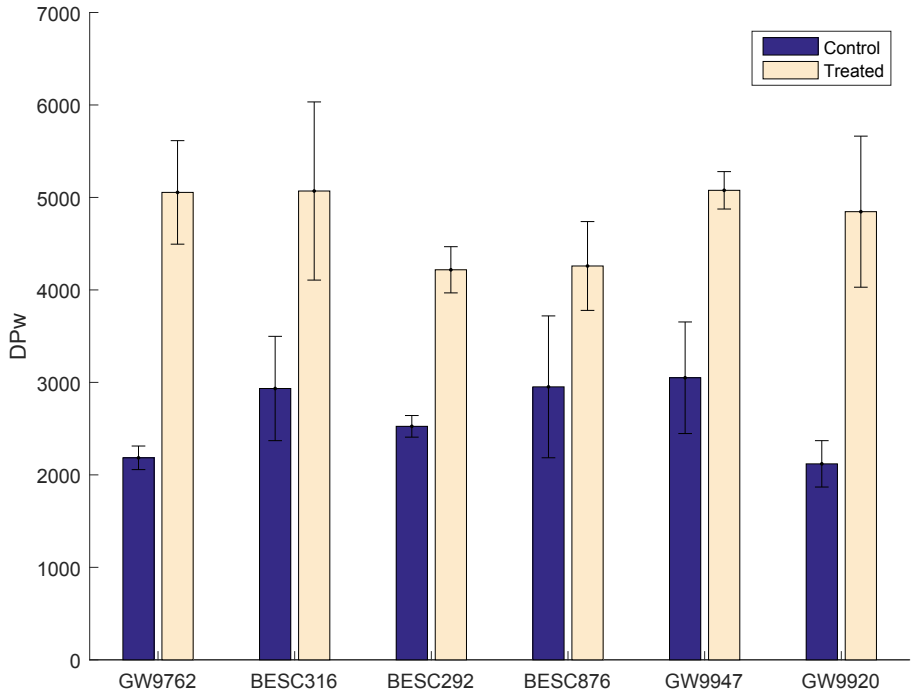

Figure 12 Cellulose DP from the control and *C. thermocellum* treated *P. trichocarpa*

4.4.2.2 Hemicellulose molecular weights

Hemicellulose molecular weights were not significantly different from one another neither in the controls nor in the treated materials ($P>0.05$). Accordingly, the molecular weights were relatively similar between the controls (between 3.6×10^4 and 5.6×10^4 g/mol) and between the treated (4.0×10^4 and 5.2×10^4 g/mol) samples. Lastly, the variability in molecular weights tended to be smaller in the treated samples than the controls.

4.4.3 *Lignin structure*

4.4.3.1 Lignin contents and S/G ratio

Lignin contents varied by less than five percent in the untreated samples. GW-9947 had the lowest lignin content (22.76%), while BESC-316 had the highest (27.23%). Although the differences appeared minor, lignin contents potentially influence fermentation in this and other studies (308, 349). Specifically, natural variants with lower lignin contents tended to generate higher lactate, ethanol, and acetate concentrations (Figure 13). It appears that higher lignin contents reduce hydrolysis efficiencies, which in turn reduces sugar yield, or inhibitors accumulate that negatively impact intracellular metabolism and fermentation yields. Both high lignin content (349, 350) and inhibitor generation (351, 352) have been linked to decreased end-product yields in *C. thermocellum*.

4.4.3.2 Lignin S/G ratio and interunit linkages

The 2D HSQC NMR spectra of a top (GW-9947), moderate (BESC-292), and

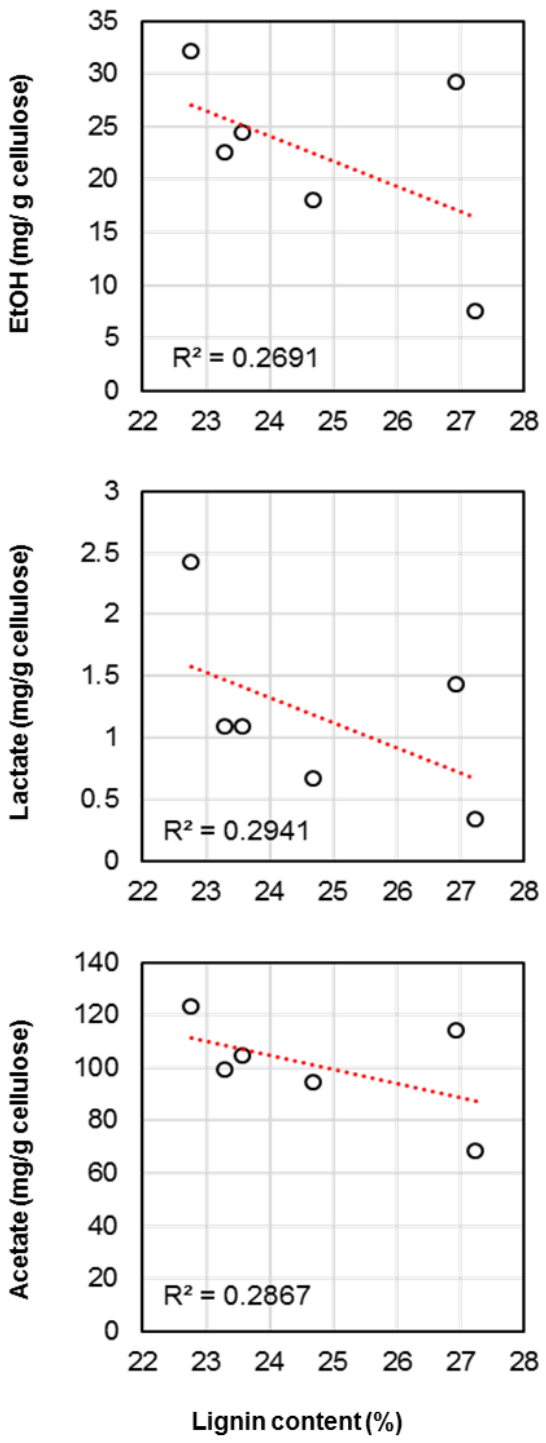

poor (BESC-316) ethanol yielding poplar were obtained to understand structural differences in lignin that potentially influence the extent of CBP (Figure 14). The primary structural differences in lignin-enriched residues between untreated BESC-292, BESC-316, and GW-9947 are listed in Table 14. NMR revealed distinct structural features in lignin that were isolated from GW-9947 that may facilitate biomass solubilization and utilization. Firstly, the relative proportion of S lignin in GW-9947 is higher. As a result, its S/G ratio is approximately 1.5 times greater than that of BESC-316 and BESC-292. Secondly, the para-hydroxybenzoate (PB) content was between 2 and 3% lower in GW-9947 than in the remaining lignin-enriched residues. Additionally, the number of β-β linkages was approximately 2% lower in GW-9947 than in BESC-316; the proportion of β-5 linkages demonstrated minor differences between samples. The data reveal that GW-9947 and BESC-316, which varied greatly in their CBP performances,

exhibited very different lignin structural features.

Figure 13 Lignin contents (%) of the six natural variants compared to the fermentation product yields

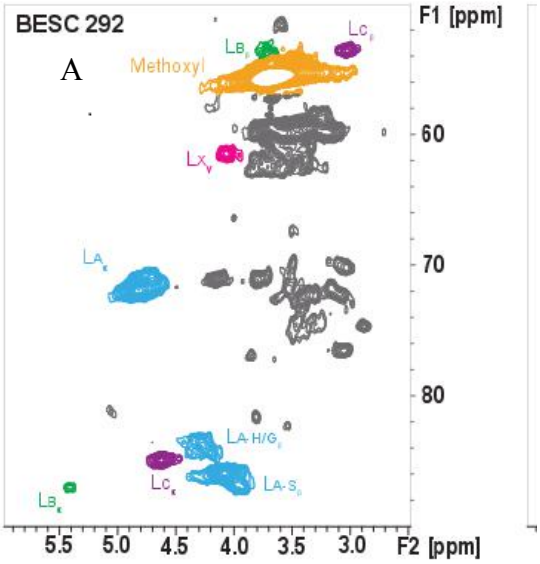
BESC 292
A
Methoxyl
F1 [ppm]
60
70
80
5.5
5.0
4.5
4.0
3.5
3.0
F2 [ppm]

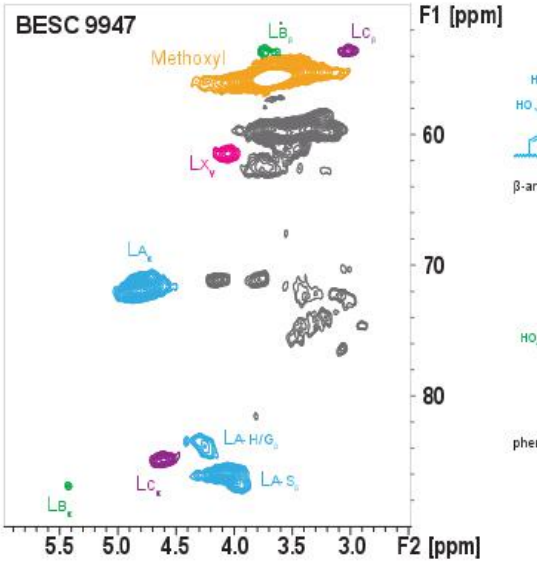
BESC 9947
Methoxyl
F1 [ppm]
60
70
80
5.5
5.0
4.5
4.0
3.5
3.0
F2 [ppm]

B

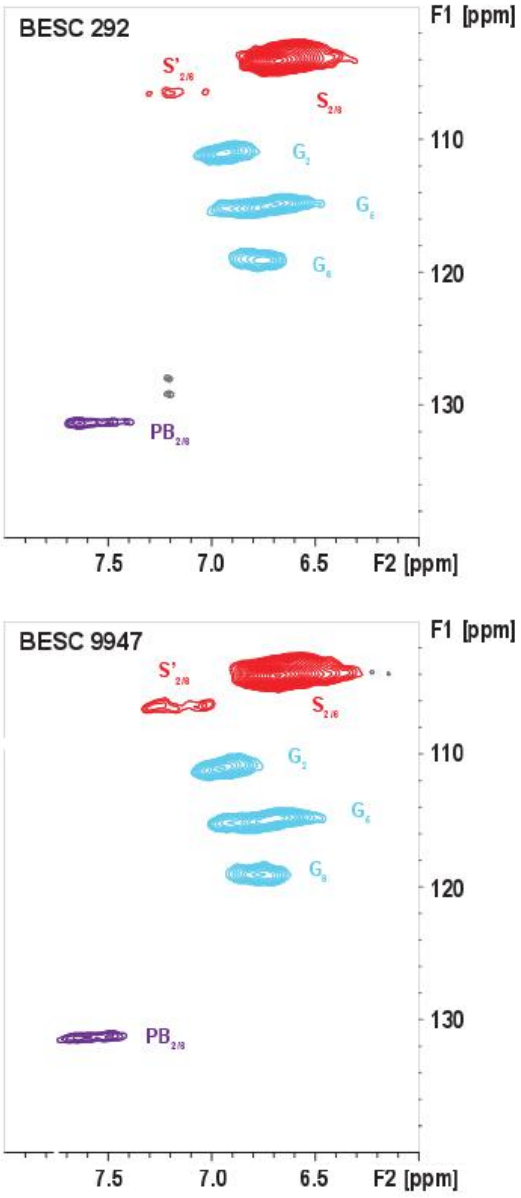

Figure 14 Illustration of the 2D ^{1}H-^{13}C HSQC NMR spectra of the (a) aliphatic and (b) aromatic regions of BESC-292, BESC-316, GW-9947 in lignin isolated from control *P. trichocarpa*.

Table 14 – Lignin S/G ratio, PB (%) content, and interunit linkages in natural variants of untreated *P. trichocarpa*

	S/G ratio	PB (%)	β-O-4 (%)	β-5 (%)	β-β (%)
BESC-292	1.85	7.73	82.2	2.85	14.9
BESC-316	1.62	8.85	79.4	3.92	16.7
GW-9947	2.62	5.78	83.3	2.26	14.4

S/G: syringyl to guaiacyl ratio

PB: para-hydroxybenzoate

4.5 Discussion

4.5.1 *Low DP cellulose is utilized before high DP cellulose*

Cellulose DP data indicate that longer cellulose chains remain after CBP. This observation suggests that *C. thermocellum* likely utilizes short chain cellulose and leaves behind longer chain cellulose. Similar studies propose that *C. thermocellum* takes cellulose size into account during enzymatic hydrolysis. For example, cellulosomes that were isolated from *C. thermocellum* have been used to hydrolyze Avicel (PH-101) and Whatman filter paper no. 1 under the same conditions; however, the conversion of shorter chain Avicel proceeded more rapidly and to a greater extent than on the Whatman filter paper (83).

In fungal cellulase systems, lower cellulose DPs are believed to facilitate enzymatic hydrolysis due to greater proportions of hydroxyl groups; however, studies that explore this relationship lack consensus (272, 353-355). In fungal cellulases, shorter chain cellulose purportedly possesses more hydroxyl groups that are available for hydrolysis

and fewer intracellular hydrogen bonds (353). Likewise, short chain cellulose may be a more favorable starting substrate for *C. thermocellum*, as exoglucanases and β-glucosidases could quickly convert cellulose into sugars that can be fermented.

4.5.2 *Cellulose crystallinities and hemicellulose molecular weights are likely minor contributors to recalcitrance during CBP*

Although several reports have argued it is a critical factor to enzymatic hydrolysis (277, 278, 356), cellulose crystallinity is likely a minor contributor to deconstruction difficulties in this study. GW-9920 differed significantly from the remaining controls ($P<0.05$); however, the CrIs were not significantly different from one another ($P>0.05$) in the treated samples. GW-9920 had the highest CrI of all the samples but did not exhibit poorer fermentation properties compared to its counterparts. It is unlikely that cellulose CrI is dominant factor that is responsible for the CBP differences observed.

Hemicellulose molecular weight may have important implications in enzyme inhibition (103) and have been found to increase in size following enzymatic hydrolysis (357). Hemicellulose molecular weights neither increased nor decreased consistently in all of the samples and were not significantly different amongst the controls or treated samples ($P>0.05$). The changes in the molecular weights indicate that hydrolysis likely occurs, but the systematic route in which these changes take place cannot be fully established by molecular weight alone. Furthermore, hemicellulose molecular weights interestingly approach 4.5×10^4 g/mol, which may suggest that the hydrolysis pattern in *C. thermocellum* focuses primarily on hemicelluloses removal to facilitate cellulose hydrolysis rather than its complete degradation for utilization.

4.5.3 *Structural variations in lignin structure are apparent between natural variants*

Though recalcitrance is not completely understood during CBP, lignin appears to influence the action of *C. thermocellum* (348, 358). The lignin contents illustrated in Figure 13, as determined by pyrolysis molecular beam mass spectroscopy (py-MBMS), indicate that fermentation yields are generally lower in the presence of higher lignin contents. Hence, high lignin concentrations may interfere with CBP due to reduced cellulose accessibilities and/or enhanced hydrophobic interactions with its cellulases and/or the cellulosome, thereby lowering the amount of sugars released. Additionally, GW-9947 contains syringyl-rich lignin and demonstrated better fermentation yields during CBP than BESC-316 and BESC-292. Similar to free cellulases (307), higher S/G ratio facilitates CBP.

PB (%) content may also influence recalcitrance. The inclusion of hydroxybenzaldehyde and hydroxybenzoate derivatives in transgenic *Arabidopsis* has been associated with lower lignin DPs and improved sugar release properties (359). GW-9947 had the lowest PB (%) content of all three lignins, while BESC-292 had the highest. Interestingly, BESC-292 was a moderately performing poplar despite its low S/G ratio, which may also be attributed to its high PB (%) content (360). It is possible that the high PB (%) content could have also promoted a similar lignin DP reducing effect and or increased terminal hydroxyl groups in lignin (361), which may reduce lignin's surface coverage and improve accessibility to cellulose; however, the latter postulation requires further investigation. Lastly, the high proportion of carbon-carbon

linkages, β-β and β-5 (%) in BESC-316 compared to the remaining two poplars may have also impeded the progression of CBP. The relative proportions of carbon-carbon linkages and aryl ether linkages influence lignin structure (362), which affects its interactions with cellulases (60).

4.6 Conclusion

While hemicellulose molecular weight, cellulose crystallinity, and cellulose DP were not prominent contributors to recalcitrance, their analysis provided structural clues regarding *C. thermocellum*'s mode of deconstruction. Lignin structural analysis indicated that lignin structural features, either individually or collectively, influenced the extent of CBP with *C. thermocellum*. Lignin structure and content contribute to the observed differences in CBP, meaning that biomass structure still presents difficulties for large-scale ethanol production. Cellulose crystallinity and size (DP) are minor contributors to recalcitrance during CBP.

CHAPTER 5. CONSOLIDATED BIOPROCESSING OF *POPULUS* USING *CLOSTRIDIUM (RUMINICLOSTRIDIUM) THERMOCELLUM*: A CASE STUDY ON THE IMPACT OF LIGNIN COMPOSITION AND STRUCTURE

5.1 Introduction

Recent advancements in lignocellulosic biofuel strategies have shown increased adoption and improved conversion of dedicated bioenergy feedstocks. For example, consolidated bioprocessing (CBP) growth on very high loads of minimally processed switchgrass has been described for *Caldicellulosiruptor bescii* (363). Yeast-based simultaneous saccharification and fermentation (SSF) and consolidated bioprocessing with *Clostridium thermocellum* have shown improved bioconversion performance for switchgrass with reduced lignin content (364). Bioconversion performances for *Saccharomyces cerevisiae* SSF and several CBP approaches have been assessed for switchgrass (*Panicum virgatum*) under different conditions (365). *C. thermocellum* has one of the highest rates for cellulose utilization (366). Metabolic engineering has generated strains that produce 70% of theoretical ethanol yield on Avicel and ethanol titers up to 73.4 mM, although further engineering is required (367).

Populus is a fast-growing woody bioenergy feedstock investigated for utilization in large scale bioconversion to alcohols (368, 369). Its inherent recalcitrance to enzymatic and microbial deconstruction is one of the largest impediments to large scale,

economically feasible biofuel production. Understanding *Populus* properties responsible for its resistance to degradation will aid in the generation of low recalcitrance plants. Lignin is an important component of lignocellulosic biomass, which is thought to act as a physical barrier towards the accessible surface of carbohydrates and adsorb and inactivate cellulases to restrict enzymatic hydrolysis (370). Lignin is a branched, heterogeneous polymer that makes up 16% to 28% of the content of undomesticated natural variants of *Populus trichocarpa* (307). When incorporated into lignin, the primary monolignols form three units: *p*-hydroxyphenylpropane (H), syringyl (S) and guaiacyl (G). S and G are the predominant units in the hardwood lignin backbone and vary in an S/G ratio between 1.0 and 3.0 (307). Lignin is most commonly linked through a labile arylglycerol-β-aryl ether (*β-O-4*) bond (371).

Compositionally, these lignin units differ by the absence of the methoxy group in position five on the benzene ring of the G unit, which results in the potential creation of two additional highly resistant bonds (372), the 5-5 and the β-5 linkages. This fundamental difference has been theorized to prompt differences in biomass degradability when the S and G lignin content varies: G-rich lignin could promote thinner cell walls that are easier to degrade (373), or it may lead to denser polymer crosslinking with increased resistance to degradation (299); S-rich lignin may form predominantly linear, shorter chains with thermoplastic properties more favorable to degradation, particularly by hydrothermal pretreatments (307).

Despite emerging hypotheses, current literature does not hold a unified mechanistic understanding on the role of lignin in the biological breakdown of lignocellulosic biomass. Still, there is general agreement that lignification significantly inhibits

deconstruction, in particular, a strong negative correlation is seen between total lignin content and sugar release by free-enzyme hydrolysis (374, 375). However, literature data do not show a generalized association between lignin composition and cellulose degradability in lignocellulose. Several reports found no discernable correlation between lignin S/G content and saccharification levels in alfalfa transgenics (375), synthetic cell wall complexes (376) and untreated *Arabidopsis thaliana* mutants (377). A high S/G ratio was found to adversely affect xylose release by acid hydrolysis in *Populus* (299), the enzymatic solubilization of maize (378) and transgenic *Populus* degradation by wood-decay fungi (378). At the same time high S/G was found to improve the saccharification of pretreated *A. thaliana* mutants (377), the efficiency of Kraft pulping (379), and enzymatic sugar release in undomesticated *Populus* (307). A challenge in comparing these published results is that many other properties beyond S/G ratio may also vary in these studies. These examples demonstrate that lignin S and G variations can be neutral or relevant depending on plant species, transgenic modifications, biomass pretreatments and the choice of degradation agent or method.

For undomesticated natural variants of *Populus trichocarpa*, the biomass tested in the current study, Studer and collaborators (307) found an S/G ratio above 2.0 to generally improve enzymatic hydrolysis, while the worst nine out of 47 performers had either very low S/G ratios (below 1.2) or very high total lignin content (above 27.8%). Cellulose properties, such as the degree of polymerization (380) and crystallinity (200), have also been of interest for characterization of lignocellulose recalcitrance and were investigated in this study in relation to lignin.

In this study, for the first time, we address whether lignin S/G variations have an impact on the consolidated bioprocessing of *Populus* biomass by a model cellulolytic organism, *Clostridium thermocellum* ATCC 27405. We evaluate the bioconversion performance of *Populus* individuals with similar average total lignin values and high or low S/G compositions to determine whether microbes have differential access to sugars, whether potential inhibitor release was linked to lignin composition and whether the abundance of S and G units was responsible for changes in biomass structural properties before and after fermentation (i.e., lignin and cellulose molecular weights, cellulose crystallinity and degree of polymerization).

5.2 Results

5.2.1 *Initial Microbial Bioconversion Screening of Populus Natural Variants*

Populus natural variants were screened and selected on the basis of average and similar total lignin (~ 24%) content. A subsection was assayed for primary carbohydrate content (i.e., glucose, xylose, galactose, arabinose and mannose) and the lignin S/G ratio. These selected *Populus* had very similar sugar contents. Three with average S/G ratios (~ 2.1) and one with the lowest possible S/G ratio (~1.2) were chosen for bioconversion performance assessment. Microbial CBP screening of these *Populus* individuals revealed a very similar performance in samples with equal S/G ratios, and a significantly lower conversion of the *Populus* with very low S/G content (Figure 15). The results are consistent with reported solubilization of undomesticated *Populus* with commercial enzyme mixtures (307).

To investigate what was responsible for the large discrepancy in the degradability of *Populus* with seemingly comparable sugar and total lignin content, but with a two-fold change in S/G content, two individuals were selected for further comparative analyses and will be referred to as the "low S/G" (natural variant BESC-102) and the "high S/G" (natural variant HARA-26-2) phenotypes.

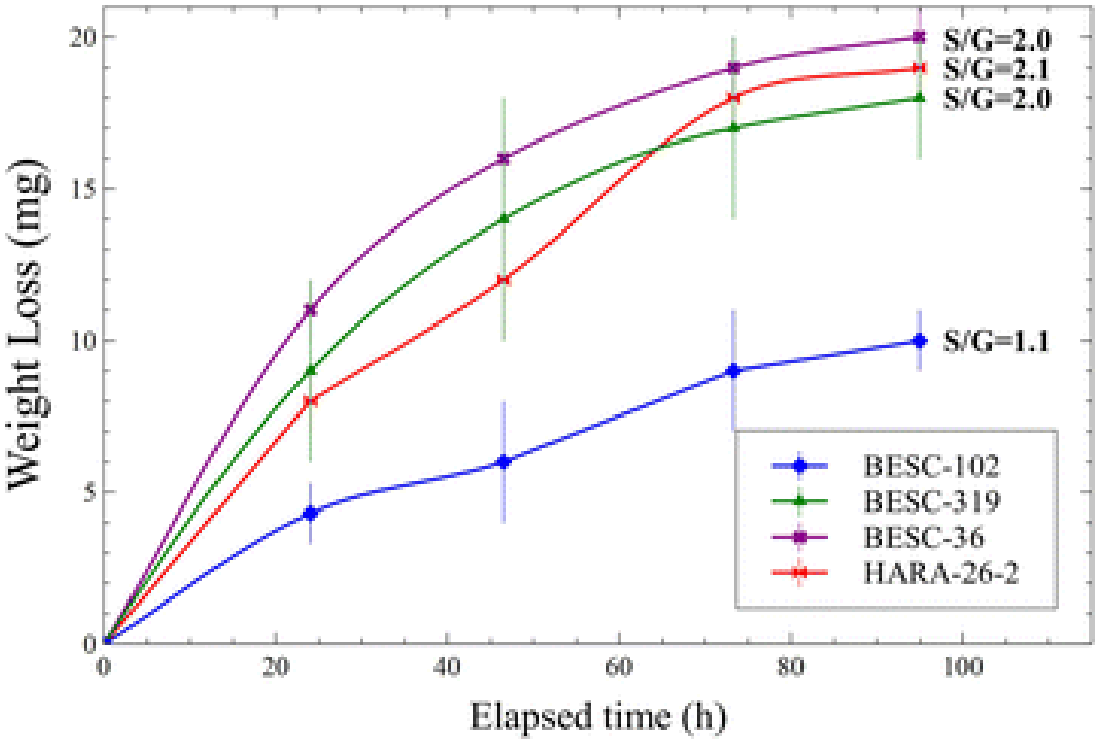

Figure 15 Bioconversion screening through time-course-weight loss measurements in batch fermentations with *C. thermocellum* ATCC 27405 at 5 g/L (dry basis) initial biomass loadings. Mean values and standard deviations are shown for triplicate fermentations

5.2.2 *Consolidated Bioprocessing (CBP): Microbial Hydrolysis and Fermentation of Low and High S/G Populus Phenotypes*

Microbial hydrolysis and fermentation of 20 g/L biomass samples (approximately 8 to 8.8 g/L glucan) in pH controlled bioreactors showed total solid solubilization of 12%

in low S/G and 20% in high S/G *Populus* (i.e., a 50% relative difference – calculated as absolute difference normalized to average solubilization for both lines). Ethanol yield (mg/g glucan) was 2.9-fold higher for the high S/G *Populus*, although fermentations of low S/G samples had their metabolic output shifted more towards acetate production - reported here as normalized to total biomass (Figure 16). Subtracting the end-point biomass-derived acetate of control samples from the total acetate in fermentation samples, the rough acetate to ethanol ratio was calculated to be 2.9:1 and 5.4:1 for the high S/G and the low S/G biomass conversions, respectively. Xylose release was proportional to total solid solubilization in both cases (data not shown). Control fermentations with 10 g/L glucan (Avicel) showed near-complete solubilization in less than 24 h. Compositional analysis of primary sugars in the two *Populus* phenotypes, before and after microbial bioconversion revealed an equal 15% reduction (g/g solid, dry basis) in the measured total carbohydrates. Glucose recorded the largest reductions in absolute values; however, with very similar relative changes (per gram solid), at 17% and 18% lower post-fermentation glucan content in the low S/G and the high S/G phenotypes, respectively (Figure 17).

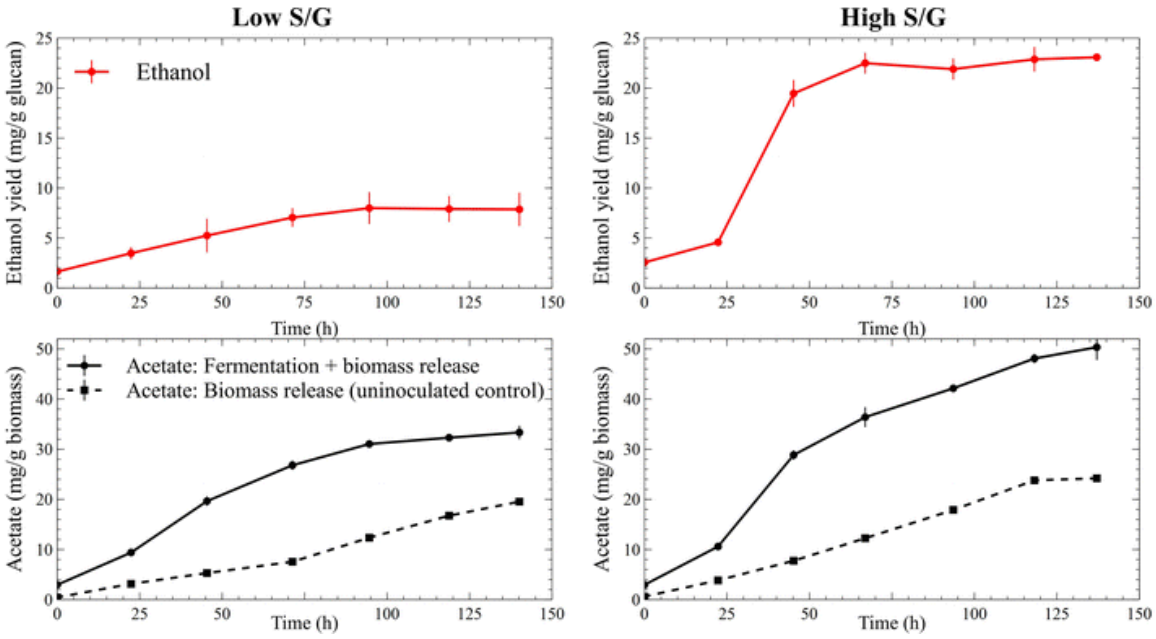

Figure 16 A 2.9-fold ethanol yield increase in the consolidated bioprocessing of high S/G *Populus* biomass over the low S/G variant (*top*); biomass-derived acetate (*below*, *dotted line*) measured in un-inoculated bioreactor controls and total acetate measured in CBP bioreactors (*below*, *solid line*)—fermentative acetate is approximately the difference between these two series. Mean values and standard deviations are shown for triplicate fermentations

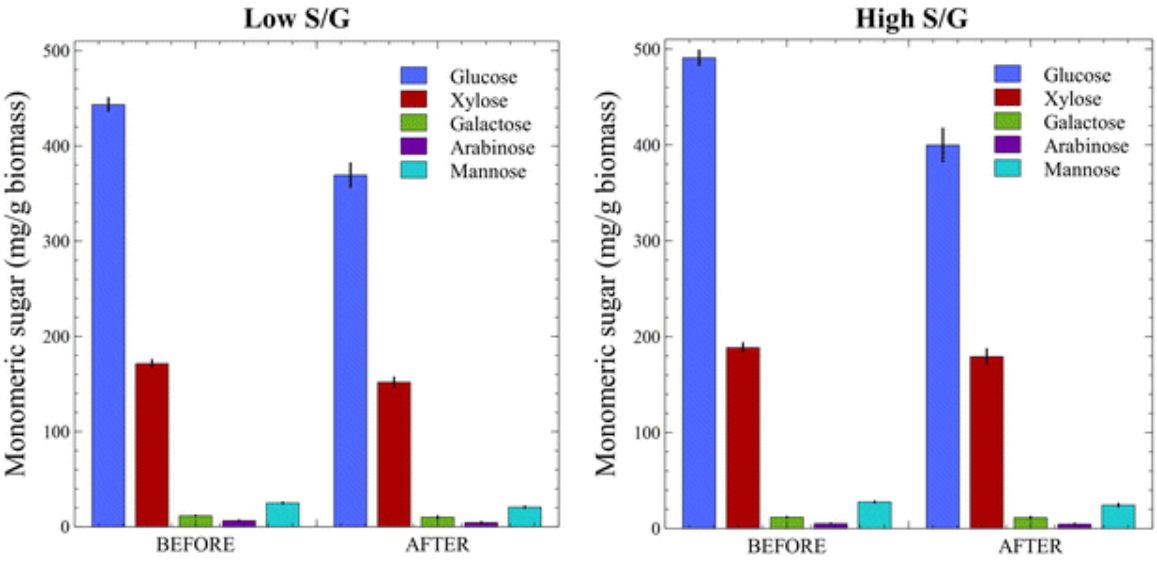

Figure 17 Sugar content per gram solid in low S/G (*left*) and high S/G (*right*) *Populus* before and after consolidated bioprocessing. Mean values and standard deviations are shown for solids of triplicate fermentations

5.2.3 *Separate Hydrolysis and Fermentation (SHF): Free-enzyme Hydrolysis and Yeast Fermentation of Low and High S/G Populus Phenotypes*

To test whether the large differences observed under CBP conversion were largely at the hydrolysis level, the two *Populus* phenotypes were also processed with a mixture of commercial cellulases, hemicellulases and a *β*-glucosidase at 50 °C. A 52% relative difference in glucose release was measured in favor of the high S/G phenotype. Xylose release measured a similar 60% relative difference (data not shown), and the subsequent yeast fermentation of solubilized sugars had similar conversion efficiency to ethanol (i.e., ethanol yield/glucose release, under 5% relative difference) (Figure 18), indicating no biomass-derived adverse effect on the yeast metabolism.

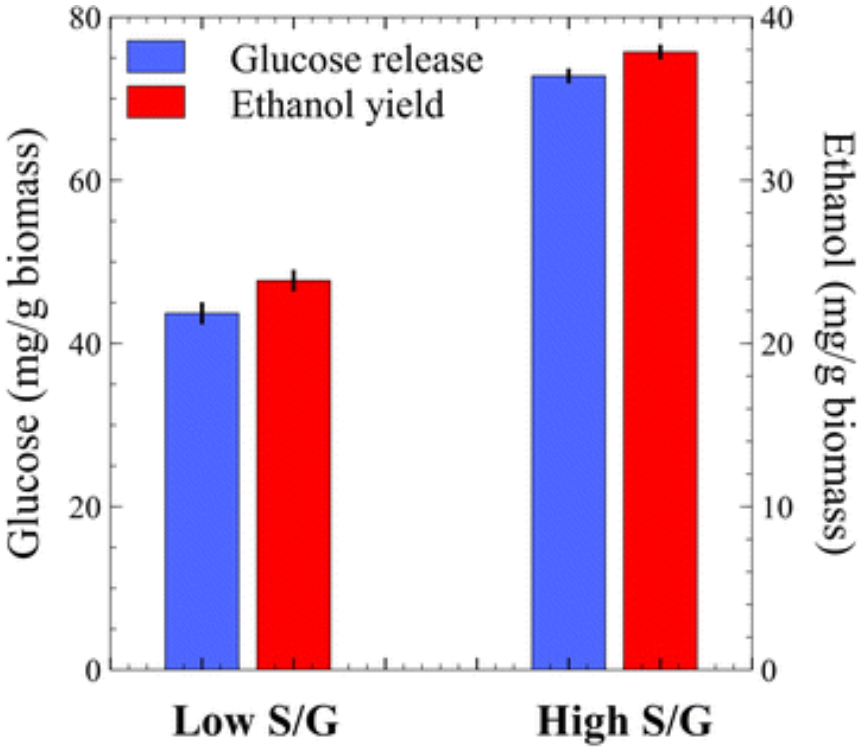

Figure 18 Glucose release and subsequent yeast fermentation to ethanol in separate hydrolysis and fermentation (SHF) of the low and high S/G *Populus*. Mean values and standard deviations are shown for triplicate fermentations

5.2.4 *GC-MS Metabolome Analysis of CBP Bioconversions for Identification of Potential Inhibitor Release*

In order to test whether biomass-derived inhibitors were contributors to differences in biomass solubilization during microbial hydrolysis, extracellular bioreactor metabolome samples were analyzed at time zero, 71 h and 140 h. Unsurprisingly, guaiacyl lignans were released in higher proportion from the low S/G *Populus*, while syringyl lignans in higher proportion from the high S/G biomass (Table 15). However, the very low detected concentrations were below what was considered inhibitory. The most common biomass-derived inhibitors (e.g., lignin precursors, HMF, furfural, etc.) were also not detected in the fermentation medium of either feedstock.

Table 15 – Time-course GC–MS metabolome analysis of CBP bioconversions; aqueous concentrations (mg/L) and the fold change (low S/G to high S/G) of potential biomass-derived inhibitors

Metabolite	Lo S/G	Hi S/G	Fold change	Lo S/G	Hi S/G	Fold change	Lo S/G	Hi S/G	Fold change
p-Hydroxybenzoic acid	1.28	0.14	*9.33*	4.54	0.56	*8.08*	6.82	1.09	*6.26*
4-Hydroxyphenethyl alcohol	0.02	0.01	*1.50*	0.26	0.77	0.34	0.46	1.73	0.27
11.64 347	0.38	0.16	*2.37*	4.62	0.97	*4.78*	8.23	1.74	*4.72*
11.00 218 100	2.13	0.55	*3.89*	5.16	1.28	*4.04*	4.20	1.30	*3.23*
10.92 218 100 277	3.38	1.08	*3.14*	9.32	3.71	*2.51*	7.73	2.41	*3.21*
14.90 Guaiacyl lignan	1.33	0.36	*3.73*	1.15	0.36	*3.19*	0.72	0.28	*2.61*
14.96 Guaiacyl lignan	2.30	0.68	*3.36*	2.27	0.81	*2.80*	1.67	0.70	*2.37*
Guaiacylglycerol	0.09	0.04	*2.17*	0.10	0.05	*2.20*	0.09	0.05	*2.00*
15.52 Syringyl lignan	0.09	0.17	0.55	0.12	0.25	0.49	0.13	0.28	0.46
15.44 Syringyl lignan	0.05	0.10	0.55	0.05	0.10	0.47	0.04	0.10	0.38

Syringylglycerol	0.09	0.09	1.04	0.13	0.12	1.09	0.12	0.13	0.92

Lo S/G represents low S/G ratio; hi represents high S/G ratio

Among the identified metabolites, *p*-hydroxybenzoic acid was released in higher concentrations (up to 6.8 µg/mL) and also showed the most pronounced fold-differences between the two *Populus* phenotypes. In order to test the potential inhibitory effect of *p*-hydroxybenzoic acid, it was added to fermentations of the high S/G *Populus* at two oncentrations and was found to have no measurable impact on fermentation performance (Figure 19).

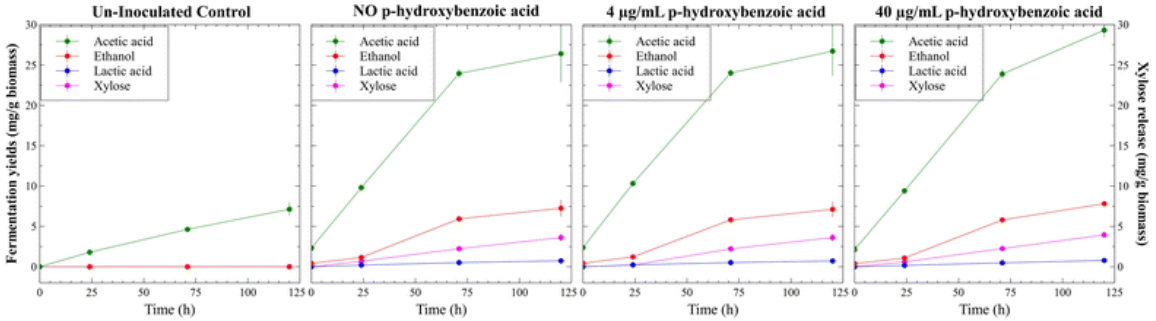

Figure 19 CBP fermentations of the high S/G *Populus* phenotype with additions of potential inhibitor *p*-hydroxybenzoic acid showed no significant effect on metabolic output. The compound was added to the culture medium in quantities that produced final concentrations close to onefold and tenfold the concentrations found in the low S/G cultures. Mean values and standard deviations are shown for triplicate fermentations

5.2.5 *Biomass Characterization: Cellulose Degree of Polymerization, Crystallinity and Lignin Molecular Weight*

Cellulose was isolated from the low and high S/G biomasses, before and after CBP fermentation. The number-average and the weight-average degree of polymerization (DP_n and DP_w, respectively) for cellulose were calculated from molecular weight determinations obtained by gel permeation chromatography (GPC) (Figure 20). The high

ratio S/G *Populus* had marginally longer cellulose chains (i.e., DP_n); however the difference became statistically insignificant after bioconversion (p=0.41). The degree of polymerization increased in both feedstocks following microbial hydrolysis by roughly 19 to 24 units. Polydispersity measurements provide indications of the broadness of molecular weight distributions for polymers. Polydispersity (DP_w/DP_n) calculations indicated the low S/G *Populus* had a wider distribution of cellulose molecular weights (19.1 for low S/G and 16.6 for high S/G *Populus*), which did not change much after fermentation.

Cellulose crystallinity was assessed using ATR-FTIR (attenuated total reflectance - Fourier transform infrared) to determine its relationship to S/G ratio. Peaks at 1430 cm^{-1} and 898 cm^{-1} in the FTIR spectrum are sensitive to changes in crystalline and amorphous cellulose content (381) [23, 24] and thus, the ratio of these peaks provides for comparisons of cellulose crystallinities through the lateral order index (LOI) (Figure 20). The low S/G *Populus* displayed an initially higher crystallinity ratio (p=0.22) compared to the starting high S/G *Populus*, which decreased following CBP conversion (p=0.29). The high S/G biomass started with a lower LOI that increased after microbial conversion (p=0.46). However, differences were not statistically significant at 95% confidence and the wider variations may be credited to heterogeneity in the small subsamples used in this analysis.

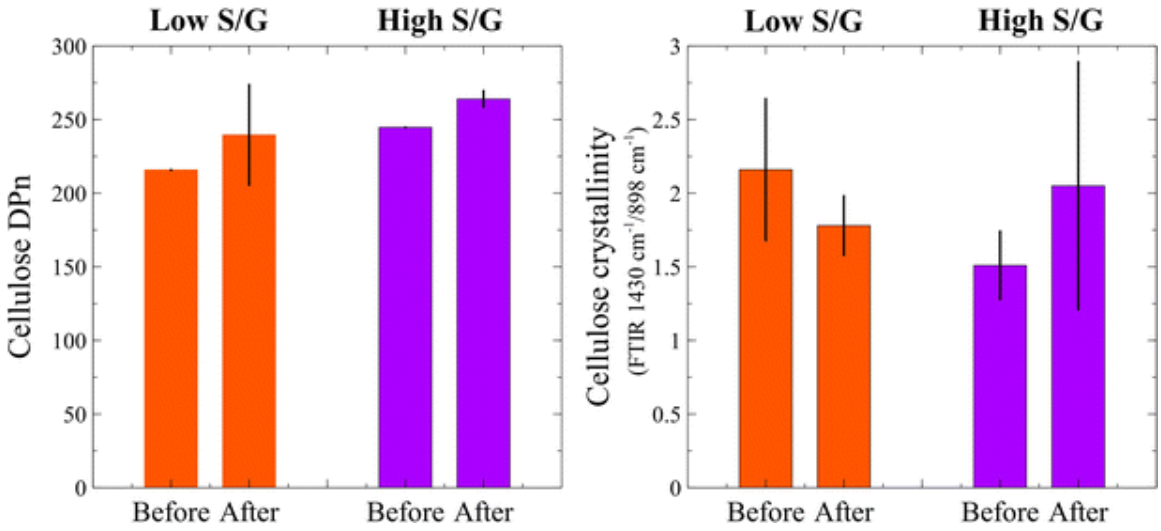

Figure 20 Cellulose number-average degree of polymerization (DP_n) for "low S/G" and "high S/G" *Populus*, before and after CBP bioconversion. In both phenotypes, cellulose chain length increased slightly after fermentation; however, differences in cellulose properties between the two feedstocks are not particularly significant (*left*); the ratio of crystalline to amorphous cellulose showed no significant differences between the two *Populus* phenotypes (*right*)

Lignin was also isolated from the two *Populus* phenotypes before and after CBP conversion and its molecular weight (in g/mol) was determined by GPC. The results pointed to the most meaningful difference between these *Populus* (Figure 21), where the high S/G variant had significantly larger lignin molecular weights than the low S/G biomass ($p<0.01$) in both the initial and the CBP-processed samples. Post-fermentation biomass had modest lignin M_w increases in both phenotypes (although with low statistical significance, $p=0.13$ and $p=0.11$). The polydispersity indices were not different between the S/G variants (i.e., 2.2) and marginally increased to 2.4 only in the high S/G *Populus* after CBP conversion.

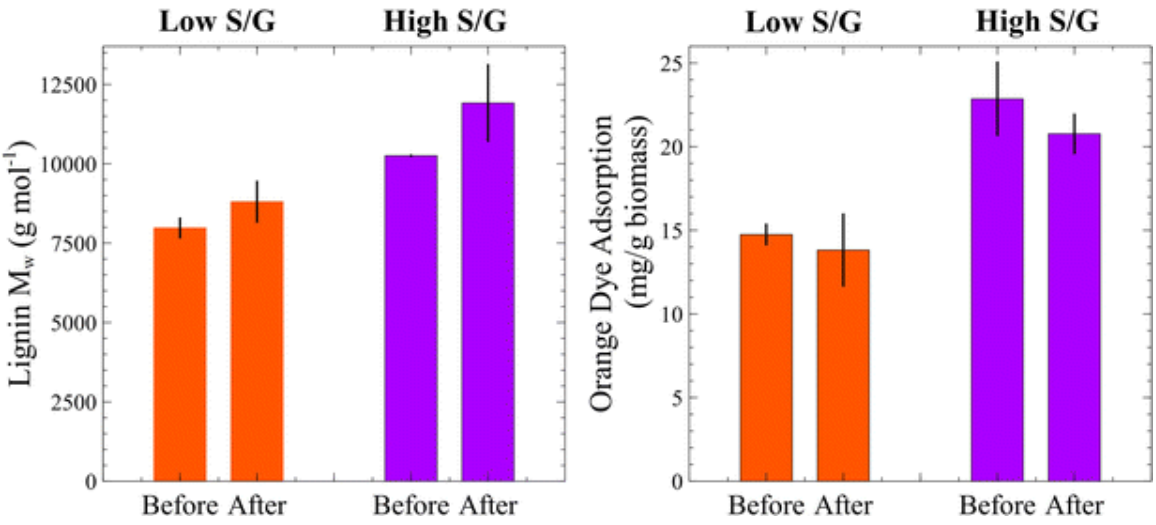

Figure 21 Lignin molecular weights (M_w) are notably larger in the high S/G *Populus* wood before and after CBP conversion (*left*); the direct orange dye adsorption, determined by modified Simons' staining, revealed better cellulose accessibility in the high S/G *Populus* phenotypes before and after fermentation (*right*)

5.2.6 *Simons' Staining: Cellulose Accessibility Measurements*

Simons' staining utilizes mixtures of a small blue dye (~1 nm molecular diameter) and a larger orange dye (~5-36 nm) to characterize cellulose surface porosity (382). In this study, we report the orange dye adsorption values (Figure 21), because the orange dye has a higher affinity to cellulose and is thought to provide a good estimation of enzymatic accessibility to cellulose surface area due to the dye's molecular weight similarity to cellulases and its high binding affinity (383). The high S/G *Populus* had better orange dye adsorption than the low S/G *Populus* ($p=0.04$); and in both cases, these values decreased by small, although statistically not significant, amounts after CBP fermentation ($p=0.60$ for low S/G and $p=0.24$ for high S/G samples).

5.3 Discussion

Based on literature investigations, to our knowledge, the impact of the syringyl and guaiacyl content in various natural and synthetic substrates has been studied almost exclusively using free-enzyme systems. Microbial lignocellulose conversion quite often relies on adherent microbes that have improved access to substrates and in general show better hydrolytic performance than their purified cellulase preparations (384). The objective of this study was to expand our comprehension of lignocellulose recalcitrance to microbial solubilization and in particular when the content of syringyl units is nearly equal to (low S/G ratio) or two-fold higher (high S/G ratio) than the guaiacyl monolignol content. The research presented here investigated a small sample size of a single plant species, and represents a case study intended to identify key biomass properties that impact solubilization of biomass by microbes and purified enzymes. Further validation requires larger sample sets and/or multiple plant species.

Our initial screening of natural *Populus* variants showed *C. thermocellum* bioconversions could be just as sensitive to biomass compositional properties, and in particular with respect to lignin, as hydrolysis with commercial enzyme preparations (307). Microbial hydrolysis of biomass in bioreactors showed a relative 50% improvement in solubilization for the unpretreated high S/G *Populus* compared the low S/G biomass. *C. thermocellum* bioconversion was comparable to the 52% relative difference in the glucose release from the hydrolysis of these plant lines with commercial enzyme blends, which indicate the performance differentiator in microbial conversion is also likely at the level of enzymatic activity, rather than due to disparities in microbial growth. Surprisingly, both *Populus* samples had an average 15% relative reduction in total measured carbohydrates following microbial conversion, while glucan alone was

reduced by 17% to 18% per gram of post-fermentation recovered solid, indicating that glucose extraction, or mining, from the lignocellulosic matrix did not occur preferentially in either *Populus* biomass. The limited solubilization in all tests is typical for the minimally processed (milled, washed and autoclaved) woody biomass that was used to accentuate lignin differences without gross alterations (130, 309). Considering the large relative difference in total solid solubilization between these phenotypes, it is reasonable to conclude that microbial hydrolysis occurred in a similar mechanistic pattern, where the high S/G *Populus* was deconstructed at a faster rate. The evidence denotes less restricted enzyme access to the carbohydrates of the biomass with higher S/G lignin ratio; unfortunately, literature provides little corroboration on the actual mechanisms of complex lignocellulose breakdown by cellulolytic organisms.

A bias towards acetate production was observed in the fermentation of the low S/G *Populus*, and it is thought to be the consequence of lower carbon availability; a phenomenon also observed during the growth of this organism on pure cellulose substrates (385). Previous reports catalogued the release of *Populus*-derived inhibitors against *C. thermocellum* after dilute acid pretreatment (386); however, our fermentation metabolome analysis performed under the same GC-MS technique, did not reveal significant accumulation of these products which may be a result of using different biomass materials and/or different preparation methods. A previously unidentified component, *p*-hydroxybenzoic acid, was observed in this study but also found non-inhibitory when it alone was added in high levels. It remains uncertain if *p*-hydroxybenzoic acid is associated with lignin or hemicelluloses. Under the

circumstances, differences in the activity of cell-bound enzymes could not be linked to the presence of aqueous inhibitors.

It was also important to compare the properties of cellulose and lignin in the two *Populus* samples that had been postulated in the literature to have a role in biomass solubilization, and to observe how these properties changed due to microbial activity. A lower cellulose degree of polymerization (DP) has been typically associated with greater availability of cellulose chain ends and therefore improved hydrolysis (380). Our *Populus* phenotypes, exhibited cellulose of similar average chain length which marginally increased after fermentation, a phenomenon also observed in the utilization of birchwood by *C. thermocellum* (348). In general, lower cellulose crystallinity improves hydrolysis with free-enzymes (200).While cellulose accessibility can be affected by crystallinity, other attributes such as lignin/hemicellulose contents and distribution, porosity can play roles in cellulose digestibility (315) and the influence of crystallinity on consolidated bioprocessing with cellulolytic bacteria is less clear. Cellulose hydrolysis by *C. thermocellum* or its cellulosome has been proposed to occur at equal rates on crystalline and amorphous cellulose (348) and in other instances to occur rapidly on microcrystalline cellulose (83, 201). In the current study, cellulose crystallinity in the two *Populus* tested was not affected by lignin composition, and did not significantly change under CBP treatment. Crystallinity is not considered a performance differentiator in the solubilization of these *Populus* phenotypes.

Lignin molecular weight was the strongest indication of structural differences in the compared biomasses; where a low S/G ratio resulted in greatly reduced lignin molecular weights. These results deviate from previous postulations that syringyl-rich

lignins possess more fragmented structures and smaller molecular weights (307). GPC separates polymers based on molecular size and assumes the polymer of interest to have spherical conformation in solution (387); therefore, variations in calculated molecular weights may be attributed to differences in polymer chain size or conformation (i.e., a given polymer may appear low weight if it was highly branched, or high weight if it was straight chain). Hypothetically, structural disparities between lignins with low and high S/G ratios may stem from the radical polymerization of lignin. Coniferyl alcohol polymerization, which incorporates G-units into lignin, generates a more condensed lignin structure due to increased proportions of carbon-carbon linkages (388). The compact structure of lignin isolated from low S/G *Populus* may manifest itself as a lower molecular weight, whereas the less compact structure of the high S/G phenotype may produce higher relative molecular weights.

Simon stains suggests the potential for greater enzyme accessibility to cellulose in samples with higher syringyl content (382), which points to higher surface porosity in the range of 5-36 nm and above. Although this may explain differences in enzymatic solubilization with free cellulases, this porosity range may not equally aid microbes with much larger footprints (i.e., micron size) which utilize complex, cell-bound cellulosome clusters. However, it remains to be determined whether the correlation between lignin composition and molecular size and the porosity of cellulose fibrils extends to future observations.

5.4 Conclusions

While microbial hydrolysis of unpretreated or minimally pretreated lignocellulosic substrates is considered more efficient than with cell-free enzyme mixtures, we found biomass properties to have equal impact on their capacity to solubilize celluloses and hemicelluloses. In particular, solubilization was greatly improved on the *Populus* phenotype with a higher ratio of syringyl-to-guaiacyl lignin. The results found the two significant properties of *Populus* tested in this study were cellulose accessibility and lignin molecular weight, both positively correlated to the S/G ratio. We suggest that higher syringyl content leads to larger, linear lignin chains, which presents less interference for carbohydrate breakdown by free-enzymes and microbes.

CHAPTER 6. EFFECTS OF BIOMASS ACCESSIBILITY AND KLASON LIGNIN CONTENTS DURING CONSOLIDATED BIOPROCESSING IN *POPULUS TRICHOCARPA*

6.1 Introduction

In biomass, pore sizes are purportedly related to the synergism between fungal enzymes. Depending on their sizes, certain pores may filter enzymes that are too large to pass, thereby separating them from smaller enzymes and reducing the synergy between these enzymes (389). During biomass deconstruction, synergism has been shown to improve the rate and extent of solubilization (390) with fungal cellulases. Hence, reductions in enzyme synergism have detrimental effects in overcoming biomass recalcitrance and lowering the production costs for cellulosic ethanol. Similarly, *Clostridium thermocellum*, a consolidated bioprocessing (CBP) microorganism, relies heavily on enzyme synergism to achieve unprecedented hydrolysis rates. The enzyme synergy is typically attributed to a specific organelle; however, these synergistic relationships in *C. thermocellum* are not clearly defined in terms of accessibility.

The Simons' stain technique assays a fiber's specific surface area (SSA) through semi-quantitative measurements. The SSA, which has been linked to favorable hydrolysis properties, estimates the fiber's exterior and interior surface areas to assess surface area per mass of cellulose. The exterior surface area depends on the fiber width and length, while the interior surface area is determined by the amount of pores and crevices in the fiber as well as the size of the lumen (391). Certain pretreatments remove plant cell wall constituents, thereby altering the cell wall structure and increasing the interior surface area. Accordingly, the Simons' stain is routinely used to determine accessibility following a pretreatment (392-394).

The Simons' stain technique is dependent on two dye, Direct Blue 1 (DB 1) and Direct Orange 15 (DO 15), which typically bind to either small (1 nm) or large (5 to 36 nm) diameter pores, respectively (395). The dye binding patterns are also related to their

individual cellulose affinities; DO 15 has a greater affinity to cellulose than DB 1. The ratio of the DO 15 and DB 1 dyes provides a basis for pore size distribution and accessibility predictions. The diameter of a representative cellulase is 5.1 nm, but cellulases may range between 4 to 7 nm in size (393, 396). There is also evidence that hemicellulose may influence accessibility measurements as determined by other Simons' staining studies (283, 392).

During consolidated bioprocessing, the bacterium deconstructs biomass using cell-bound and cell-free cellulosomes and utilizes cellulose-derived degradation products to yield ethanol amongst other fermentation products. The cell-bound cellulosome is anchored to the bacterial surface via a scaffoldin, whereas the cell-free cellulosome is secreted. The carbohydrate-active enzymes of the cellulosome complex anchor to the scaffoldin through hydrophobic mediated cohesin-dockerin interactions. The cellulosome is 18 nm in diameter —much larger than the estimated 5.1 cellulase diameter. The pore-dependent filtering effect, and therefore accessibility, may exert much less of an impact during consolidated bioprocessing, as many of the enzymes involved in deconstruction are cellulosomal bound. *C. thermocellum* likely peels cellulose microfibrils from the biomass surface as opposed to fungal enzyme systems, which cause pitting in biomass (397). This mode of action may also make pore size (and accessibility) irrelevant as *C. thermocellum* may not require entrance in to pores to carry out CBP; however, Dumitrache et al. have identified accessibility differences with the Simons' stain before and after CBP, which were possibly linked to structural differences in lignin, as contributors to the observed ethanol yields (275).

The negative correlation between biomass porosity and density (398, 399) provides a starting point for the selection and comparison of wood for Simons' staining. Wood density and surface roughness also appear to be interconnected (400), which is possibly due to their relationship to the number of pores. Therefore, these variables may provide useful information for the proposed surface deconstruction of biomass with *C. thermocellum*. Because density has been linked to surface roughness (400) and porosity (398, 399), either of these parameters may provide indications of accessibility through Simons' staining even if the cellulosome does not need to enter the pores.

This investigation examines Simons' staining's relevance to consolidated bioprocessing to assess biomass' susceptibility to microbial solubilization. Biomass porosity, Klason lignin content, surface roughness, and cellulose degree of polymerization were all considered as factors that may affect deconstruction during separate hydrolysis and fermentation (SHF) and CBP.

6.2 Experimental

6.2.1 *Wood Density Characterization*

Wood density analyses were performed on wood cores collected from field grown 4-year-old *Populus trichocarpa* trees in Clatskanie, OR and 3-year old *Populus trichocarpa* trees in Corvallis, OR. All *Populus trichocarpa* used in this study were natural variants. Field establishment, growth conditions, harvesting and process was previously described by Muchero et al. (401) Density was determined using the water displacement method as described by Chave (2005) with no modifications (402). Reproducibility of the density phenotype across the two sites was assessed based on a

common set of 462 genotypes using Spearmann rank correlation analysis. Eight genotypes representing the extreme tails of the phenotypic distribution were selected for accessibility measurements.

6.2.2 *Consolidated Bioprocessing and Separate Hydrolysis and Fermentation*

Non-pretreated milled (0.84 mm screen) poplar was used at 50 g/L, on a dry-weight basis, for the preparation of sterile MTC media for small scale consolidated bioprocessing (CBP) screening. Media for each poplar natural variant was prepared anaerobically at 50 mL culture volume in independent biological duplicates, as previously described (Dumitrache et al., 2016) (275). *Clostridium thermocellum* ATCC 27405, grown in freshly prepared cultures, was used at 10% v/v as inoculum of CBP bottles. Aqueous samples were collected from each bottle immediately after inoculation and following 96 h of incubation at 60°C with constant shaking. Ethanol content was quantified against known standards by HPLC according to standard procedure NREL/TP-510-42623 (403).

Replicate samples of non-pretreated milled poplar were also subjected to a separate hydrolysis and fermentation (SHF) bioconversion process according to previously described methodology (Dumitrache et al., 2016) (275). In short, poplar samples were first enzymatically hydrolyzed at 50°C for 5 days with a mixture of Cellic Ctec2 cellulases (Novozymes North America, Franklinton, NC, USA), Htec2 hemicellulases (Novozymes North America, Franklinton, NC, USA) and the Novozymes 188 β-glucosidase (Novozymes North America, Franklinton, NC, USA) and the resulting aqueous sugars were then fermented at 35°C for 3 days with *Saccharomyces cerevisiae* D7A ATCC 200062 (American Type Culture Collection, Manassas, VA, USA). At end-

point fermentation ethanol yield was determined by HPLC with the same procedure utilized for the CBP process.

6.2.3 *Simons' Stain*

The Simons' stain procedure was based on published methodology (Dumitrache et al., 2016), and no modifications were made (275). The Direct Orange 15 (DO15) and Direct Blue 1 (DB1) dyes, which were supplied by the Pylam Products, Corp. (Garden City, NY) were prepared in Milli-Q water (10 mg/mL). The DB1 dye solution was used as prepared. The DO15 dye was filtered through a 100 K membrane on an Amicon ultrafiltration apparatus (EMD Millipore Corp., Billerica, MA) under 200 kPa of nitrogen gas to remove low molecular mass components of the dye (<100 KDa). Following filtration, 1 mL of the concentrated DO15 dye was weighed and dried for three d in a 105°C oven. After the three d drying period, the mass of DO15 was recorded and diluted to 10 mg/mL. A standard curve was constructed individually for the orange and blue dyes. Each tube contained 0.1 ml of phosphate buffered saline solution (aqueous 0.3 M sodium phosphate and 1.4 mM sodium chloride at pH 6). DO15 or DB1 were added to test tubes in their respective volumes for a total of seven test tubes (0, 0.1, 0.2, 0.3, 0.4, 0.6, 0.8 mL). The test tubes were diluted to volume (1 mL) with water.

Untreated *P. trichocarpa* (10 mg) was weighed into seven centrifuge tubes. DO15 and DB1 were added in a 1:1 ratio in increasing concentrations. Phosphate buffered saline solution was added to each test tube (0.1 mL), and water was added to dilute the mixture to volume (1 mL). The mixture incubated at 70°C for 6 h in a shaking incubator and subsequently centrifuged at 10,252 g for 5 min to separate the remaining dye from the biomass. The supernatant was recovered, and its absorbance was measured

on a Lambda 35 UV-Vis Spectrophotometer (PerkinElmer, Waltham, MA). The absorbance was transformed into O:B ratio according to calculations from Chandra et al. (404).

6.2.4 *Klason Lignin Content Determinations*

Klason lignin contents were determined using a modified version of NREL's *Determination of Structural Carbohydrates and Lignin in Biomass*. Dry, milled (0.84 mm screen) poplar (0.175 g ± 0.005 g) was weighed in flat-bottomed tubes, and 1.5 mL of 72% v/v sulfuric acid (VWR North America, Radnor, PA) was subsequently added. The tubes were placed into the Digiblock digital block heater (Sigma Aldrich, St. Louis, MO) to maintain the temperature at 30°C and stirred every 3 to 5 min for 1 h. Each sample was diluted to 42 mL, while minimizing Klason lignin losses. The diluted samples were autoclaved for 1 h at 121°C and cooled to room temperature. Following acid hydrolysis, the hydrolysis tubes were diluted to volume (50 ml). The hydrolysate was filtered through G8 glass filters to separate sugars from the Klason lignin. The samples were filtered through glass filters to separate the filtrate from the retentate. The remaining solids were heated at 105°C and weighed 24 h later to determine Klason lignin content. The Klason lignin content was calculated by determining the weight (g) of lignin that remains after 24 h as a percentage of the initial mass of the biomass.

The sugars were diluted accordingly and analyzed on a high-performance anion exchange chromatography with pulsed amperometric detection (Dionex ICS-3000, Dionex Corp., USA). The instrument was equipped with a PC10 pneumatic controller, CarboPac PA1 guard column (2 by 50 mm, Dionex, Dionex Corp., USA), a CarboPac

PA1 column (2 by 250 mm, Dionex, Dionex Corp., USA), a conductivity detector, and an AS40 automated sampler. The eluent (0.2 M and 0.4 M NaOH) flow rate was 0.4 ml/min, and the analysis duration was 70 min per sample. The sugar contents were quantified with five standard curves for glucose, mannose, galactose, xylose, and arabinose concentrations. Fucose (1 mg/ml) was used as an internal standard.

6.2.5 *Surface Roughness Measurements*

The logs for the surface roughness measurements were cut to form slices that were further cut to yield 100 mm thick slices. The surfaces of the logs were sanded with 109 μm sandpaper (405) to mitigate irregularities on the log surface from cutting with the band saw. The logs were held at 65% relative humidity until the moisture content of the wood was approximately 12% (340). The surface roughness measurements were carried out at room temperature with a stylus type profilometer (Alpha Step® D-600 Stylus Profiler, KLA Tencor, Milpitas, CA, USA) with a 5 μm diameter stylus tip and a 90° pin angle. The force of stylus tip was 5 mN, and the tracing length spanned 2 mm at a scanning 50 μm/s. The data were acquired in 2D.

6.2.6 *Cellulose Degree of Polymerization*

Cellulose degrees of polymerization (DP) were obtained following delignification of *P. trichocarpa* with peracetic acid (3.5s g/g biomass) (339), Cellulose and hemicellulose were subsequently separated from the resulting holocellulose using two successive sodium hydroxide treatments. During the first treatment, 17.5% sodium hydroxide was added to the holocellulose and stirred for 2 h. The NaOH was then diluted to 8.75% and stirred for an additional 2 h. Cellulose, which was insoluble in solution,

was separated from hemicellulose through filtration through a 0.45 μm polyamide filter. The cellulose was washed via filtration with Milli-Q water, frozen, and freeze-dried. The dry cellulose was vacuum-dried overnight and derivatized with phenyl isocyanate (0.5 mL) in pyridine (4 mL). The derivatization took place over 3 d at 55°C, and the derivatized cellulose was recovered through precipitation in 7:3 methanol:water. The derivatized cellulose was separated from the solution with centrifugation at 8228 g for 10 min, washed 7:3 methanol:water once, and rinsed 2 additional times with Millli-Q water. The solid was air-dried and vacuum dried prior to dissolution (1-2 mg/mL) in the mobile phase (THF).

6.2.7 *Statistical Analysis*

Outlier detection was assessed using the modified z-score (275). Any datum possessing a modified z-score of ±1.5 was considered an outlier and removed from the data set. Statistical analysis for the Simon's stain were conducted on the orange and blue dyes individually for the calculation of the O:B ratio. One-way ANOVA and Tukey's tests were used at 95% confidence to determine significant differences between means.

6.3 Results and Discussion

6.3.1 *Wood Density*

Significant phenotypic variation was observed for the 462 *P. trichocarpa* genotypes at both field sites. At Clatskanie, wood density ranged from 0.22 to 0.72 g/cm^3 while ranges of 0.29 to 0.55 g/cm^3 were observed at the Corvallis field site. Furthermore, the wood density phenotype exhibited significant levels of reproducibility across the two field sites

($r^2 = 0.35$, $p = 0.00$). Based on these data, eight genotypes that exhibited consistently high and low density at both sites were selected for accessibility assessment (Table 16).

Table 16 - Densities (g/cm^3) of the eight biomasses, as determined by the water displacement values

Low density biomass		
	Clatskanie (g/cm^3)	Corvallis (g/cm^3)
GW-9585	0.32	0.33
BESC-316	0.33	0.35
GW-9914	0.34	0.35
GW-9588	0.34	0.35
High density biomass		
	Clatskanie (g/cm^3)	Corvallis (g/cm^3)
KLNA-20-4	0.50	0.53
YALE-27-3	0.50	0.50
BESC-251	0.47	0.53
BESC-7	0.50	0.50

6.3.2 *Simons' Stain*

During Simons' staining, accessibility differences are quantified with the ratio of the orange and blue dyes bound to the biomass, where higher O:B ratios are associated with higher accessibilities. Figure 22 describes the natural variants and their associated O:B ratios. Although the O:B ratios are not optimally grouped into four high and four low extremes, the data illustrate that higher O:B ratios, and therefore higher accessibilities (r^2=0.53), were generally associated with lower density poplar. Theoretically, lower density wood has more void space as density and porosity are inversely correlated (406). Although the Simons' stain is commonly applied to pretreated substrates (283, 404, 407-

409), this study demonstrates that accessibility differences can be observed in non-pretreated biomass with Simons' staining.

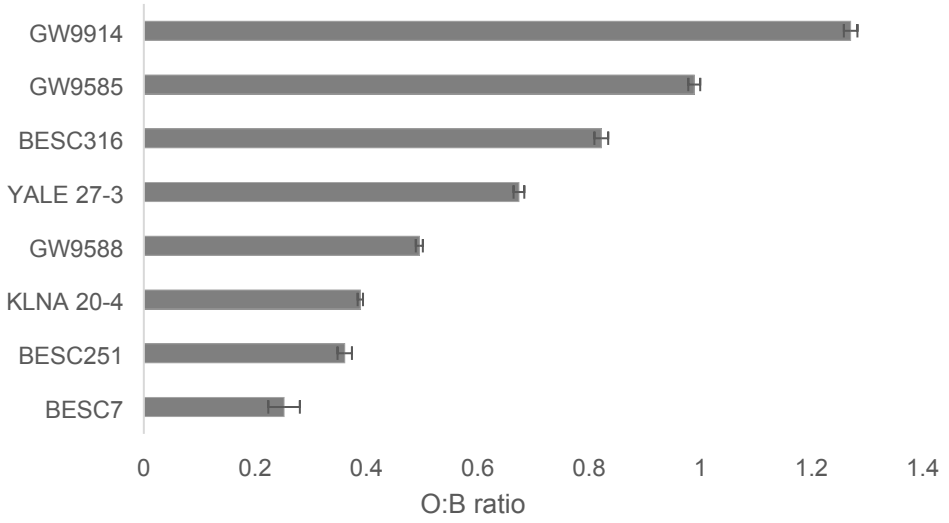

Figure 22 The association between Simons' stain O:B ratios and *P. trichocarpa* (harvested in Clatskanie) densities (g/cm^3).

6.3.3 *Cellulose DPw*

Scanning electron microscopy imaging data has suggested that cellulose structural changes (i.e. fragmentation and deformation) result from pretreatments (410). Accordingly, these changes may influence the cellulose fiber's interior and exterior surface areas, which are assessed during Simons' staining. Though the *P. trichocarpa* in this study were not pretreated, we assessed cellulose degree of polymerizations (DPws) in the natural variants to establish its relationship to accessibility on this basis. Although the cellulose DPws varied by as much as 4000 units between natural variants (Table 17), it appears to be unrelated to O:B ratio (r^2=0.17). Furthermore, it appears that cellulose

DPws are not grouped into high and low extremes as densities are, which further support the lack of relationship.

Table 17 – Cellulose DPws and polydispersity indices from the low and high density *P. trichocarpa*

		Cellulose DPw	SD	PDI	SD
High density	YALE 27-3	2939	56	4.18	0.20
	BESC-251	5452	28	4.11	0.13
	KLNA 20-4	5966	20	6.65	0.03
	BESC-7	3207	114	3.11	0.49
Low density	GW-9914	7250	68	3.59	0.11
	GW-9585	5436	64	4.46	0.10
	GW-9588	5870	418	3.97	0.30
	BESC-316	3932	4	3.07	0.0

SD: standard deviation

6.3.4 *Klason Lignin*

The Klason lignin contents of the eight natural variants, which varied between 20.3 and 25.1%, are displayed in Figure 23. Klason lignin contents may influence the progression of CBP as *C. thermocellum*'s cellulases have been found to adsorb to lignin.(358) Significant differences in Klason lignin contents existed between several poplar including GW-9914 and BESC-7, GW-9914 and BESC-316, and GW-9914 and YALE 27-3 ($P<0.05$). Interestingly, Klason lignin contents exhibited a weak linear relationship with O:B ratio ($r^2=0.33$). A linear plot between Klason lignin contents and O:B ratio revealed two relatively well-defined groupings of high Klason lignin contents and low accessibilities and vice-versa (Figure 24). Hemicellulose contents did not demonstrate significant differences between BESC-251, GW-9914, and BESC-7 ($P>0.05$).

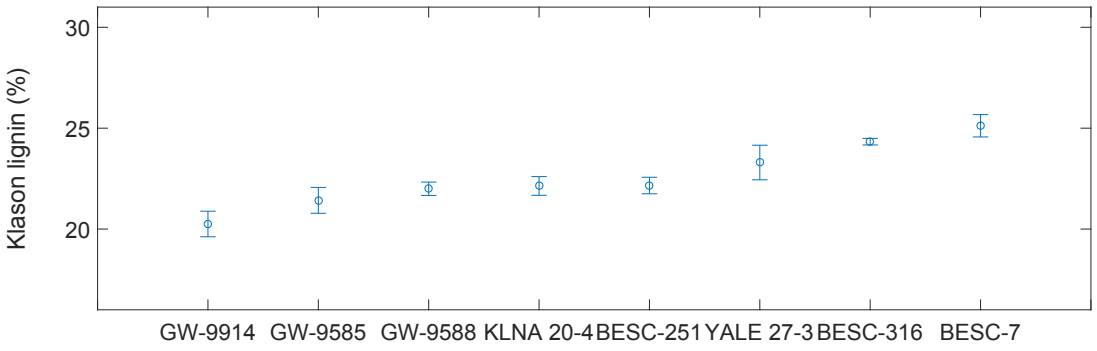

Figure 23 The Klason lignin contents of the eight natural variants of *P. trichocarpa*

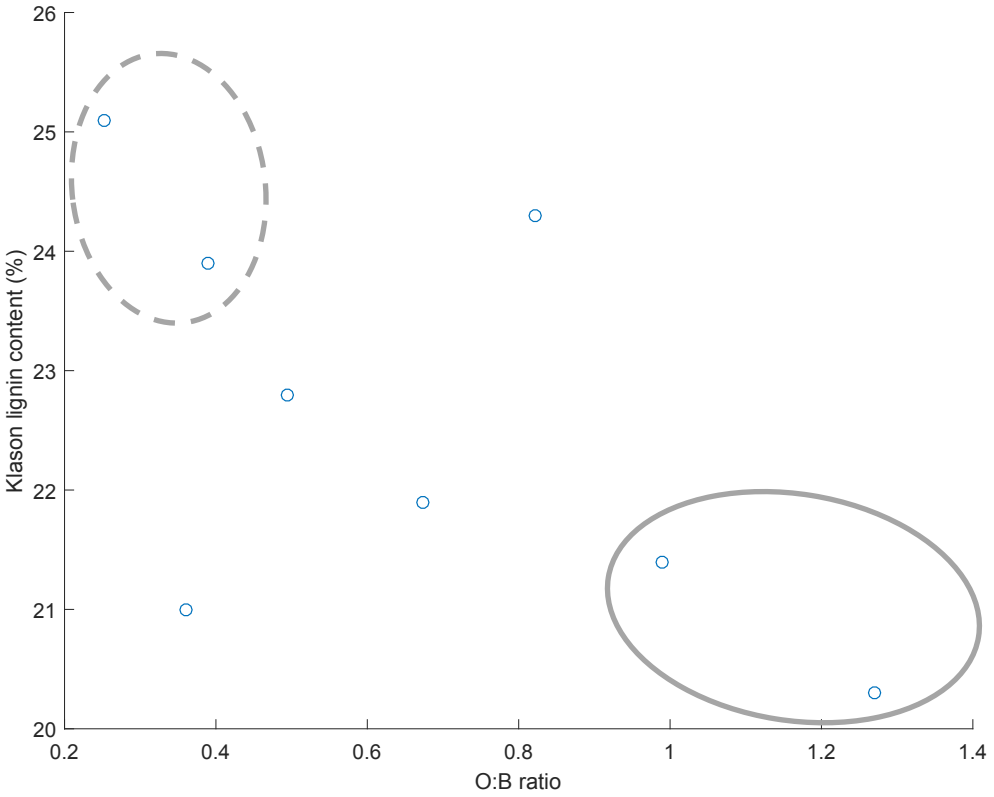

Figure 24 The association between O:B ratio and Klason lignin content (%). Dotted circle represents high Klason lignin contents and low O:B ratio, and solid circle represents low Klason lignin contents and high O:B ratio.

6.3.5 *Surface Roughness*

Surface roughness measurements were expected to identify whether the porosity extremes are manifested at the biomass surface, where *C. thermocellum* is believed to carry out CBP. Surface roughness measurements were designed to determine if these irregularities influence *C. thermocellum*'s interactions with the wood surface and promote the hydrolytic activity of a CBP microorganism. In Figure 25, the low density biomasses generally possessed higher average roughness (Ra), reduced valley depth (Rv), and reduced peak depth (Rp) values than the high density biomasses. The surface roughness measurements, similar to the density data, were grouped into two extremes, which verify that the porosity differences are manifested at the surface of the wood.

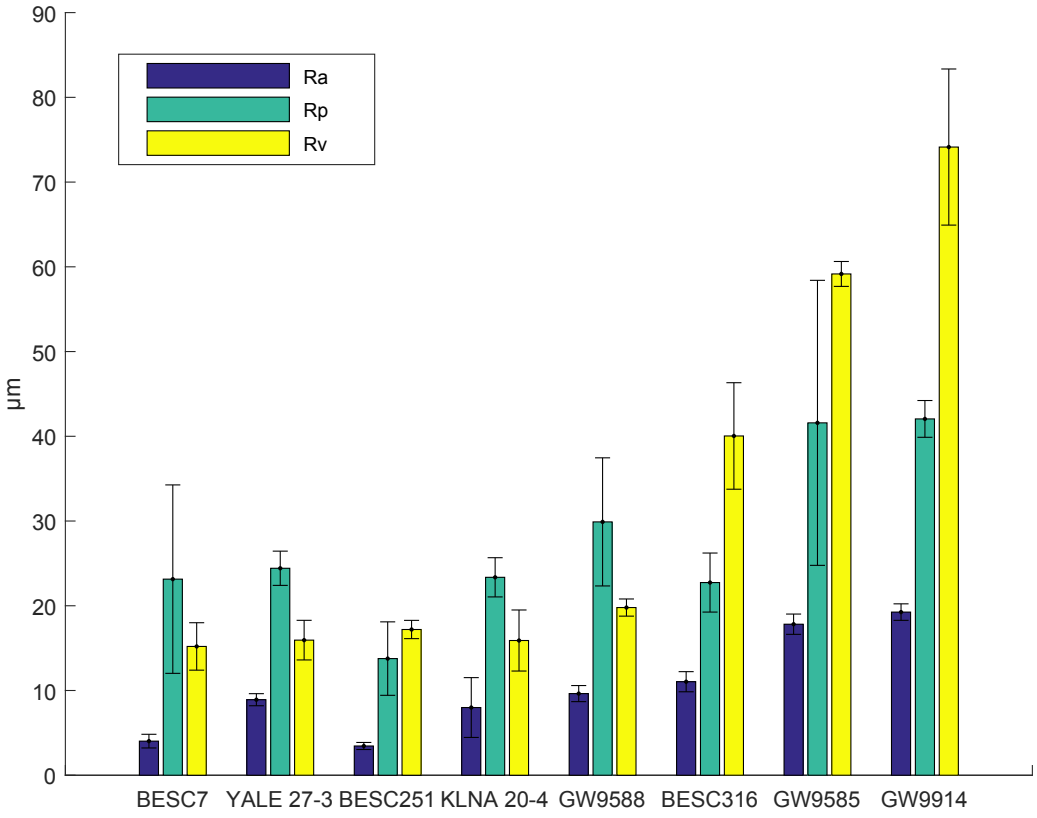

Figure 25 Average roughness (Ra), reduced peak height (Rp), and reduced peak depth (Rv) of the high and low density biomass

6.3.6 *Ethanol Yields from SHF and CBP*

Although SHF generated better ethanol yields than CBP, BESC-7 consistently produced low ethanol yields, whereas GW-9914 consistently produced one of the highest ethanol yields (Table 18). While the differences in ethanol production were not significantly different between BESC-251 and GW-9914 during CBP ($P>0.05$), the two means were found to be different in SHF ($P<0.05$). During SHF, the higher porosities may have facilitated cellulase entry during hydrolysis. and the higher concentrations of glucose may account for the ~20 mg/g discrepancy in ethanol yields between GW-9914 and BESC-251, assuming the threshold for sugar inhibition was not reached. *S.*

cerevisiae possesses impressive ethanol tolerance (411) and achieves high ethanol productivities (412), which may account for the higher ethanol yields during SHF than with CBP.

Surface irregularities, which are likely associated with porosity in this study, appear to be relevant to CBP with *C. thermocellum*. Surface roughness values identified GW-9914 and BESC-7 with the roughest and smoothest surfaces, respectively. Hence, Simons' staining porosity measurements can provide useful information about the biomass surface.

Klason lignin content may hold importance in the observed CBP trends. Total lignin content alone, when above 20% (w/w), has not been strongly correlated with improved enzymatic hydrolysis of poplar (307). In this study, however, Klason lignin content and accessibility may be indirectly related to hydrolysis by fermentation yields. The best and poorest ethanol yielding biomass demonstrated noticeable differences in Klason lignin content and accessibility. GW-9914 possessed the lowest Klason lignin content, whereas BESC-7 possessed the highest. Furthermore, GW-9914 was predicted to be most accessible, whereas BESC-7 was predicted to be least accessible. Hence, the Klason lignin contents and accessibility appear to be related to the extent of fermentation.

SHF			CBP		
	Ethanol Yield (mg/g biomass)	SD		Ethanol Yield (mg/g biomass)	SD
BESC-7	24.24	0.24	BESC-7	0.17	0.04
KLNA-20-4	30.44	1.12	BESC-316	0.34	0.03
GW-9585	33.41	0.57	GW-9588	0.35	0.01
BESC-316	35.96	0.36	GW-9585	0.50	0.08
GW-9588	37.34	1.29	YALE-27-3	1.69	0.16
YALE-27-3	39.23	0.68	KLNA-20-4	1.81	0.33
BESC-251	39.52	0.11	GW-9914	2.68	0.59
GW-9914	61.83	2.61	BESC-251	2.77	0.89

SD: standard deviation

Table 18 – Ethanol yields (mg/g biomass) from SHF with *Saccharomyces cerevisiae* and CBP with *C. thermocellum*

6.4 Discussion

Few studies have suggested that lignin content and/or structure play a role in the efficiency of CBP (67, 309); however, there is only one known study that establishes a relationship between the Simons' stain and CBP (275). Neither the SHF nor the CBP ethanol yields clearly pointed towards a dominating effect of either variable; however, the two may be related as higher Klason lignin contents may limit enzyme or cellulosomal accessibilities. Regardless, studies suggest that lignin content contributions amongst other factors impact ethanol production (413, 414). For example, Grabber et al. reported that lignin content, in addition to lignin-ferulate crosslinking, was more influential than lignin composition during fermentation. In Grabber's study, elevated Klason lignin contents (128 mg/g biomass) were linked to 12-fold increases in hydrolysis

lag times compared to the nonlignified counterparts (5 mg/g biomass), when fungal cellulases were employed (413). In this study, we observed much lower ethanol yields during CBP as compared to SHF, which may be attributed to a more potent or confounded effect of lignin on *C. thermocellum*'s cellulases and cellulosome.

Although accessibility and density were related in this investigation, their relationship with ethanol yields, lignin content, and cellulose DP are less well-defined. There was no significant correlation between wood density and lignin content in the 462 genotypes evaluated ($r^2 = 0.004$, $p = 0.92$); however, this observation suggests that the two phenotypes may have synergist but independent effects on cell wall deconstruction. During SHF and CBP, low and high density biomasses regularly produced ethanol yields that were not significantly different from one another ($P>0.05$). The observed trends in BESC-7 and GW-9914 suggest that Klason lignin contents play a role in O:B Simons' stain measurements. Meng et al. (2015) have proposed that lignin exerts a minimal impact on cellulose accessibility; however, lignin likely limits xylan accessibility, which negatively influences cellulase accessibility to cellulose (392). Shao et al. formed similar conclusions, arguing that hemicellulose influences accessibility during CBP (415). Higher Klason lignin contents may indicate a similar trend of lignin on hemicellulose accessibility and the binding of orange and blue dyes to cellulose.

The predicted least and most accessible poplar generated some of the worst and best ethanol yields, respectively. Klason lignin contents and accessibilities of the aforementioned poplar may work together in restricting ethanol yields. To further understand this occurrence, future studies can assess the CBP ethanol yields when lignin contents are not significantly different from one another and accessibility varies or when

accessibilities remain constant while lignin contents vary. In this study, Simons' staining successfully identifies accessibility differences that are present in top and poor-performing poplar, but Klason lignin content appears to be an important factor in ethanol yields. Accessibility alone, as predicted by Simons' staining, does not appear to be a sole predictor of biomass susceptibility to CBP.

CHAPTER 7. THE STRUCTURAL CHANGES TO *POPULUS* LIGNIN DURING CONSOLIDATED BIOPROCESSING WITH *CLOSTRIDIUM THERMOCELLUM*

7.1 Introduction

Consolidated bioprocessing (CBP) has often been regarded as an effective and potentially revolutionary process for the commercialization of cellulosic ethanol (132, 416-418). CBP microorganisms address challenges associated with enzyme production (419) and biomass recalcitrance (2) that plagued ethanol production from fungal cellulases. *Clostridium thermocellum*, a thermophilic and anaerobic CBP microorganism, produces cellulosomes to deconstruct the plant cell wall architecture and utilizes primarily cellobiose and glucose to generate fermentation products such as ethanol and acetate. Few investigations have successfully identified changes to cellulose (280, 348) and hemicellulose (196) during CBP, while the current understanding of the structural changes to lignin during CBP still remain in its infancy (275).

Lignin is a key contributor to biomass recalcitrance. For instance, it inhibits enzyme accessibility and reduces enzyme activity by non-productive enzyme adsorption (370). Likewise, lignin influences biomass conversion during CBP (365), and the interactions between lignin and CBP microorganisms suggest that

lignin content and structure affect CBP (275, 364). Even though lignin introduces recalcitrance during CBP, *Clostridium thermocellum* contains at least 70 enzymes (420) that alter plant cell wall components, which in some cases reduce recalcitrance. Its pectinanses (421), chitinases (422), cellulases (423), amylases (424), β-glucanases (425), and hemicellulases (196, 426) include the host of enzymes available to *C. thermocellum* to modify the plant cell wall components and access cellulose. Although lignin is a major cell wall component and known contributor to recalcitrance, *C. thermocellum* contains no known lignin modifying enzymes, whose presence would be especially useful in accessing cellulose. To verify the static nature of lignin during CBP, lignin structure was studied using two spectroscopic techniques: NMR and FTIR spectroscopy.

7.2 Experimental

7.2.1 *Materials*

Two natural variants of *Populus trichocarpa*, which were harvested from Clatskanie, OR, were supplied by the Biosciences Division at Oak Ridge National Laboratory. All chemicals including ethanol, toluene, dimethylsulfoxide (DMSO-d_6) and hexamethylphosphoramide (HMPA-d_{18}) that were used in this study were purchased from VWR, Sigma-Aldrich or Armar Chemicals.

7.2.2 *Consolidated bioprocessing*

Consolidated bioprocessing was conducted with autoclaved *Populus trichocarpa.* Sterile media for thermophilic *Clostridia* (MTC) were prepared in 50 mL culture volumes

under anaerobic conditions. Freshly prepared *Clostridium thermocellum* ATCC 27405 was used at a 10% (v/v) inoculum in batch bottle fermentations. CBP was conducted at 50 g/L (dry basis) biomass loading for five days at 58 °C and 300 rpm. The fermentation broth was centrifuged to separate the solid residuals from the spent enzyme broth. The recovered residuals were freeze-dried for spectroscopic analyses.

7.2.3 *Whole-cell Wall Analysis with Nuclear Magnetic Resonance (NMR) spectroscopy*

P. trichocarpa were Soxhlet-extracted with an ethanol/toluene mixture (1:2, v/v) for 8 h to remove extractives. The extractive-free samples were air-dried and ball-milled using a planetary ball mill (Retsch PM 100) at 600 rpm. Grinding occurred in zirconium dioxide (ZrO_2) vessels (50 mL) using ZrO_2 ball bearings (10 mm × 10) for 2 h and 26 min (5 min grinding and 5 min break) for whole cell wall NMR analysis. The ball-milled biomasses (~50 mg) and DMSO-d_6/HMPA-d_{18} (4:1 v/v, ~0.5 mL) were loaded in a 5 mm NMR tube. The biomass and NMR solvents were vortexed to form a uniform gel, and placed in a sonicator for 1-2 h before analysis. The NMR spectra were measured at 298 K using a Bruker Avance III 400 MHz console equipped with a 5 mm Broadband Observe (BBO) probe. Two-dimensional (2D) ^{1}H–^{13}C heteronuclear single quantum coherence (HSQC) spectra were collected using a Bruker standard pulse sequence ('hsqcetgpsi2'). The measurement parameters are as follow: spectral width of 11 ppm in F2 (^{1}H) with 2048 data points and 190 ppm in F1 (^{13}C) with 256 data points, 64 scans (NS) and 1 s interscan delay (D1). Volume integration of contours in NMR spectra was carried out using Bruker's TopSpin 3.5 software. For quantitating lignin subunits, the $S_{2/6}$, $S'_{2/6}$ (oxidized), G_2, and $PB_{2/6}$ contours were used. Lignin interunit linkages were also

measured with the α-position of each unit (β-*O*-4, β-5, and β-β) as described in our previous study (427).

7.2.4 *Fourier Transform Infrared (FTIR) spectroscopy*

Lignin-enriched residues, which were prepared according to a previous study (275), were analyzed with a Perkin Elmer 100 FTIR spectrometer (Wellesley, MA) with a universal attenuated total reflection (ATR) accessory. The FTIR spectra were acquired with 32 scans at 4 cm^{-1} resolution from 4000 to 800 cm^{-1}. The S/G index was measured by normalizing the spectra to 1505 cm^{-1} and subsequently dividing the peak at 1328 cm^{-1} (C-O in syringyl lignin) by 1233 cm^{-1} (C-O in guaiacyl lignin), as discussed in the previous study (428).

7.3 Results

7.3.1.1 Whole-cell Wall Analysis

To establish structural changes during CBP with *Clostridium thermocellum*, lignin structure in two natural variants (BESC-102 and BESC-922) of *P. trichocarpa* was characterized. Nuclear magnetic resonance (NMR) spectroscpic analysis was conducted to analyze the structural properties of lignins in the whole plant cell wall before and after CBP with *Clostridium thermocellum.* Figure 26 presents the 2D two-dimensional heteronuclear single quantum coherence (HSQC) $^{1}H–^{13}C$ NMR spectra of the whole-cell walls for a control (BESC-102 and BESC-922) and CBP-treated (BESC-102T and BESC-922T) *P. trichocarpa*. Qualitative analysis identified syringyl (S), guaiacyl (G), and hydroxycinnamates (*p*-

hydroxybenzoate) in the aromatic regions of the NMR spectra. Also, the relative contents of S and G lignins were determined by integration at the $S_{2/6}$ and G_2 contours, which occurred at approximately δ_C/δ_H 104.0/6.66 and 111.2/6.98 ppm, respectively. The *p*-hydroxybenzoate (PB) content was measured with the $PB_{2/6}$ contour at 131/7.63 ppm. The lignin inter-unit linkages were also observed in the aliphatic region of the NMR spectra. The cross peaks for β-aryl ether (β-*O*-4), resinols (β-β), and phenylcoumaran (β-5) were quantified at the α-position of each linkage at δ_C/δ_H 72.2/4.90, 87.0/5.48, and 85.0/4.74 ppm, respectively

Table 19 displays the semi-quantitative analysis of lignin S/G ratio, PB content, and the three major inter-unit linkage contents in the *P. trichocarpa* examined in this study. Lignin S/G ratios increased in both *P. trichocarpa* natural variants following CBP. In particular, the *P. trichocarpa* with a higher initial lignin S/G ratio (BESC-922) showed a more notable increase in lignin S/G ratio from 2.69 to 2.95. The PB content experienced a 1-2% decrease with both *P. trichocarpa* natural variants. The β-*O*-4 linkage represented the largest relative proportions (66-68% over total lignin subunits) among lignin inter-unit linkages in the untreated *P. trichocarpa*. The β-*O*-4 content in both *P. trichocarpa* natural variants decreased by 7-8% after CBP. The relative proportions of the carbon-carbon linkages such as β-5 and β-β did not show noteworthy changes as compared to β-*O*-4 content after CBP. In BESC 922, more than half of β-5 linkages were removed, while the change in β-β content was minor after CBP.

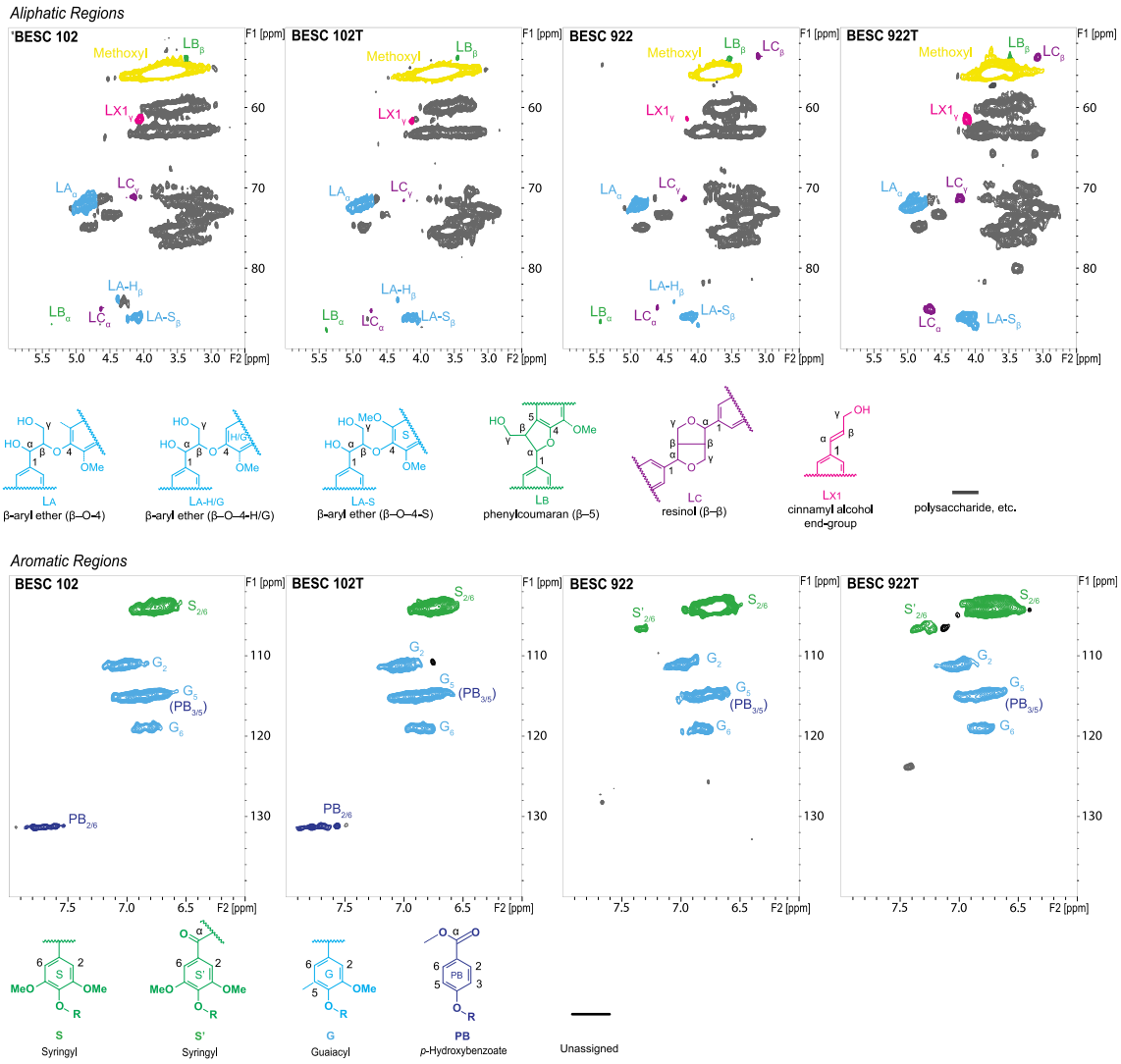

Figure 26 The 2D HSQC ^{1}H – ^{13}C NMR spectra of the whole-cell wall for the control (BESC-102 and BESC-922) and CBP-treated (BESC-102T and BESC-922T) *P. trichocarpa*.

Table 19 – Lignin S/G ratio, hydroxycinnamates (p-hydroxybenzoate, PB), and inter-unit linkages as determined by whole cell wall NMR analysis.

	Aromatic region		Aliphatic region		
	S/G	PB (%)	β-O-4 (%)	β-5 (%)	β-β (%)
BESC-102	0.96	13	66	1.3	1.5
BESC-102T	1.00	12	59	1.5	1.1
BESC-922	2.69	4	68	2.2	4.8
BESC-922T	2.95	2	60	0.8	4.3

7.3.1.2 Lignin structural analysis with ATR-FTIR

In previous studies, Fourier transform infrared (FTIR) has been applied to observe changes to lignin with fungal cellulases (429, 430). For example, studies have found that the carbonyl peak intensities in lignin's fingerprint region, 1800 to 600 cm^{-1}, decreased as lignin-degrading enzymatic activities ensued (429, 430). Lignin also elucidates structural changes to lignin (428). In this study, ATR-FTIR was used to assess changes to S and G lignins in lignin-enriched residues from untreated and CBP-treated *P. trichocarpa*. The peak intensities, which were normalized to 1505 cm^{-1}, were compared in Figure 27. The ratio of peak intensities at 1328 and 1233 cm^{-1}, which represent C—O in syringyl lignin and

C—O in guaiacyl lignins respectively, were used to calculate an alternative index for S/G ratio (428). Similar to the 2D NMR experiments, the S/G index for BESC-102 (1.08) was lower than that of BESC-922 (1.11). In BESC-102, the index was essentially unchanged between lignin from control and CBP-treated samples, as the difference may have been too small for FTIR to detect; however, BESC-922's S/G index increased from 1.11 to 1.15 following CBP. In this study, both NMR and FTIR analysis results indicated similar trends in lignin S/G ratio due to CBP.

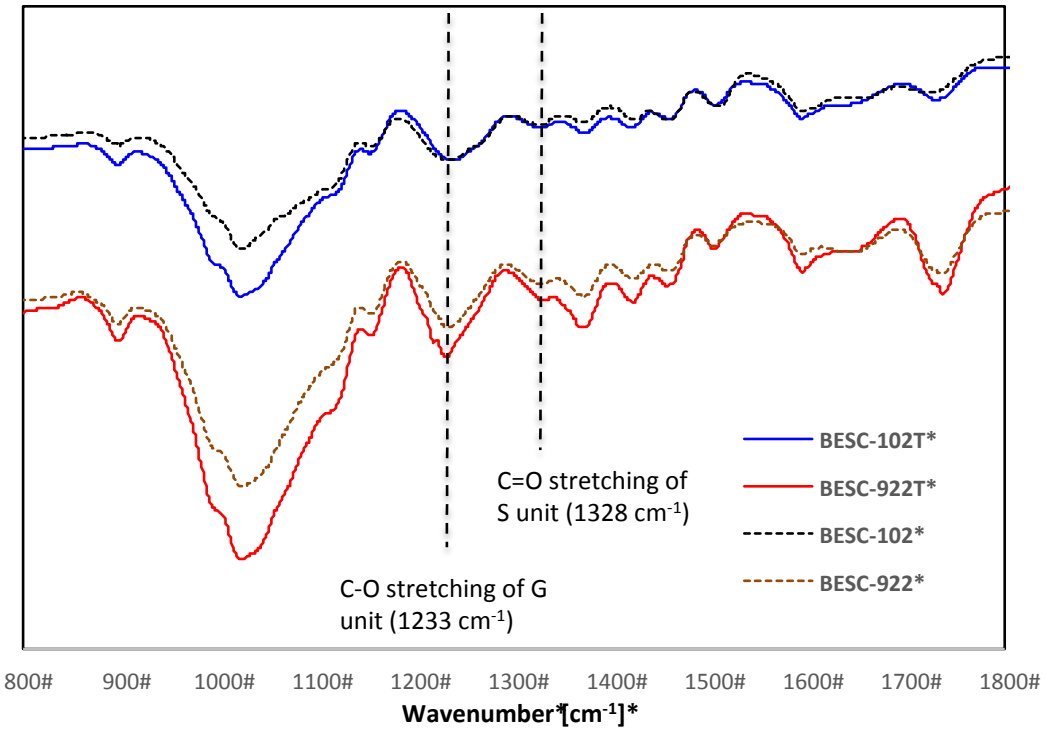

Figure 27 FTIR spectra of the four *P. trichocarpa* before and after CBP with *C. thermocellum*

7.4 Discussion

The observed transformations in lignin reported in this and our previous study (275) suggest that *C. thermocellum* catalyzes bond cleavage in lignin. Any

enzymes that catalyze these changes (i.e. increased S/G ratio, decreased β-O-4, and decreased β-5) would be different from the fungal enzymes that are known to catalyze similar reactions. Wei et al. studied gene expression in *C. thermocellum* during CBP on pretreated yellow poplar and found that the genes that traditionally encoded lignin degradation involving enzymes such as lignin peroxidase (LiP), laccase, or manganese peroxidase (MnP) were not identified from transcriptomic profiling (431). The absence of these enzymes does not negate the presence of other lignin modifying enzymes in *C. thermocellum* that are specific to bacteria. For example, the bacterium *Pantoea anantis* Sd-1 hydrolyzes cellulose, hemicellulose, and lignin (431). Nonetheless, microbial β-etherases, a class of microbe specific enzymes that remove β-*O*-4 bonds in lignin, could be possible enzymes for the lignin alteration (432, 433). However, additional studies are needed to identify the enzymes involved in lignin degradation by *C. thermocellum*.

Phenolic groups have been recognized as a common initiation site for enzymatic depolymerization of lignin (434). Additionally, steric effects and substituent properties largely influence the ease of phenolic radical generation (435). The increase in lignin S/G ratio is attributed to the removal of G lignin, whose phenolic group is less sterically hindered than S lignin. The reduced peak integration intensities, as determined by HSQC, in G lignin following CBP further support this notion. *C. thermocellum* may also remove PB during biomass deconstruction, according to the data collected during this study. PB's unhindered phenolic group renders it a viable starting site for chemical reactions; however, the

strong electron withdrawing substituent at the *para* position on the aromatic ring may negatively impact its reactivity.

Lignin modification may also be important in that lignin has been found to participate in electron transfer reactions with enzymes that facilitate its degradation. Versatile peroxidases isolated from *Pleurotus eryngii*, a fungus, appear to rely on lignin for direct electron transfer reactions (436). Harvey et al. argue that the peroxidases in the fungus *Phanerochaete chrysosporium* begin the breakdown of lignin following the single electron transfer from the aromatic ring to its oxy-ferryl active site (437). To our current knowledge, similar relationships between lignin and cellulosomal enzymes have not been established in *C. thermocellum*. Although additional research will pinpoint lignin-degrading enzymes, structural changes to lignin were observed during pH controlled CBP. Nonetheless, this heteropolymer remains a hindrance to CBP.

Aside from glucose, the core substrate of current cellulosic ethanol, lignin has several growing outlets for biomass valorization (438). Various studies have proposed using lignin generated from ethanol production for biomass-derived materials, chemicals, and fuels using catalysis (439), enzymes (440), microorganisms (441, 442) and pyrolysis (443) to achieve the desired end products. The structure of lignin, whether derived from biomass, pretreatment, or cellulosic ethanol processing, influence its suitability for future processing. Oftentimes, it is desirable that lignin possesses certain structural features such as high S/G ratio or high β-*O*-4 contents that facilitate subsequent processing (444).

The resultant lignin in the fermentation residues is relevant to a number of applications. Industrial scale ethanol production from CBP will warrant lignin valorization to maximize the profitability of the major biomass components. Accordingly, lignin structure following CBP will dictate the ease and choice of processing. The results in this study show that modification to lignin structure are minor following CBP. Therefore, lignin structure is expected to be reasonably preserved during CBP, which has important implications for β-*O*-4 content and S/G ratio. Several recent studies into pyrolysis and its product heterogeneity employed β-*O*-4 model compounds (445-449), which indicate that these bonds are of particular interest in lignin upgrading. In other lignin valorization applications, chemical conversions commonly target the β-*O*-4 linkage (450-453). *Populus* lignin after CBP still contained ≥59% β-*O*-4 contents over total lignin subunits in this investigation, which render lignin from CBP especially relevant to valorization.

The S/G ratios also exhibited relatively minor changes, meaning that CBP did not drastically alter lignin. The low S/G ratio lignin natural variant would be a competitive starting material for carbon fibers, because low S/G ratios have been associated with higher glass transition temperatures, greater cross-linking, and higher molecular weights, which promotes its function in carbon fibers (454).

7.5 Conclusions

In sum, the effects of *C. thermocellum* on *P. trichocarpa* lignin structure were investigated using 2D HSQC NMR and FTIR analyses. The alteration of

lignin, such as lignin S/G ratio and β-*O*-4 content, during CBP indicated that *C. thermocellum* presumably interacts with lignin in the biomass; however, these changes were not significant. Accordingly, the CBP-treated lignin without significant modification of structural properties possesses properties that improve its attractiveness for valorization.

CONCLUSION

Biomass is an underutilized resource for renewable energy; however, biomass requires a cost-effective process to improve its economic feasibility as a cellulosic ethanol fuel source. Integration of the conventional four-stage process scheme opens opportunities for drastic cost reduction. Integration manages variables such as temperature gradients between former and subsequent stages as well as reduces chemical and energy demands required to produce ethanol. *C. thermocellum* not only inherently carries out process integration to generate ethanol but also possesses a cellulosome, a powerful accessory that promotes synergistic relationships between enzymes during deconstruction.

Several reports have successfully modified the metabolic processes required to enhance ethanol yields (455-457) in *C. thermocellum* to redefine its relevance to large-scale cellulosic ethanol production. Although these reports signify substantial strides towards advancing *C. thermocellum*, these studies oftentimes underemphasize the

chemistries of cellulose, hemicellulose, and lignin and their resulting impact on CBP. In particular, the studies presented in this work have demonstrated that biomass structure influences the extent of CBP.

Although CBP can potentially lower ethanol production costs, lignin remains a substantial barrier. In each investigation, lignin negatively impacted hydrolysis and/or fermentation during CBP. Lignin may impair cellulosomal hydrolysis efficiencies because *C. thermocellum*'s enzymes are inhibited by previously established recalcitrant features (i.e. low S/G ratio, high lignin contents, etc.) that result in nonproductive binding and reduced accessibility. Unlike in *C. thermocellum*, the limited hydrolysis of fungal cellulases poses the greatest concern during the hydrolysis stage as large-scale fermentations for ethanol production are well-established. Costs are driven up as more vigorous chemical and energy inputs are required to convert cellulose into ethanol. In *C. thermocellum*, recalcitrance appears to have a multi-fold effect. Limited hydrolysis may reduce the concentrations of available sugars, which in turn decreases ethanol production as there are fewer starting materials available for metabolism. Though it was not fully explored in these studies, lignin may also generate products that interfere with metabolism in during CBP.

Overall, *C. thermocellum* is a feasible alternative to fungal enzymes, and its benefits over fungal cellulases warrant further research. Unfortunately, modifications to biomass structure are inevitable to make ethanol more competitive on an industrial scale in either matrix. Lignin is once again a major impediment to biomass solubilization as recalcitrance may limit hydrolysis, fermentation, and bacterial metabolism.

FUTURE RECOMMENDATIONS

The works presented consistently identified lignin as a limiting agent to CBP. Specifically, lignin content and structure were regularly identified as prominent, influential factors. Although the data gathered provide a compelling case for the role of lignin, additional experimentation will provide more detail surrounding the conclusions reached.

Firstly, future studies into recalcitrance should be carried out with *C. thermocellum*'s cellulosome to provide an alternative view of the challenges biomass presents during hydrolysis. For example, the inhibitory effect of lignin content on cellulosomal hydrolysis could be studied by hydrolyzing Avicel in the presence of lignin model compounds. Lignin adsorption measurements could also be conducted to provide support for nonproductive binding to cellulases associated with the cellulosome.

Cellulosomal studies would also clarify if the lignin degrading enzymes are cellulosomal bound or not. Both 2D HSQC NMR and ^{31}P NMR would provide valuable evidence of cellulosomal induced lignin structural changes. 2D HSQC NMR would provide a holistic view of lignin S/G ratio and interunit linkages, while ^{31}P NMR would provide estimations of the phenolic group contents. If 2D HSQC NMR identifies structural changes to lignin in several natural variants, phenolic group estimations will help to determine whether the phenolic –OH participates in lignin structural modifications. If these techniques determine that negligible changes occur, lignin structure may have a greater bearing its interactions with cellulases.

This work also warrants further investigation into lignin S/G ratio and its relationship to lignin structure. Higher S/G ratio lignin was associated with improved biomass solubilization. Lignin molecular weight and biomass accessibility were the only properties that demonstrated noteworthy differences between the low and high S/G ratio biomass. Because lignin molecular weight was determined using a relative technique, molecular structure can influence the apparent molecular size and hence the estimations of molecular weight. To determine the absolute molecular weight of lignin, light scattering can be used. If the data gathered during light scattering verify the trend observed with the GPC, high S/G ratio lignin is heavier in molecular weight than low S/G ratio lignin. If absolute molecular weights are not significantly different from one another, then the differences in molecular weight as determined by the GPC is likely due to structure (i.e. linearity or compactness).

While the properties of cellulose and hemicellulose require additional attention to assess their contributions to recalcitrance, lignin has demonstrated its involvement reducing the efficiency of CBP. Understanding lignin's detrimental effect will open opportunities for combating recalcitrance in this promising process, and ideally pave the way for cost-effective ethanol production.

REFERENCES

1. Alcántara MÁB, Dobruchowska J, Azadi P, García BD, Molina-Heredia FP, Reyes-Sosa FM. Recalcitrant carbohydrates after enzymatic hydrolysis of pretreated lignocellulosic biomass. Biotechnology for Biofuels. 2016;9(1):207.

2. Himmel ME, Ding S-Y, Johnson DK, Adney WS, Nimlos MR, Brady JW, et al. Biomass Recalcitrance: Engineering Plants and Enzymes for Biofuels Production. Science. 2007;315(5813):804-7.

3. Yang B, Dai Z, Ding S-Y, Wyman CE. Enzymatic hydrolysis of cellulosic biomass. Biofuels. 2011;2(4):421-49.

4. Pu Y, Hu F, Huang F, Davison BH, Ragauskas AJ. Assessing the molecular structure basis for biomass recalcitrance during dilute acid and hydrothermal pretreatments. Biotechnol Biofuels. 2013;6.

5. Tolbert A, Akinosho H, Khunsupat R, Naskar AK, Ragauskas AJ. Characterization and analysis of the molecular weight of lignin for biorefining studies. Biofuels, Bioproducts and Biorefining. 2014;8(6):836-56.

6. Li M, Pu Y, Ragauskas AJ. Current Understanding of the Correlation of Lignin Structure with Biomass Recalcitrance. Frontiers in Chemistry. 2016;4:45.

7. Kursunogammalu BN, Mintz SL, Perlmutter A. Global Energy Demand in Transition: The New Role of Electricity: Springer US; 2013.

8. Cleveland CJ. Concise Encyclopedia of the History of Energy: Elsevier Science; 2009.

9. Administration UEI. Short-Term Energy and Winter Fuels Outlook 2017 [updated February 19, 2017. Available from: http://www.eia.gov/forecasts/steo/report/us_oil.cfm.

10. Cazalot C. Advancing Technology for America's Transpotaion Future. National Petroleum Council; 2012.

11. Nerurkar N. U.S. Oil Imports and Exports. 2012. Report No.: R42465.

12. Urbanchuk J. Contribution of the Ethanol industry to the Economy of the United States in 2015 2016 [updated February 5, 2016. Available from: http://www.ethanolrfa.org/wp-content/uploads/2016/02/Ethanol-Economic-Impact-for-2015.pdf.

13. Administration USEI. How much carbon dioxide is produced by burning gasoline and diesel fuel? 2016 [updated May 6, 2016.

14. Hill J, Nelson E, Tilman D, Polasky S, Tiffany D. Environmental, economic, and energetic costs and benefits of biodiesel and ethanol biofuels. Proceedings of the National Academy of Sciences. 2006;103(30):11206-10.

15. Energy EER. Energy Independence and Security Act of 2007 [updated 06/04/2014 10/17/2015]. Available from: http://www.afdc.energy.gov/laws/eisa.html.

16. Schnepf R, Yacobucci B. Renewable Fuel Standard (RFS): Overview and Issues Service CR; 2013 March 4. 2013. Report No.: R40155.

17. Downing L. Clean Fuel From Trash, Crop Waste to Match Corn-Ethanol by 2016. Bloomberg New Energy Finance. 2013.

18. Fang Z, Xu CC. Near-critical and Supercritical Water and Their Applications for Biorefineries: Springer Netherlands; 2014.

19. Stephen JD, Mabee WE, Saddler JN. Will second-generation ethanol be able to compete with first-generation ethanol? Opportunities for cost reduction. Biofuels, Bioproducts and Biorefining. 2012;6(2):159-76.

20. Cheng JJ, Timilsina GR. Status and barriers of advanced biofuel technologies: A review. Renewable Energy. 2011;36(12):3541-9.

21. Tuskan GA, DiFazio S, Jansson S, Bohlmann J, Grigoriev I, Hellsten U, et al. The Genome of Black Cottonwood, *Populus trichocarpa* (Torr. & Gray). Science. 2006;313(5793):1596-604.

22. Cao S, Pu Y, Studer M, Wyman CL, Ragauskas AJ. Chemical transformations of *Populus trichocarpa* during dilute acid pretreatment. RSC Advances. 2012;2.

23. Liu TX, Kang L. Recent Advances in Entomological Research: From Molecular Biology to Pest Management: Springer Berlin Heidelberg; 2011.

24. Albersheim P, Darvill A, Roberts K, Sederoff R, Staehelin A. Plant Cell Walls: Taylor & Francis Group; 2010.

25. Wikberg H, Liisa Maunu S. Characterisation of thermally modified hard- and softwoods by 13C CPMAS NMR. Carbohydrate Polymers. 2004;58(4):461-6.

26. Hallac BB, Ragauskas AJ. Analyzing cellulose degree of polymerization and its relevancy to cellulosic ethanol. Biofuels, Bioproducts and Biorefining. 2011;5(2):215-25.

27. da Silva ASA, Teixeira RSS, Endo T, Bon EPS, Lee S-H. Continuous pretreatment of sugarcane bagasse at high loading in an ionic liquid using a twin-screw extruder. Green Chemistry. 2013;15(7):1991-2001.

28. Andersson S, Wikberg H, Pesonen E, Maunu SL, Serimaa R. Studies of crystallinity of Scots pine and Norway spruce cellulose. Trees. 2004;18(3):346-53.

29. Newman RH. Homogeneity in cellulose crystallinity between samples of *Pinus radiata* wood. Holzforschung2004. p. 91.

30. Sannigrahi P, Ragauskas AJ, Tuskan GA. Poplar as a feedstock for biofuels: a review of compositional characteristics. Biofuel Bioprod Bior. 2010;4.

31. Scheller HV, Ulvskov P. Hemicelluloses. Annual Review of Plant Biology. 2010;61(1):263-89.

32. Chen H. Chemical Composition and Structure of Natural Lignocellulose. Biotechnology of Lignocellulose: Springer Netherlands; 2014. p. 25-71.

33. Xu L, Tschirner UW. Peracetic Acid Pretreatment of Alfalfa Stem and Aspen Biomass. Bioresourcescom. 2011;7(1).

34. Chen X, Shekiro J, Pschorn T, Sabourin M, Tao L, Elander R, et al. A highly efficient dilute alkali deacetylation and mechanical (disc) refining process for the conversion of renewable biomass to lower cost sugars. Biotechnology for Biofuels. 2014;7(1):98.

35. Socha AM, Plummer SP, Stavila V, Simmons BA, Singh S. Comparison of sugar content for ionic liquid pretreated Douglas-fir woodchips and forestry residues. Biotechnology for Biofuels. 2013;6(1):61.

36. Santos RB, Gomide JL, Hart PW. Impact of wood chip leaching pretreatment on wood chemical composition. Tappi Journal (2002). 2015;14(1):9-14.

37. Mark MFDD, Gerald GATT, Peggy PPP, Timothy TJTT, Richard RMM. Assessment of *Populus* wood chemistry following the introduction of a Bt toxin gene. Tree Physiology. 2006;26(5):557-64.

38. Cheng Y-S, Zheng Y, Yu CW, Dooley TM, Jenkins BM, VanderGheynst JS. Evaluation of High Solids Alkaline Pretreatment of Rice Straw. Applied Biochemistry and Biotechnology. 2010;162(6):1768-84.

39. Samuel R, Pu Y, Raman B, Ragauskas AJ. Structural Characterization and Comparison of Switchgrass Ball-milled Lignin Before and After Dilute Acid Pretreatment. Applied Biochemistry and Biotechnology. 2010;162(1):62-74.

40. Jacobs A, Dahlman O. Characterization of the Molar Masses of Hemicelluloses from Wood and Pulps Employing Size Exclusion Chromatography and Matrix-Assisted Laser Desorption Ionization Time-of-Flight Mass Spectrometry. Biomacromolecules. 2001;2(3):894-905.

41. Li M, Pu Y, Yoo CG, Gjersing E, Decker SR, Doeppke C, et al. Study of traits and recalcitrance reduction of field-grown COMT down-regulated switchgrass. Biotechnology for Biofuels. 2017;10(1):12.

42. Del Río JC, Marques G, Rencoret J, Martínez ÁT, Gutiérrez A. Occurrence of Naturally Acetylated Lignin Units. Journal of Agricultural and Food Chemistry. 2007;55(14):5461-8.

43. del Río JC, Rencoret J, Marques G, Gutiérrez A, Ibarra D, Santos JI, et al. Highly Acylated (Acetylated and/or p-Coumaroylated) Native Lignins from Diverse Herbaceous Plants. Journal of Agricultural and Food Chemistry. 2008;56(20):9525-34.

44. Pawar P, Koutaniemi S, Tenkanen M, Mellerowicz E. Acetylation of woody lignocellulose: significance and regulation. Frontiers in Plant Science. 2013;4(118).

45. Morreel K, Ralph J, Kim H, Lu F, Goeminne G, Ralph S, et al. Profiling of Oligolignols Reveals Monolignol Coupling Conditions in Lignifying Poplar Xylem. Plant Physiology. 2004;136(3):3537-49.

46. Lu F, Ralph J, Morreel K, Messens E, Boerjan W. Preparation and relevance of a cross-coupling product between sinapyl alcohol and sinapyl p-hydroxybenzoate. Organic & Biomolecular Chemistry. 2004;2(20):2888-90.

47. Eudes A, George A, Mukerjee P, Kim JS, Pollet B, Benke PI, et al. Biosynthesis and incorporation of side-chain-truncated lignin monomers to reduce lignin polymerization and enhance saccharification. Plant Biotechnol J. 2012;10.

48. Yelle DJ, Kaparaju P, Hunt CG, Hirth K, Kim H, Ralph J, et al. Two-dimensional NMR evidence for cleavage of lignin and xylan substituents in wheat straw through hydrothermal pretreatment and enzymatic hydrolysis. Bioenergy Research. 2013;6.

49. Mnich E, Vanholme R, Oyarce P, Liu S, Lu F, Goeminne G, et al. Degradation of lignin β-aryl ether units in *Arabidopsis thaliana* expressing LigD, LigF and LigG from Sphingomonas paucimobilis SYK-6. Plant Biotechnology Journal. 2016:n/a-n/a.

50. Santos JI, Fillat Ú, Martín-Sampedro R, Ballesteros I, Manzanares P, Ballesteros M, et al. Lignin-enriched Fermentation Residues from Bioethanol Production of Fast-growing Poplar and Forage Sorghum2015.

51. Stewart JJ, Akiyama T, Chapple C, Ralph J, Mansfield SD. The Effects on Lignin Structure of Overexpression of Ferulate 5-Hydroxylase in Hybrid Poplar. Plant Physiology. 2009;150(2):621-35.

52. Wen J-L, Xue B-L, Xu F, Sun R-C. Unveiling the Structural Heterogeneity of Bamboo Lignin by In Situ HSQC NMR Technique. BioEnergy Research. 2012;5(4):886-903.

53. Achyuthan KE, Achyuthan AM, Adams PD, Dirk SM, Harper JC, Simmons BA, et al. Supramolecular self-assembled chaos: polyphenolic lignin's barrier to cost-effective lignocellulosic biofuels. Molecules. 2010;15.

54. Sangha AK, Davison BH, Standaert RF, Davis MF, Smith JC, Parks JM. Chemical Factors that Control Lignin Polymerization. The Journal of Physical Chemistry B. 2014;118(1):164-70.

55. Samuel R, Pu Y, Jiang N, Fu C, Wang Z-Y, Ragauskas A. Structural Characterization of Lignin in Wild-Type versus COMT Down-Regulated Switchgrass. Frontiers in Energy Research. 2014;1(14).

56. Santos J, I., Martin-Sampedro R, et al. Evaluating Lignin-Rich Residues from Biochemical Ethanol Production of Wheat Straw and Olive Tree Pruning by FTIR and 2D-NMR. International Journal of Polymer Science. 2015;2015:11.

57. Timilsena YP, Abeywickrama CJ, Rakshit SK, Brosse N. Effect of different pretreatments on delignification pattern and enzymatic hydrolysability of miscanthus, oil palm biomass and typha grass. Bioresource Technology. 2013;135:82-8.

58. Stewart JJ, Akiyama T, Chapple C, Ralph J, Mansfield SD. The Effects on Lignin Structure of Overexpression of Ferulate 5-Hydroxylase in Hybrid Poplar(1). Plant Physiology. 2009;150(2):621-35.

59. Zeng J, Tong Z, Wang L, Zhu JY, Ingram L. Isolation and structural characterization of sugarcane bagasse lignin after dilute phosphoric acid plus steam explosion pretreatment and its effect on cellulose hydrolysis. Bioresource Technology. 2014;154:274-81.

60. Pan X. Role of Functional Groups in Lignin Inhibition of Enzymatic Hydrolysis of Cellulose to Glucose. Journal of Biobased Materials and Bioenergy. 2008;2(1):25-32.

61. Lai Y-Z. Determination of Phenolic Hydroxyl Groups. In: Lin SY, Dence CW, editors. Methods in Lignin Chemistry. Berlin, Heidelberg: Springer Berlin Heidelberg; 1992. p. 423-34.

62. Brosse N, El Hage R, Chaouch M, Pétrissans M, Dumarçay S, Gérardin P. Investigation of the chemical modifications of beech wood lignin during heat treatment. Polymer Degradation and Stability. 2010;95(9):1721-6.

63. Moon S-J, Eom I-Y, Kim J-Y, Kim T-S, Lee SM, Choi I-G, et al. Characterization of lignin-rich residues remaining after continuous super-critical water hydrolysis of poplar wood (*Populus albaglandulosa*) for conversion to fermentable sugars. Bioresource Technology. 2011;102(10):5912-6.

64. Samuel R, Cao S, Das BK, Hu F, Pu Y, Ragauskas AJ. Investigation of the fate of poplar lignin during autohydrolysis pretreatment to understand the biomass recalcitrance. RSC Advances. 2013;3(16):5305-9.

65. Ziebell A, Gracom K, Katahira R, Chen F, Pu Y, Ragauskas AJ, et al. Increase in 4-coumaryl alcohol units during lignification in alfalfa (Medicago sativa) alters the extractability and molecular weight of lignin. J Biol Chem. 2010;285.

66. Huang F, Singh PM, Ragauskas AJ. Characterization of Milled Wood Lignin (MWL) in Loblolly Pine Stem Wood, Residue, and Bark. Journal of Agricultural and Food Chemistry. 2011;59(24):12910-6.

67. Fu C, Mielenz JR, Xiao X, Ge Y, Hamilton CY, Rodriguez M, et al. Genetic manipulation of lignin reduces recalcitrance and improves ethanol production from switchgrass. Proceedings of the National Academy of Sciences. 2011;108(9):3803-8.

68. Bhagia S, Muchero W, Kumar R, Tuskan GA, Wyman CE. Natural genetic variability reduces recalcitrance in poplar. Biotechnology for Biofuels. 2016;9(1):106.

69. Taherzadeh MJ, Karimi K. Enzyme-based hydrolysis processes for ethanol from lignocellulosic materials: A review. BioResources. 2007;2(4):707-38.

70. Kumar R, Hu F, Sannigrahi P, Jung S, Ragauskas AJ, Wyman CE. Carbohydrate derived-pseudo-lignin can retard cellulose biological conversion. Biotechnology and Bioengineering. 2013;110(3):737-53.

71. Fang H, Xia L. High activity cellulase production by recombinant T*richoderma reesei* ZU-02 with the enhanced cellobiohydrolase production. Bioresource Technology. 2013;144(0):693-7.

72. Engel P, Krull S, Seiferheld B, Spiess AC. Rational approach to optimize cellulase mixtures for hydrolysis of regenerated cellulose containing residual ionic liquid. Bioresource Technology. 2012;115(0):27-34.

73. Hu J, Arantes V, Saddler J. The enhancement of enzymatic hydrolysis of lignocellulosic substrates by the addition of accessory enzymes such as xylanase: Is it an additive or synergistic effect? Biotechnol Biofuels. 2011;4(1):1-14.

74. Chen F, Dixon RA. Lignin modification improves fermentable sugar yields for biofuel production. Nat Biotechnol. 2007;25(7):759-61.

75. Fu C, Mielenz JR, Xiao X, Ge Y, Hamilton CY, Rodriguez M, et al. Genetic manipulation of lignin reduces recalcitrance and improves ethanol production from switchgrass. Proceedings of the National Academy of Sciences. 2011;108(9):3803-8.

76. Hisano H, Nandakumar R, Wang ZY. Genetic modification of lignin biosynthesis for improved biofuel production. In Vitro Cellular & Developmental Biology - Plant. 2009;45(3):306-13.

77. Shen H, Poovaiah CR, Ziebell A, Tschaplinski TJ, Pattathil S, Gjersing E, et al. Enhanced characteristics of genetically modified switchgrass (*Panicum virgatum* L.) for high biofuel production. Biotechnology for Biofuels. 2013;6(1):71-86.

78. Zhang X, Yu H, Huang H, Liu Y. Evaluation of biological pretreatment with white rot fungi for the enzymatic hydrolysis of bamboo culms. International Biodeterioration & Biodegradation. 2007;60(3):159-64.

79. Zhang X, Xu C, Wang H. Pretreatment of bamboo residues with *Coriolus versicolor* for enzymatic hydrolysis. Journal of Bioscience and Bioengineering. 2007;104(2):149-51.

80. Intanakul P, Krairiksh M, Kitchaiya P. Enhancement of enzymatic hydrolysis of lignocellulosic wastes by microwave pretreatment under atmospheric pressure. Journal of Wood Chemistry and Technology. 2003;23(2):217-25.

81. Pu Y, Hu F, Huang F, Davison BH, Ragauskas AJ. Assessing the molecular structure basis for biomass recalcitrance during dilute acid and hydrothermal pretreatments. Biotechnology for Biofuels. 2013;6(1):1-13.

82. Alvira P, Tomás-Pejó E, Ballesteros M, Negro MJ. Pretreatment technologies for an efficient bioethanol production process based on enzymatic hydrolysis: A review. Bioresource Technology. 2010;101(13):4851-61.

83. Resch MG, Donohoe BS, Baker JO, Decker SR, Bayer EA, Beckham GT, et al. Fungal cellulases and complexed cellulosomal enzymes exhibit synergistic mechanisms in cellulose deconstruction. Energy & Environmental Science. 2013;6(6):1858-67.

84. Fathi-Afshar S, Rudd DF. Biomass ethanol as a chemical feedstock in the United States. Biotechnology and Bioengineering. 1980;22(3):677-9.

85. Szczodrak J, Targoński Z. Selection of thermotolerant yeast strains for simultaneous saccharification and fermentation of cellulose. Biotechnology and Bioengineering. 1988;31(4):300-3.

86. Bazua CD, Wilke CR. Ethanol effects on the kinetics of a continuous fermentation with saccharomyces cerevisiae1975. Medium: X; Size: Pages: 30 p.

87. Ghose TK, Tyagi RD. Rapid ethanol fermentation of cellulose hydrolysate. II. Product and substrate inhibition and optimization of fermentor design. Biotechnology and Bioengineering. 1979;21(8):1401-20.

88. Ghose TK, Tyagi RD. Rapid ethanol fermentation of cellulose hydrolysate. I. Batch versus continuous systems. Biotechnology and Bioengineering. 1979;21(8):1387-400.

89. Chang T, Yao S. Thermophilic, lignocellulolytic bacteria for ethanol production: current state and perspectives. Applied Microbiology and Biotechnology. 2011;92(1):13-27.

90. Alfani F, Gallifuoco A, Saporosi A, Spera A, Cantarella M. Comparison of SHF and SSF processes for the bioconversion of steam-exploded wheat straw. J Ind Microbiol Biotech. 2000;25(4):184-92.

91. Jin M, Gunawan C, Balan V, Yu X, Dale BE. Continuous SSCF of AFEX™ pretreated corn stover for enhanced ethanol productivity using commercial enzymes and Saccharomyces cerevisiae 424A (LNH-ST). Biotechnology and Bioengineering. 2013;110(5):1302-11.

92. Zhu M, Li P, Gong X, Wang J. A Comparison of the Production of Ethanol between Simultaneous Saccharification and Fermentation and Separate Hydrolysis and Fermentation Using Unpretreated Cassava Pulp and Enzyme Cocktail. Bioscience, Biotechnology, and Biochemistry. 2012;76(4):671-8.

93. Nitsos CK, Matis KA, Triantafyllidis KS. Optimization of Hydrothermal Pretreatment of Lignocellulosic Biomass in the Bioethanol Production Process. ChemSusChem. 2013;6(1):110-22.

94. Chandel AK, Gonçalves BCM, Strap JL, da Silva SS. Biodelignification of lignocellulose substrates: An intrinsic and sustainable pretreatment strategy for clean energy production. Critical Reviews in Biotechnology. 2015;35(3):281-93.

95. Yang B, Wyman CE. Pretreatment: the key to unlocking low-cost cellulosic ethanol. Biofuels, Bioproducts and Biorefining. 2008;2(1):26-40.

96. Tao L, Aden A, Elander RT, Pallapolu VR, Lee YY, Garlock RJ, et al. Process and technoeconomic analysis of leading pretreatment technologies for lignocellulosic ethanol production using switchgrass. Bioresource Technology. 2011;102(24):11105-14.

97. Nguyen TY, Cai CM, Kumar R, Wyman CE. Co-solvent Pretreatment Reduces Costly Enzyme Requirements for High Sugar and Ethanol Yields from Lignocellulosic Biomass. ChemSusChem. 2015;8(10):1716-25.

98. Nguyen TY, Cai CM, Osman O, Kumar R, Wyman CE. CELF pretreatment of corn stover boosts ethanol titers and yields from high solids SSF with low enzyme loadings. Green Chemistry. 2016.

99. Smith MD, Mostofian B, Cheng X, Petridis L, Cai CM, Wyman CE, et al. Cosolvent pretreatment in cellulosic biofuel production: effect of tetrahydrofuran-water on lignin structure and dynamics. Green Chemistry. 2016;18(5):1268-77.

100. Kumar R, Mago G, Balan V, Wyman CE. Physical and chemical characterizations of corn stover and poplar solids resulting from leading pretreatment technologies. Bioresour Technol. 2009;100.

101. Shekiro J, Kuhn EM, Selig MJ, Nagle NJ, Decker SR, Elander RT. Enzymatic Conversion of Xylan Residues from Dilute Acid-Pretreated Corn Stover. Applied Biochemistry and Biotechnology. 2012;168(2):421-33.

102. Qing Q, Wyman CE. Supplementation with xylanase and β-xylosidase to reduce xylo-oligomer and xylan inhibition of enzymatic hydrolysis of cellulose and pretreated corn stover. Biotechnology for Biofuels. 2011;4(1):18.

103. Qing Q, Yang B, Wyman CE. Xylooligomers are strong inhibitors of cellulose hydrolysis by enzymes. Bioresource Technology. 2010;101(24):9624-30.

104. Kim Y, Kreke T, Hendrickson R, Parenti J, Ladisch MR. Fractionation of cellulase and fermentation inhibitors from steam pretreated mixed hardwood. Bioresource Technology. 2013;135:30-8.

105. Bellido C, Bolado S, Coca M, Lucas S, González-Benito G, García-Cubero MT. Effect of inhibitors formed during wheat straw pretreatment on ethanol fermentation by Pichia stipitis. Bioresource Technology. 2011;102(23):10868-74.

106. Saritha M, Arora A, Lata. Biological Pretreatment of Lignocellulosic Substrates for Enhanced Delignification and Enzymatic Digestibility. Indian Journal of Microbiology. 2012;52(2):122-30.

107. Lu X, Zhang Y, Angelidaki I. Optimization of H2SO4-catalyzed hydrothermal pretreatment of rapeseed straw for bioconversion to ethanol: Focusing on pretreatment at high solids content. Bioresource Technology. 2009;100(12):3048-53.

108. Sun Y, Cheng J. Hydrolysis of lignocellulosic materials for ethanol production: a review. Bioresource Technology. 2002;83(1):1-11.

109. Petersen MØ, Larsen J, Thomsen MH. Optimization of hydrothermal pretreatment of wheat straw for production of bioethanol at low water consumption without addition of chemicals. Biomass and Bioenergy. 2009;33(5):834-40.

110. Yang B, Dai Z, Ding S-Y, Wyman CE. Enzymatic hydrolysis of cellulosic biomass. Biofuels. 2011;2.

111. Hong Y, Nizami A-S, Pour Bafrani M, Saville BA, MacLean HL. Impact of cellulase production on environmental and financial metrics for lignocellulosic ethanol. Biofuels, Bioproducts and Biorefining. 2013;7(3):303-13.

112. Zhuang J, Marchant M, Nokes S, Strobel H. Economic analysis of cellulase production methods for bio-ethanol. Applied Engineering in Agriculture. 2007;23(5):679-87.

113. Klein-Marcuschamer D, Oleskowicz-Popiel P, Simmons BA, Blanch HW. The challenge of enzyme cost in the production of lignocellulosic biofuels. Biotechnology and Bioengineering. 2012;109(4):1083-7.

114. He J, Wu A-m, Chen D, Yu B, Mao X, Zheng P, et al. Cost-effective lignocellulolytic enzyme production by Trichoderma reesei on a cane molasses medium. Biotechnology for Biofuels. 2014;7(1):1-9.

115. Deswal D, Khasa YP, Kuhad RC. Optimization of cellulase production by a brown rot fungus Fomitopsis sp. RCK2010 under solid state fermentation. Bioresource Technology. 2011;102(10):6065-72.

116. Sohail M, Siddiqi R, Ahmad A, Khan SA. Cellulase production from Aspergillus niger MS82: effect of temperature and pH. New Biotechnology. 2009;25(6):437-41.

117. Fujii T, Inoue H, Ishikawa K. Enhancing cellulase and hemicellulase production by genetic modification of the carbon catabolite repressor gene, creA, in Acremonium cellulolyticus. AMB Express. 2013;3:73-.

118. Sathitsuksanoh N, Zhu Z, Ho T-J, Bai M-D, Zhang Y-HP. Bamboo saccharification through cellulose solvent-based biomass pretreatment followed by enzymatic hydrolysis at ultra-low cellulase loadings. Bioresource Technology. 2010;101(13):4926-9.

119. Du R, Su R, Zhang M, Qi W, He Z. Cellulase Recycling after High-Solids Simultaneous Saccharification and Fermentation of Combined Pretreated Corncob. Frontiers in Energy Research. 2014;2(24).

120. Sambasivarao SV, Granum DM, Wang H, Maupin CM. Identifying the Enzymatic Mode of Action for Cellulase Enzymes by Means of Docking Calculations and a Machine Learning Algorithm. AIMS Molecular Science. 2014;1:59-80.

121. Arantes V, Saddler JN. Access to cellulose limits the efficiency of enzymatic hydrolysis: the role of amorphogenesis. Biotechnol Biofuels. 2010;3.

122. Chen H. Chemical Composition and Structure of Natural Lignocellulose. Biotechnology of Lignocellulose: Theory and Practice. Dordrecht: Springer Netherlands; 2014. p. 25-71.

123. Walker G, Stewart G. Saccharomyces cerevisiae in the Production of Fermented Beverages. Beverages. 2016;2(4):30.

124. Yuan D, Rao K, Relue P, Varanasi S. Fermentation of biomass sugars to ethanol using native industrial yeast strains. Bioresource Technology. 2011;102(3):3246-53.

125. Cripps RE, Eley K, Leak DJ, Rudd B, Taylor M, Todd M, et al. Metabolic engineering of Geobacillus thermoglucosidasius for high yield ethanol production. Metabolic Engineering. 2009;11(6):398-408.

126. Johnson E. Integrated enzyme production lowers the cost of cellulosic ethanol. Biofuels, Bioproducts and Biorefining. 2016;10(2):164-74.

127. Lynd LR, Laser MS, Bransby D, Dale BE, Davison B, Hamilton R, et al. How biotech can transform biofuels. Nat Biotech. 2008;26(2):169-72.

128. El-Mansi EMT, Bryce CFA, Demain AL, Allman AR. Fermentation Microbiology and Biotechnology, Second Edition: Taylor & Francis; 2006.

129. Amarasekara AS. Fermentation I – Microorganisms. Handbook of Cellulosic Ethanol: John Wiley & Sons, Inc.; 2013. p. 283-337.

130. Akinosho H, Yee K, Close D, Ragauskas A. The emergence of *Clostridium thermocellum* as a high utility candidate for consolidated bioprocessing applications. Front Chem. 2014;2.

131. Chung D, Cha M, Guss AM, Westpheling J. Direct conversion of plant biomass to ethanol by engineered Caldicellulosiruptor bescii. Proceedings of the National Academy of Sciences. 2014;111(24):8931-6.

132. Olson DG, McBride JE, Joe Shaw A, Lynd LR. Recent progress in consolidated bioprocessing. Current Opinion in Biotechnology. 2012;23(3):396-405.

133. Bokinsky G, Peralta-Yahya PP, George A, Holmes BM, Steen EJ, Dietrich J, et al. Synthesis of three advanced biofuels from ionic liquid-pretreated switchgrass using engineered *Escherichia coli*. Proceedings of the National Academy of Sciences. 2011;108(50):19949-54.

134. Lee SJ, Warnick TA, Pattathil S, Alvelo-Maurosa JG, Serapiglia MJ, McCormick H, et al. Biological conversion assay using Clostridium phytofermentans to estimate plant feedstock quality. Biotechnology for Biofuels. 2012;5:5-.

135. Zuroff TR, Xiques SB, Curtis WR. Consortia-mediated bioprocessing of cellulose to ethanol with a symbiotic Clostridium phytofermentans/yeast co-culture. Biotechnology for Biofuels. 2013;6(1):59.

136. Lynd LR, Van Zyl WH, McBride JE, Laser M. Consolidated bioprocessing of cellulosic biomass: an update. Curr Opin Biotecnol. 2005;16.

137. Tracy BP, Jones SW, Fast AG, Indurthi DC, Papoutsakis ET. *Clostridia*: The importance of their exceptional substrate and metabolite diversity for biofuel and biorefinery applications. Curr Opin Biotechnol. 2012;23(3):364-81.

138. Vermerris W. Genetic Improvement of Bioenergy Crops: Springer; 2008.

139. Lynd LR, Van Zyl WH, McBRIDE JE, Laser M. Consolidated bioprocessing of cellulosic biomass: An update. Curr Opin Biotechnol. 2005;16(5):577-83.

140. Xu Q, Singh A, Himmel ME. Perspectives and new directions for the production of bioethanol using consolidated bioprocessing of lignocellulose. Current Opinion in Biotechnology. 2009;20(3):364-71.

141. Olson DG, Tripathi SA, Giannone RJ, Lo J, Caiazza NC, Hogsett DA, et al. Deletion of the Cel48S cellulase from *Clostridium thermocellum*. Proceedings of the National Academy of Sciences. 2010;107(41):17727-32.

142. Dien B, Cotta M, Jeffries T. Bacteria engineered for fuel ethanol production: Current status. Appl Microbiol Biotechnol. 2003;63(3):258-66.

143. Lynd LR. Overview and evaluation of fuel ethanol from cellulosic biomass: Technology, economics, the environment, and policy. Annual Review of Energy and the Environment. 1996;21(1):403-65.

144. Alper H, Stephanopoulos G. Engineering for biofuels: Exploiting innate microbial capacity or importing biosynthetic potential? Nat Rev Microbiol. 2009;7(10):715-23.

145. Blumer-Schuette SE, Brown SD, Sander KB, Bayer EA, Kataeva I, Zurawski JV, et al. Thermophilic lignocellulose deconstruction. FEMS Microbiology Reviews. 2013;38:393-448.

146. Demain AL, Newcomb M, Wu JD. Cellulase, *Clostridia*, and ethanol. Microbiology and Molecular Biology Reviews. 2005;69(1):124-54.

147. Egorova K, Antranikian G. Industrial relevance of thermophilic Archaea. Current Opinion in Microbiology. 2005;8(6):649-55.

148. Lynd LR, Weimer PJ, Van Zyl WH, Pretorius IS. Microbial cellulose utilization: Fundamentals and biotechnology. Microbiology and Molecular Biology Reviews. 2002;66(3):506-77.

149. Zhang YHP. What is vital (and not vital) to advance economically-competitive biofuels production. Process Biochemistry. 2011;46(11):2091-110.

150. Hasunuma T, Okazaki F, Okai N, Hara KY, Ishii J, Kondo A. A review of enzymes and microbes for lignocellulosic biorefinery and the possibility of their application to consolidated bioprocessing technology. Bioresource Technology. 2013;135(0):513-22.

151. Taylor MP, Eley KL, Martin S, Tuffin MI, Burton SG, Cowan DA. Thermophilic ethanologenesis: Future prospects for second-generation bioethanol production. Trends in Biotechnology. 2009;27(7):398-405.

152. Lu Y, Zhang Y-HP, Lynd LR. Enzyme – microbe synergy during cellulose hydrolysis by *Clostridium thermocellum*. Proceedings of the National Academy of Sciences. 2006;103(44):16165-9.

153. Johnson EA, Sakajoh M, Halliwell G, Madia A, Demain AL. Saccharification of complex cellulosic substrates by the cellulase system from *Clostridium thermocellum*. Applied and Environmental Microbiology. 1982;43(5):1125-32.

154. Viljoen J, Fred E, Peterson W. The fermentation of cellulose by thermophilic bacteria. The Journal of Agricultural Science. 1926;16(01):1-17.

155. McBee R. The characteristics of *Clostridium thermocellum*. Journal of Bacteriology. 1954;67(4):505-6.

156. McBee R. The anaerobic thermophilic cellulolytic bacteria. Bacteriological Reviews. 1950;14(1):51-63.

157. McBee R. The culture and physiology of a thermophilic cellulose-fermenting bacterium. Journal of Bacteriology. 1948;56(5):653-63.

158. Fleming R, Quinn L. Chemically defined medium for growth of *Clostridium thermocellum*, a cellulolytic thermophilic anaerobe. Applied Microbiology. 1971;21(5):967.

159. Johnson EA, Madia A, Demain AL. Chemically defined minimal medium for growth of the anaerobic cellulolytic thermophile *Clostridium thermocellum*. Applied and Environmental Microbiology. 1981;41(4):1060-2.

160. Freier D, Mothershed CP, Wiegel J. Characterization of *Clostridium thermocellum* JW20. Applied and Environmental Microbiology. 1988;54(1):204-11.

161. Lynd LR, Grethlein HE, Wolkin RH. Fermentation of cellulosic substrates in batch and continuous culture by *Clostridium thermocellum*. Applied and Environmental Microbiology. 1989;55(12):3131-9.

162. Dumitrache A, Wolfaardt G, Allen G, Liss SN, Lynd LR. Form and function of *Clostridium thermocellum* biofilms. Applied and Environmental Microbiology. 2013;79(1):231-9.

163. Zhang YHP, Lynd LR. Cellulose utilization by *Clostridium thermocellum*: Bioenergetics and hydrolysis product assimilation. Proceedings of the National Academy of Sciences. 2005;102(20):7321-5.

164. Herrero A, Gomez R. Development of ethanol tolerance in *Clostridium thermocellum*: Effect of growth temperature. Applied and Environmental Microbiology. 1980;40(3):571-7.

165. Timmons MD, Knutson BL, Nokes SE, Strobel HJ, Lynn BC. Analysis of composition and structure of *Clostridium thermocellum* membranes from wild-type and ethanol-adapted strains. Appl Microbiol Biotechnol. 2009;82(5):929-39.

166. Feinberg L, Foden J, Barrett T, Davenport KW, Bruce D, Detter C, et al. Complete genome sequence of the cellulolytic thermophile *Clostridium thermocellum* DSM1313. Journal of Bacteriology. 2011;193(11):2906-7.

167. Mohr G, Hong W, Zhang J, Cui GZ, Yang Y, Cui Q, et al. A targetron system for gene targeting in thermophiles and its application in *Clostridium thermocellum*. PLoS ONE. 2013;8(7):e69032.

168. Olson DG, Lynd LR. Transformation of *Clostridium thermocellum* by electroporation. In: Gilbert H, editor. Methods in Enzymology. 510. Waltham, MA: Academic Press; 2012. p. 317-30.

169. Tripathi SA, Olson DG, Argyros DA, Miller BB, Barrett TF, Murphy DM, et al. Development of *pyrF*-based genetic system for targeted gene deletion in *Clostridium thermocellum* and creation of a *pta* mutant. Applied and Environmental Microbiology. 2010;76(19):6591-9.

170. Tyurin MV, Desai SG, Lynd LR. Electrotransformation of *Clostridium thermocellum*. Applied and Environmental Microbiology. 2004;70(2):883-90.

171. Uversky VN, Kataeva IA. Cellulosome: Nova Science Publishers; 2006.

172. Bayer EA, Henrissat B, Lamed R. The cellulosome: A natural bacterial strategy to combat biomass recalcitrance. Biomass Recalcitrance: Blackwell Publishing Ltd.; 2009. p. 407-35.

173. Wertz JL, Bédué O. Lignocellulosic Biorefineries: EFPL Press; 2013.

174. Spinnler HE, Lavigne B, Blachere H. Pectinolytic activity of *Clostridium thermocellum*: Its use for anaerobic fermentation of sugar beet pulp. Applied Microbiology and Biotechnology. 1986;23(6):434-7.

175. Zverlov VV, Kellermann J, Schwarz WH. Functional subgenomics of *Clostridium thermocellum* cellulosomal genes: Identification of the major catalytic components in the extracellular complex and detection of three new enzymes. PROTEOMICS. 2005;5(14):3646-53.

176. Lamed R, Setter E, Bayer E. Characterization of a cellulose-binding, cellulase-containing complex in *Clostridium thermocellum*. Journal of Bacteriology. 1983;156(2):828-36.

177. Bayer EA, Kenig R, Lamed R. Adherence of *Clostridium thermocellum* to cellulose. Journal of Bacteriology. 1983;156(2):818-27.

178. Bayer E, Setter E, Lamed R. Organization and distribution of the cellulosome in *Clostridium thermocellum*. Journal of Bacteriology. 1985;163(2):552-9.

179. Bayer EA, Lamed R. Ultrastructure of the cell surface cellulosome of *Clostridium thermocellum* and its interaction with cellulose. Journal of Bacteriology. 1986;167(3):828-36.

180. Garcia-Martinez DV, Shinmyo A, Madia A, Demain AL. Studies on cellulase production by *Clostridium thermocellum*. European J Appl Microbiol Biotechnol. 1980;9(3):189-97.

181. Dror TW, Rolider A, Bayer EA, Lamed R, Shoham Y. Regulation of expression of scaffoldin-related genes in *Clostridium thermocellum*. Journal of Bacteriology. 2003;185(17):5109-16.

182. Shimon LJW, Bayer EA, Morag E, Lamed R, Yaron S, Shoham Y, et al. A cohesin domain from *Clostridium thermocellum*: The crystal structure provides new insights into cellulosome assembly. Structure. 1997;5(3):381-90.

183. Gilbert HJ. Cellulosomes: microbial nanomachines that display plasticity in quaternary structure. Molecular Microbiology. 2007;63(6):1568-76.

184. Carvalho AL, Dias FMV, Prates JAM, Nagy T, Gilbert HJ, Davies GJ, et al. Cellulosome assembly revealed by the crystal structure of the cohesin–dockerin complex. Proceedings of the National Academy of Sciences. 2003;100(24):13809-14.

185. Xu J, Crowley MF, Smith JC. Building a foundation for structure-based cellulosome design for cellulosic ethanol: Insight into cohesin-dockerin complexation from computer simulation. Protein Science. 2009;18(5):949-59.

186. Sakka K, Kishino Y, Sugihara Y, Jindou S, Sakka M, Inagaki M, et al. Unusual binding properties of the dockerin module of *Clostridium thermocellum* endoglucanase CelJ (Cel9D-Cel44A). FEMS Microbiology Letters. 2009;300(2):249-55.

187. Borne R, Bayer EA, Pagès S, Perret S, Fierobe HP. Unraveling enzyme discrimination during cellulosome assembly independent of cohesin – dockerin affinity. FEBS Journal. 2013;280(22):5764-79.

188. Krauss J, Zverlov VV, Schwarz WH. *In vitro* reconstitution of the complete *Clostridium thermocellum* cellulosome and synergistic activity on crystalline cellulose. Applied and Environmental Microbiology. 2012;78(12):4301-7.

189. Mitsuzawa S, Kagawa H, Li Y, Chan SL, Paavola CD, Trent JD. The rosettazyme: A synthetic cellulosome. Journal of Biotechnology. 2009;143(2):139-44.

190. Gefen G, Anbar M, Morag E, Lamed R, Bayer EA. Enhanced cellulose degradation by targeted integration of a cohesin-fused β-glucosidase into the *Clostridium thermocellum* cellulosome. Proceedings of the National Academy of Sciences. 2012;109(26):10298-303.

191. Bomble YJ, Beckham GT, Matthews JF, Nimlos MR, Himmel ME, Crowley MF. Modeling the self-assembly of the cellulosome enzyme complex. Journal of Biological Chemistry. 2011;286(7):5614-23.

192. Nataf Y, Yaron S, Stahl F, Lamed R, Bayer EA, Scheper TH, et al. Cellodextrin and laminaribiose ABC transporters in *Clostridium thermocellum*. Journal of Bacteriology. 2009;191(1):203-9.

193. Zhou J, Olson DG, Argyros DA, Deng Y, van Gulik WM, van Dijken JP, et al. Atypical Glycolysis in *Clostridium thermocellum*. Applied and Environmental Microbiology. 2013;79(9):3000-8.

194. Rydzak T, Levin DB, Cicek N, Sparling R. End-product induced metabolic shifts in *Clostridium thermocellum* ATCC 27405. Appl Microbiol Biotechnol. 2011;92(1):199-209.

195. Zverlov VV, Schantz N, Schmitt-Kopplin P, Schwarz WH. Two new major subunits in the cellulosome of *Clostridium thermocellum*: Xyloglucanase Xgh74A and endoxylanase Xyn10D. Microbiology. 2005;151(10):3395-401.

196. Wiegel J, Mothershed CP, Puls J. Differences in Xylan Degradation by Various Noncellulolytic Thermophilic Anaerobes and *Clostridium thermocellum*. Applied and Environmental Microbiology. 1985;49(3):656-9.

197. Ding SY, Liu YS, Zeng Y, Himmel ME, Baker JO, Bayer EA. How does plant cell wall nanoscale architecture correlate with enzymatic digestibility? Science. 2012;338(6110):1055-60.

198. Puls J, Wood TM. The degradation pattern of cellulose by extracellular cellulases of aerobic and anaerobic microorganisms. Bioresource Technology. 1991;36(1):15-9.

199. Zhao X, Zhang L, Liu D. Biomass recalcitrance. Part I: The chemical compositions and physical structures affecting the enzymatic hydrolysis of lignocellulose. Biofuels, Bioproducts and Biorefining. 2012;6(4):465-82.

200. Hall M, Bansal P, Lee JH, Realff MJ, Bommarius AS. Cellulose crystallinity – a key predictor of the enzymatic hydrolysis rate. FEBS Journal. 2010;277(6):1571-82.

201. Shao X, Jin M, Guseva A, Liu C, Balan V, Hogsett D, et al. Conversion for Avicel and AFEX pretreated corn stover by *Clostridium thermocellum* and simultaneous saccharification and fermentation: Insights into microbial conversion of pretreated cellulosic biomass. Bioresource Technology. 2011;102(17):8040-5.

202. Hörmeyer HF, Tailliez P, Millet J, Girard H, Bonn G, Bobleter O, et al. Ethanol production by *Clostridium thermocellum* grown on hydrothermally and organosolv-pretreated lignocellulosic materials. Appl Microbiol Biotechnol. 1988;29(6):528-35.

203. Yee KL, Rodriguez Jr M, Tschaplinski TJ, Engle NL, Martin MZ, Fu C, et al. Evaluation of the bioconversion of genetically modified switchgrass using simultaneous saccharification and fermentation and a consolidated bioprocessing approach. Biotechnology for Biofuels. 2012;5:81-93.

204. Bothun GD, Knutson BL, Berberich JA, Strobel HJ, Nokes SE. Metabolic selectivity and growth of *Clostridium thermocellum* in continuous culture under elevated hydrostatic pressure. Applied Microbiology and Biotechnology. 2004;65(2):149-57.

205. Hauser L, Land M, Larimer F. *Clostridium thermocellum* ATCC 27405 analysis files 2010 [Available from: http://genome.ornl.gov/microbial/cthe/.

206. Brown SD, Lamed R, Morag E, Borovok I, Shoham Y, Klingeman DM, et al. Draft genome sequences for *Clostridium thermocellum* wild-type strain YS and derived cellulose adhesion-defective mutant strain AD2. Journal of Bacteriology. 2012;194(12):3290-1.

207. Hemme CL, Mouttaki H, Lee YJ, Zhang G, Goodwin L, Lucas S, et al. Sequencing of multiple clostridial genomes related to biomass conversion and biofuel production. Journal of Bacteriology. 2010;192(24):6494-6.

208. Shao X, Raman B, Zhu M, Mielenz JR, Brown SD, Guss AM, et al. Mutant selection and phenotypic and genetic characterization of ethanol-tolerant strains of *Clostridium thermocellum*. Appl Microbiol Biotechnol. 2011;92(3):641-52.

209. Riederer A, Takasuka TE, Makino S-i, Stevenson DM, Bukhman YV, Elsen NL, et al. Global gene expression patterns in *Clostridium thermocellum* as determined by microarray analysis of chemostat cultures on cellulose or cellobiose. Applied and Environmental Microbiology. 2011;77(4):1243-53.

210. Raman B, McKeown CK, Rodriguez M, Brown SD, Mielenz JR. Transcriptomic analysis of *Clostridium thermocellum* ATCC 27405 cellulose fermentation. BMC Microbiology. 2011;11(1):134-52.

211. Wei H, Fu Y, Magnusson L, Baker JO, Maness PC, Xu Q, et al. Comparison of transcriptional profiles of *Clostridium thermocellum* grown on cellobiose and pretreated yellow poplar using RNA-Seq. Frontiers in Microbiology. 2014;5(142):1-16.

212. Wilson CM, Rodriguez Jr M, Johnson CM, Martin SL, Chu TM, Wolfinger RD, et al. Global transcriptome analysis of *Clostridium thermocellum* ATCC 27405 during growth on dilute acid pretreated *Populus* and switchgrass. Biotechnology for Biofuels. 2013;6(1):179-97.

213. Rydzak T, McQueen PD, Krokhin OV, Spicer V, Ezzati P, Dwivedi RC, et al. Proteomic analysis of *Clostridium thermocellum* core metabolism: Relative protein expression profiles and growth phase-dependent changes in protein expression. BMC Microbiology. 2012;12(1):214-53.

214. Gold ND, Martin VJ. Global view of the *Clostridium thermocellum* cellulosome revealed by quantitative proteomic analysis. Journal of Bacteriology. 2007;189(19):6787-95.

215. Raman B, Pan C, Hurst GB, Rodriguez Jr M, McKeown CK, Lankford PK, et al. Impact of pretreated switchgrass and biomass carbohydrates on *Clostridium thermocellum* ATCC 27405 cellulosome composition: A quantitative proteomic analysis. PLoS ONE. 2009;4(4):e5271.

216. Williams TI, Combs JC, Lynn BC, Strobel HJ. Proteomic profile changes in membranes of ethanol-tolerant *Clostridium thermocellum*. Appl Microbiol Biotechnol. 2007;74(2):422-32.

217. Burton E, Martin VJ. Proteomic analysis of *Clostridium thermocellum* ATCC 27405 reveals the upregulation of an alternative transhydrogenase–malate pathway and nitrogen assimilation in cells grown on cellulose. Canadian Journal of Microbiology. 2012;58(12):1378-88.

218. Roberts SB, Gowen CM, Brooks JP, Fong SS. Genome-scale metabolic analysis of *Clostridium thermocellum* for bioethanol production. BMC Systems Biology. 2010;4(1):31-48.

219. Saddler J, Chan M. Optimization of *Clostridium thermocellum* growth on cellulose and pretreated wood substrates. European Journal of Applied Microbiology and Biotechnology. 1982;16(2-3):99-104.

220. Brown SD, Raman B, McKeown CK, Kale SP, He Z, Mielenz JR. Construction and evaluation of a *Clostridium thermocellum* ATCC 27405 whole-genome oligonucleotide microarray. In: Mielenz JR, Klasson KT, Adney WS, McMillan JD,

editors. Applied Biochemistry and Biotecnology. 27. Nashville, TN: Humana Press; 2007. p. 663-74.

221. Ellis LD, Holwerda EK, Hogsett D, Rogers S, Shao X, Tschaplinski T, et al. Closing the carbon balance for fermentation by *Clostridium thermocellum* (ATCC 27405). Bioresource Technology. 2012;103(1):293-9.

222. Islam R, Cicek N, Sparling R, Levin D. Influence of initial cellulose concentration on the carbon flow distribution during batch fermentation by *Clostridium thermocellum* ATCC 27405. Appl Microbiol Biotechnol. 2009;82(1):141-8.

223. Li HF, Knutson BL, Nokes SE, Lynn BC, Flythe MD. Metabolic control of *Clostridium thermocellum* via inhibition of hydrogenase activity and the glucose transport rate. Appl Microbiol Biotechnol. 2012;93(4):1777-84.

224. Stevenson DM, Weimer PJ. Expression of 17 genes in *Clostridium thermocellum* ATCC 27405 during fermentation of cellulose or cellobiose in continuous culture. Applied and Environmental Microbiology. 2005;71(8):4672-8.

225. Wilson CM, Yang S, Rodriguez Jr M, Ma Q, Johnson CM, Dice L, et al. *Clostridium thermocellum* transcriptomic profiles after exposure to furfural or heat stress. Biotechnology for Biofuels. 2013;6(1):131-44.

226. Linville JL, Rodriguez Jr M, Land M, Syed MH, Engle NL, Tschaplinski TJ, et al. Industrial robustness: Understanding the mechanism of tolerance for the *Populus* hydrolysate-tolerant mutant strain of *Clostridium thermocellum*. PLoS ONE. 2013;8(10):e78829.

227. Brown SD, Guss AM, Karpinets TV, Parks JM, Smolin N, Yang S, et al. Mutant alcohol dehydrogenase leads to improved ethanol tolerance in *Clostridium thermocellum*. Proceedings of the National Academy of Sciences. 2011;108(33):13752-7.

228. Lv W, Yu Z. Isolation and characterization of two thermophilic cellulolytic strains of *Clostridium thermocellum* from a compost sample. Journal of Applied Microbiology. 2013;114(4):1001-7.

229. Tachaapaikoon C, Kosugi A, Pason P, Waeonukul R, Ratanakhanokchai K, Kyu KL, et al. Isolation and characterization of a new cellulosome-producing *Clostridium thermocellum* strain. Biodegradation. 2012;23(1):57-68.

230. Dror TW, Morag E, Rolider A, Bayer EA, Lamed R, Shoham Y. Regulation of the cellulosomal *celS* (*cel48A*) gene of *Clostridium thermocellum* is growth rate dependent. Journal of Bacteriology. 2003;185(10):3042-8.

231. Dror TW, Rolider A, Bayer EA, Lamed R, Shoham Y. Regulation of major cellulosomal endoglucanases of *Clostridium thermocellum* differs from that of a prominent cellulosomal xylanase. Journal of Bacteriology. 2005;187(7):2261-6.

232. Fernandes A, Fontes C, Gilbert H, Hazlewood G, FERNANDES T, Ferreira L. Homologous xylanases from *Clostridium thermocellum*: Evidence for bi-functional activity, synergism between xylanase catalytic modules and the presence of xylan-binding domains in enzyme complexes. Biochemical Journal. 1999;342:105-10.

233. Lamed R, Lobos J, Su T. Effects of stirring and hydrogen on fermentation products of *Clostridium thermocellum*. Applied and Environmental Microbiology. 1988;54(5):1216-21.

234. Poole DM, Morag E, Lamed R, Bayer EA, Hazlewood GP, Gilbert HJ. Identification of the cellulose-binding domain of the cellulosome subunit S1 from *Clostridium thermocellum* YS. FEMS Microbiology Letters. 1992;99(2):181-6.

235. Ng TK, Ben-Bassat A, Zeikus J. Ethanol production by thermophilic bacteria: Fermentation of cellulosic substrates by cocultures of *Clostridium thermocellum* and *Clostridium thermohydrosulfuricum*. Applied and Environmental Microbiology. 1981;41(6):1337-43.

236. Ng TK, Zeikus JG. Purification and characterization of an endoglucanase (1, 4-beta-D-glucan glucanohydrolase) from *Clostridium thermocellum*. Biochemical Journal. 1981;199:341-50.

237. Lamed R, Zeikus J. Ethanol production by thermophilic bacteria: Relationship between fermentation product yields of and catabolic enzyme activities in *Clostridium thermocellum* and *Thermoanaerobium brockii*. Journal of Bacteriology. 1980;144(2):569-78.

238. Koeck DE, Wibberg D, Koellmeier T, Blom J, Jaenicke S, Winkler A, et al. Draft genome sequence of the cellulolytic *Clostridium thermocellum* wild-type strain BC1 playing a role in cellulosic biomass degradation. Journal of Biotechnology. 2013;168(1):62-3.

239. Weimer P, Zeikus J. Fermentation of cellulose and cellobiose by *Clostridium thermocellum* in the absence of *Methanobacterium thermoautotrophicum*. Applied and Environmental Microbiology. 1977;33(2):289-97.

240. Wiegel J, Dykstra M. *Clostridium thermocellum*: Adhesion and sporulation while adhered to cellulose and hemicellulose. Appl Microbiol Biotechnol. 1984;20(1):59-65.

241. Fontes CM, Gilbert HJ. Cellulosomes: Highly efficient nanomachines designed to deconstruct plant cell wall complex carbohydrates. Annu Rev Biochem. 2010;79:655-81.

242. Rani KS, Swamy M, Sunitha D, Haritha D, Seenayya G. Improved ethanol tolerance and production in strains of *Clostridium thermocellum*. World Journal of Microbiology and Biotechnology. 1996;12(1):57-60.

243. Argyros DA, Tripathi SA, Barrett TF, Rogers SR, Feinberg LF, Olson DG, et al. High ethanol titers from cellulose by using metabolically engineered thermophilic, anaerobic microbes. Applied and Environmental Microbiology. 2011;77(23):8288-94.

244. Deng Y, Olson DG, Zhou J, Herring CD, Joe Shaw A, Lynd LR. Redirecting carbon flux through exogenous pyruvate kinase to achieve high ethanol yields in *Clostridium thermocellum*. Metabolic Engineering. 2013;15:151-8.

245. Van Der Veen D, Lo J, Brown SD, Johnson CM, Tschaplinski TJ, Martin M, et al. Characterization of *Clostridium thermocellum* strains with disrupted fermentation end-product pathways. J Ind Microbiol Biotechnol. 2013;40(7):725-34.

246. Haruta S, Cui Z, Huang Z, Li M, Ishii M, Igarashi Y. Construction of a stable microbial community with high cellulose-degradation ability. Appl Microbiol Biotechnol. 2002;59(4-5):529-34.

247. Izquierdo JA, Sizova MV, Lynd LR. Diversity of bacteria and glycosyl hydrolase family 48 genes in cellulolytic consortia enriched from thermophilic biocompost. Applied and Environmental Microbiology. 2010;76(11):3545-53.

248. Kato S, Haruta S, Cui ZJ, Ishii M, Igarashi Y. Effective cellulose degradation by a mixed-culture system composed of a cellulolytic *Clostridium* and aerobic non-cellulolytic bacteria. FEMS Microbiol Ecol. 2004;51(1):133-42.

249. Sizova M, Izquierdo J, Panikov N, Lynd L. Cellulose- and xylan-degrading thermophilic anaerobic bacteria from biocompost. Applied and Environmental Microbiology. 2011;77(7):2282-91.

250. Zuroff TR, Curtis WR. Developing symbiotic consortia for lignocellulosic biofuel production. Appl Microbiol Biotechnol. 2012;93(4):1423-35.

251. Geng A, He Y, Qian C, Yan X, Zhou Z. Effect of key factors on hydrogen production from cellulose in a co-culture of *Clostridium thermocellum* and *Clostridium thermopalmarium*. Bioresource Technology. 2010;101(11):4029-33.

252. He Q, Hemme CL, Jiang H, He Z, Zhou J. Mechanisms of enhanced cellulosic bioethanol fermentation by co-cultivation of *Clostridium* and *Thermoanaerobacter* spp. Bioresource Technology. 2011;102(20):9586-92.

253. Le Ruyet P, Dubourguier H, Albagnac G. Homoacetogenic fermentation of cellulose by a coculture of *Clostridium thermocellum* and *Acetogenium kivui*. Applied and Environmental Microbiology. 1984;48(4):893-4.

254. Lü Y, Li N, Yuan X, Hua B, Wang J, Ishii M, et al. Enhancing the cellulose-degrading activity of cellulolytic bacteria CTL-6 (*Clostridium thermocellum*) by co-culture with non-cellulolytic bacteria W2-10 (*Geobacillus* sp.). Applied Biochemistry and Biotechnology. 2013;171(7):1578-88.

255. Mori Y. Characterization of a symbiotic coculture of *Clostridium thermohydrosulfuricum* YM3 and *Clostridium thermocellum* YM4. Applied and Environmental Microbiology. 1990;56(1):37-42.

256. Blumer-Schuette SE, Kataeva I, Westpheling J, Adams MW, Kelly RM. Extremely thermophilic microorganisms for biomass conversion: Status and prospects. Curr Opin Biotechnol. 2008;19(3):210-7.

257. Wang WK, Kruus K, Wu JH. Cloning and DNA sequence of the gene coding for *Clostridium thermocellum* cellulase Ss (CelS), a major cellulosome component. Journal of Bacteriology. 1993;175(5):1293-302.

258. Kannuchamy S, Mukund N, Saleena LM. Genetic engineering of *Clostridium thermocellum* DSM1313 for enhanced ethanol production. BMC Biotechnology. 2016;16(1):34.

259. Groom J, Chung D, Olson DG, Lynd LR, Guss AM, Westpheling J. Promiscuous plasmid replication in thermophiles: Use of a novel hyperthermophilic replicon for genetic manipulation of *Clostridium thermocellum* at its optimum growth temperature. Metabolic Engineering Communications. 2016;3:30-8.

260. Tyurin MV, Sullivan CR, Lynd LR. Role of spontaneous current oscillations during high-efficiency electrotransformation of thermophilic anaerobes. Applied and Environmental Microbiology. 2005;71(12):8069-76.

261. Olson DG, Lynd LR. Computational design and characterization of a temperature-sensitive plasmid replicon for gram positive thermophiles. Journal of Biological Engineering. 2012;6(1):1-10.

262. Cheng XY, Liu CZ. Hydrogen production via thermophilic fermentation of cornstalk by *Clostridium thermocellum*. Energy & Fuels. 2011;25(4):1714-20.

263. Carere CR, Cicek N, Levin DB, Kalia V, Sparling R. Pyruvate catabolism and hydrogen synthesis pathway genes of *Clostridium thermocellum* ATCC 27405. Indian Journal of Microbiology. 2008;48(2):252-66.

264. Lalaurette E, Thammannagowda S, Mohagheghi A, Maness PC, Logan BE. Hydrogen production from cellulose in a two-stage process combining fermentation and electrohydrogenesis. International Journal of Hydrogen Energy. 2009;34(15):6201-10.

265. Hou CT, Shaw JF. Biocatalysis and Bioenergy: Wiley; 2008.

266. Acton QA. Acetates — Advances in Research and Application: 2013 Edition. Acton QA, editor. Atlanta, GA: Scholarly Editions; 2013.

267. Sparling R, Islam R, Cicek N, Carere C, Chow H, Levin DB. Formate synthesis by *Clostridium thermocellum* during anaerobic fermentation. Canadian Journal of Microbiology. 2006;52(7):681-8.

268. Gheshlaghi R, Scharer J, Moo-Young M, Chou C. Metabolic pathways of *Clostridia* for producing butanol. Biotechnology Advances. 2009;27(6):764-81.

269. Nakayama S, Kiyoshi K, Kadokura T, Nakazato A. Butanol production from crystalline cellulose by cocultured *Clostridium thermocellum* and *Clostridium saccharoperbutylacetonicum* N1-4. Applied and Environmental Microbiology. 2011;77(18):6470-5.

270. Kastelowitz N, Sammond D, Akahuhta M, Wui H, Lin P, Guss A, et al. Engineering more thermostable metabolic enzymes for improving CBP organisms. 36th Symposium on Biotechnology for Fuels and Chemicals; April 28, 2014; Clearwater, FL: Society for Industrial Microbiology; 2014.

271. Lynd LR, Weimer PJ, Zyl WHV, Pretorius IS. Microbial cellulose utilization: fundamentals and biotechnology. Microbiol Mol Biol R. 2002;66.

272. Zhang YHP, Lynd LR. Determination of the Number-Average Degree of Polymerization of Cellodextrins and Cellulose with Application to Enzymatic Hydrolysis. Biomacromolecules. 2005;6(3):1510-5.

273. Puri VP. Effect of crystallinity and degree of polymerization of cellulose on enzymatic saccharification. Biotechnology and Bioengineering. 1984;26(10):1219-22.

274. Puls J, Wood TM. Enzymatic Hydrolysis of Cellulose The degradation pattern of cellulose by extracellular cellulases of aerobic and anaerobic microorganisms. Bioresource Technology. 1991;36(1):15-9.

275. Dumitrache A, Akinosho H, Rodriguez M, Meng X, Yoo CG, Natzke J, et al. Consolidated bioprocessing of *Populus* using Clostridium (Ruminiclostridium) thermocellum: a case study on the impact of lignin composition and structure. Biotechnology for Biofuels. 2016;9:31.

276. Hamad WY. Cellulosic Materials: Fibers, Networks and Composites: Springer US; 2013.

277. Sathitsuksanoh N, Zhu Z, Wi S, Percival Zhang YH. Cellulose solvent-based biomass pretreatment breaks highly ordered hydrogen bonds in cellulose fibers of switchgrass. Biotechnology and Bioengineering. 2011;108(3):521-9.

278. Xiros C, Vafiadi C, Topakas E, Christakopoulos P. Decrement of cellulose recalcitrance by treatment with ionic liquid (1-ethyl-3-methylimidazolium acetate) as a strategy to enhance enzymatic hydrolysis. Journal of Chemical Technology & Biotechnology. 2012;87(5):629-34.

279. Li C, Knierim B, Manisseri C, Arora R, Scheller HV, Auer M, et al. Comparison of dilute acid and ionic liquid pretreatment of switchgrass: Biomass recalcitrance, delignification and enzymatic saccharification. Bioresource Technology. 2010;101(13):4900-6.

280. Boisset C, Chanzy H, Henrissat B, Lamed R, Shoham Y, Bayer EA. Digestion of crystalline cellulose substrates by the *Clostridium thermocellum* cellulosome: structural and morphological aspects. Biochemical Journal. 1999;340(Pt 3):829-35.

281. Wang QQ, He Z, Zhu Z, Zhang YHP, Ni Y, Luo XL, et al. Evaluations of cellulose accessibilities of lignocelluloses by solute exclusion and protein adsorption techniques. Biotechnology and Bioengineering. 2012;109(2):381-9.

282. Rollin JA, Zhu Z, Sathitsuksanoh N, Zhang YHP. Increasing cellulose accessibility is more important than removing lignin: A comparison of cellulose solvent-based lignocellulose fractionation and soaking in aqueous ammonia. Biotechnology and Bioengineering. 2011;108(1):22-30.

283. Chandra RP, Arantes V, Saddler J. Steam pretreatment of agricultural residues facilitates hemicellulose recovery while enhancing enzyme accessibility to cellulose. Bioresource Technology. 2015;185:302-7.

284. Bali G, Meng X, Deneff JI, Sun Q, Ragauskas AJ. The Effect of Alkaline Pretreatment Methods on Cellulose Structure and Accessibility. ChemSusChem. 2015;8(2):275-9.

285. Dumitrache A, Wolfaardt GM, Allen DG, Liss SN, Lynd LR. Tracking the cellulolytic activity of *Clostridium thermocellum* biofilms. Biotechnology for Biofuels. 2013;6(1):1-14.

286. Pareek N, Gillgren T, Jönsson LJ. Adsorption of proteins involved in hydrolysis of lignocellulose on lignins and hemicelluloses. Bioresource Technology. 2013;148:70-7.

287. Wang X, Li K, Yang M, Zhang J. Hydrolyzability of xylan after adsorption on cellulose: Exploration of xylan limitation on enzymatic hydrolysis of cellulose. Carbohydrate Polymers. 2016;148:362-70.

288. Zhang J, Tang M, Viikari L. Xylans inhibit enzymatic hydrolysis of lignocellulosic materials by cellulases. Bioresource Technology. 2012;121:8-12.

289. Pawar PM-A, Koutaniemi S, Tenkanen M, Mellerowicz EJ. Acetylation of woody lignocellulose: significance and regulation. Frontiers in Plant Science. 2013;4:118.

290. Grohmann K, Mitchell DJ, Himmel ME, Dale BE, Schroeder HA. The role of ester groups in resistance of plant cell wall polysaccharides to enzymatic hydrolysis. Applied Biochemistry and Biotechnology. 1989;20(1):45-61.

291. Silveira RL, Stoyanov SR, Gusarov S, Skaf MS, Kovalenko A. Plant Biomass Recalcitrance: Effect of Hemicellulose Composition on Nanoscale Forces that Control Cell Wall Strength. Journal of the American Chemical Society. 2013;135(51):19048-51.

292. Öhgren K, Bura R, Saddler J, Zacchi G. Effect of hemicellulose and lignin removal on enzymatic hydrolysis of steam pretreated corn stover. Bioresource Technology. 2007;98(13):2503-10.

293. Xu N, Zhang W, Ren S, Liu F, Zhao C, Liao H, et al. Hemicelluloses negatively affect lignocellulose crystallinity for high biomass digestibility under NaOH and H2SO4 pretreatments in Miscanthus. Biotechnology for Biofuels. 2012;5(1):1-12.

294. Bhagia S, Muchero W, Kumar R, Tuskan GA, Wyman CE. Natural genetic variability reduces recalcitrance in poplar. Biotechnology for Biofuels. 2016;9(1):1-12.

295. Carmona C, Langan P, Smith JC, Petridis L. Why genetic modification of lignin leads to low-recalcitrance biomass. Physical Chemistry Chemical Physics. 2015;17(1):358-64.

296. Poovaiah CR, Nageswara-Rao M, Soneji JR, Baxter HL, Stewart CN. Altered lignin biosynthesis using biotechnology to improve lignocellulosic biofuel feedstocks. Plant Biotechnology Journal. 2014;12(9):1163-73.

297. Guo F, Shi W, Sun W, Li X, Wang F, Zhao J, et al. Differences in the adsorption of enzymes onto lignins from diverse types of lignocellulosic biomass and the underlying mechanism. Biotechnology for Biofuels. 2014;7(1):1-10.

298. Lu X, Zheng X, Li X, Zhao J. Adsorption and mechanism of cellulase enzymes onto lignin isolated from corn stover pretreated with liquid hot water. Biotechnology for Biofuels. 2016;9(1):118.

299. Davison BH, Drescher SR, Tuskan GA, Davis MF, Nghiem NP. Variation of S/G ratio and lignin content in a *Populus* family influences the release of xylose by dilute acid hydrolysis. Appl Biochem Biotechnol. 2006;130.

300. Dien BS, Sarath G, Pedersen JF, Sattler SE, Chen H, Funnell-Harris DL, et al. Improved sugar conversion and ethanol yield for forage sorghum (Sorghum bicolor L. Moench) lines with reduced lignin contents. Bioenergy Res. 2009;2.

301. Grabber JH, Mertens DR, Kim H, Funk C, Lu F, Ralph J. Cell wall fermentation kinetics are impacted more by lignin content and ferulate cross-linking than by lignin composition. J Sci Food Agric. 2009;89.

302. Mooney CA, Mansfield SD, Touhy MG, Saddler JN. The effect of initial pore volume and lignin content on the enzymatic hydrolysis of softwoods. Bioresour Technol. 1998;64.

303. Li Y, Sun Z, Ge X, Zhang J. Effects of lignin and surfactant on adsorption and hydrolysis of cellulases on cellulose. Biotechnology for Biofuels. 2016;9(1):1-9.

304. Seo DJ, Fujita H, Sakoda A. Effects of a non-ionic surfactant, Tween 20, on adsorption/desorption of saccharification enzymes onto/from lignocelluloses and saccharification rate. Adsorption. 2011;17.

305. Wi SG, Cho EJ, Lee D-S, Lee SJ, Lee YJ, Bae H-J. Lignocellulose conversion for biofuel: a new pretreatment greatly improves downstream biocatalytic hydrolysis of various lignocellulosic materials. Biotechnology for Biofuels. 2015;8(1):228.

306. Chen F, Dixon RA. Lignin modification improves fermentable sugar yields for biofuel production. Nat Biotech. 2007;25(7):759-61.

307. Studer MH, DeMartini JD, Davis MF, Sykes RW, Davison B, Keller M, et al. Lignin content in natural *Populus* variants affects sugar release. Proc Natl Acad Sci USA. 2011;108.

308. Fu C, Mielenz JR, Xiao X, Ge Y, Hamilton CY, Rodriguez M, et al. Genetic manipulation of lignin reduces recalcitrance and improves ethanol production from switchgrass. Proc Natl Acad Sci. 2011;108.

309. Yee KL, Rodriguez Jr M, Thompson OA, Fu C, Wang Z-Y, Davison BH, et al. Consolidated bioprocessing of transgenic switchgrass by an engineered and evolved *Clostridium thermocellum*strain. Biotechnology for Biofuels. 2014;7(1):1-6.

310. A. Sluiter BH, R. Ruiz, C. Scarlata, J. Sluiter, D. Templeton, and D. Crocker editor. Determination of Structural Carbohydrates and Lignin in Biomass2012.

311. Oberlerchner J, Rosenau T, Potthast A. Overview of Methods for the Direct Molar Mass Determination of Cellulose. Molecules. 2015;20(6):10313.

312. Cathala B, Saake B, Faix O, Monties B. Association behaviour of lignins and lignin model compounds studied by multidetector size-exclusion chromatography. Journal of Chromatography A. 2003;1020(2):229-39.

313. Asikkala J, Tamminen T, Argyropoulos DS. Accurate and Reproducible Determination of Lignin Molar Mass by Acetobromination. Journal of Agricultural and Food Chemistry. 2012;60(36):8968-73.

314. Engel P, Hein L, Spiess AC. Derivatization-free gel permeation chromatography elucidates enzymatic cellulose hydrolysis. Biotechnology for Biofuels. 2012;5(1):1-8.

315. Park S, Baker JO, Himmel ME, Parilla PA, Johnson DK. Cellulose crystallinity index: measurement techniques and their impact on interpreting cellulase performance. Biotechnology for Biofuels. 2010;3(1):1-10.

316. Coates J. Interpretation of Infrared Spectra, A Practical Approach. Encyclopedia of Analytical Chemistry: John Wiley & Sons, Ltd; 2006.

317. Synytsya A, Novak M. Structural analysis of glucans. Annals of Translational Medicine. 2014;2(2):17.

318. Newmann RH, Hemmingson JA. Determination of the degree of cellulose crystallinity in wood by carbon-13- nuclear magnetic resonance spectroscopy. International Journal of the Biology, Chemistry, Physics, and Technology of Wood. 1990;44(5):351-6.

319. Liitiä T, Maunu SL, Hortling B, Tamminen T, Pekkala O, Varhimo A. Cellulose crystallinity and ordering of hemicelluloses in pine and birch pulps as revealed by solid-state NMR spectroscopic methods. Cellulose. 2003;10.

320. Newman RH. Homogeneity in cellulose crystallinity between samples of *Pinus radiata* wood. Holzforschung. 2004;58.

321. Teeäär R, Serimaa R, Paakkarl T. Crystallinity of cellulose, as determined by CP/MAS NMR and XRD methods. Polym Bull. 1987;17.

322. Thygesen A, Oddershede J, Lilholt H, Thomsen AB, Stahl K. On the determination of crystallinity and cellulose content in plant fibers. Cellulose. 2005;12.

323. Yoshida M, Liu Y, Uchida S, Kawarada K, Ukagami Y, Ichinose H, et al. Effects of cellulose crystallinity, hemicellulose, and lignin on the enzymatic hydrolysis of Miscanthus sinensis to monosaccharides. Biosci Biotech Bioch. 2008;72.

324. Zhao H, Kwak JH, Wang Y, Franz JA, White JM, Holladay JE. Effects of crystallinity on dilute acid hydrolysis of cellulose by cellulose ball-milling study. Energy Fuels. 2006;20.

325. Aimin T, Hongwei Z, Gang C, Guohui X, Wenzhi L. Influence of ultrasound treatment on accessibility and regioselective oxidation reactivity of cellulose. Ultrasonics Sonochemistry. 2005;12(6):467-72.

326. Wiman M, Dienes D, Hansen MAT, van der Meulen T, Zacchi G, Lidén G. Cellulose accessibility determines the rate of enzymatic hydrolysis of steam-pretreated spruce. Bioresource Technology. 2012;126:208-15.

327. Esteghlalian AR, Bilodeau M, Mansfield SD, Saddler JN. Do enzymatic hydrolyzability and Simons' stain reflect the changes in the accessibility of lignocellulosic substrates to cellulase enzymes? Biotechnol Prog. 2001;17.

328. Beecher JF, Hunt CG, Zhu JY. Tools for the Characterization of Biomass at the Nanometer Scale. The Nanoscience and Technology of Renewable Biomaterials: John Wiley & Sons, Ltd; 2009. p. 61-90.

329. Hong J, Ye X, Zhang YHP. Quantitative Determination of Cellulose Accessibility to Cellulase Based on Adsorption of a Nonhydrolytic Fusion Protein Containing CBM and GFP with Its Applications. Langmuir. 2007;23(25):12535-40.

330. Yu X, Atalla RH, Minor JL. Mechanism of action of Simons' stain. Tappi journal. 1995;78(6):175-80.

331. Rencoret J, Gutiérrez A, Nieto L, Jiménez-Barbero J, Faulds CB, Kim H, et al. Lignin Composition and Structure in Young versus Adult Eucalyptus globulus Plants. Plant Physiology. 2011;155(2):667-82.

332. Morreel K, Dima O, Kim H, Lu F, Niculaes C, Vanholme R, et al. Mass Spectrometry-Based Sequencing of Lignin Oligomers. Plant Physiology. 2010;153(4):1464-78.

333. Hu G, Cateto C, Pu Y, Samuel R, Ragauskas AJ. Structural Characterization of Switchgrass Lignin after Ethanol Organosolv Pretreatment. Energy & Fuels. 2012;26(1):740-5.

334. Trajano HL, Engle NL, Foston M, Ragauskas AJ, Tschaplinski TJ, Wyman CE. The fate of lignin during hydrothermal pretreatment. Biotechnology for Biofuels. 2013;6(1):110.

335. Teramura H, Sasaki K, Oshima T, Aikawa S, Matsuda F, Okamoto M, et al. Changes in Lignin and Polysaccharide Components in 13 Cultivars of Rice Straw following Dilute Acid Pretreatment as Studied by Solution-State 2D 1H-13C NMR. PLOS ONE. 2015;10(6):e0128417.

336. Marita JM, Ralph J, Hatfield RD, Chapple C. NMR characterization of lignins in Arabidopsis altered in the activity of ferulate 5-hydroxylase. Proceedings of the National Academy of Sciences of the United States of America. 1999;96(22):12328-32.

337. De Souza AP, Kamei CLA, Torres AF, Pattathil S, Hahn MG, Trindade LM, et al. How cell wall complexity influences saccharification efficiency in Miscanthus sinensis. Journal of Experimental Botany. 2015.

338. Lupoi JS, Gjersing E, Davis MF. Evaluating Lignocellulosic Biomass, Its Derivatives, and Downstream Products with Raman Spectroscopy. Frontiers in Bioengineering and Biotechnology. 2015;3:50.

339. Kumar R, Hu F, Hubbell CA, Ragauskas AJ, Wyman CE. Comparison of laboratory delignification methods, their selectivity, and impacts on physiochemical characteristics of cellulosic biomass. Bioresource Technology. 2013;130:372-81.

340. Kılıç M. Effects of Machining Methods on the Surface Roughness Values of Pinus nigra Arnold Wood2015.

341. Iglewicz B, Hoaglin DC. How to Detect and Handle Outliers: ASQC Quality Press; 1993.

342. Pu Y, Hu F, Huang F, Davison BH, Ragauskas AJ. Assessing the molecular structure basis for biomass recalcitrance during dilute acid and hydrothermal pretreatments. Biotechnology for Biofuels. 2013;6(1):15.

343. Baxter HL, Mazarei M, Labbe N, Kline LM, Cheng Q, Windham MT, et al. Two-year field analysis of reduced recalcitrance transgenic switchgrass. Plant Biotechnology Journal. 2014;12(7):914-24.

344. Akinosho H, Yee K, Close D, Ragauskas A. The emergence of *Clostridium thermocellum* as a high utility candidate for consolidated bioprocessing applications. Frontiers in Chemistry. 2014;2(66).

345. Shao X, Jin M, Guseva A, Liu C, Balan V, Hogsett D, et al. Conversion for Avicel and AFEX pretreated corn stover by *Clostridium thermocellum* and simultaneous saccharification and fermentation: insights into microbial conversion of pretreated cellulosic biomass. Bioresour Technol. 2011;102.

346. Dumitrache A, Akinosho H, Rodriguez M, Meng X, Yoo CG, Natzke J, et al. Consolidated bioprocessing of *Populus* using Clostridium (Ruminiclostridium) thermocellum: a case study on the impact of lignin composition and structure. Biotechnology for Biofuels. 2016;9(1):31.

347. Sluiter A, Hames, B., Ruiz, R., Scarlata, C.,, Sluiter J, Templeton, J., and Crocker. D. . Determination of Structural Carbohydrates and Lignin in Biomass. 2012. Contract No.: NREL/TP-510-42618.

348. Puls J, Wood TM. The degradation pattern of cellulose by extracellular cellulases of aerobic and anaerobic microorganisms. Bioresour Technol. 1991;36.

349. Yee KL, Rodriguez M, Thompson Oa, Fu C, Wang Z-Y, Davison BH, et al. Consolidated bioprocessing of transgenic switchgrass by an engineered and evolved *Clostridium thermocellum* strain. Biotechnol Biofuels. 2014;7.

350. Fu C, Mielenz JR, Xiao X, Ge Y, Hamilton CY, Rodriguez M, et al. Genetic manipulation of lignin reduces recalcitrance and improves ethanol production from switchgrass. Proc Natl Acad Sci U S A. 2011;108.

351. Poudel S, Giannone RJ, Rodriguez M, Raman B, Martin MZ, Engle NL, et al. Integrated omics analyses reveal the details of metabolic adaptation of *Clostridium thermocellum* to lignocellulose-derived growth inhibitors released during the deconstruction of switchgrass. Biotechnology for Biofuels. 2017;10(1):14.

352. Rydzak T, Levin DB, Cicek N, Sparling R. End-product induced metabolic shifts in *Clostridium thermocellum* ATCC 27405. Applied Microbiology and Biotechnology. 2011;92(1):199.

353. Zhang M, Su R, Qi W, Du R, He Z. Enzymatic Hydrolysis of Cellulose with Different Crystallinities Studied by Means of SEC-MALLS. Chinese Journal of Chemical Engineering. 2011;19(5):773-8.

354. Dadi AP, Schall CA, Varanasi S. Mitigation of cellulose recalcitrance to enzymatic hydrolysis by ionic liquid pretreatment. Applied Biochemistry and Biotechnology. 2007;137(1):407-21.

355. Ioelovich M, Morag E. Effect of Cellulose Structure on Enzymatic Hydrolysis. BioResources. 2011;6(3).

356. Yoshida M, Liu Y, Uchida S, Kawarada K, Ukagami Y, Ichinose H, et al. Effects of Cellulose Crystallinity, Hemicellulose, and Lignin on the Enzymatic Hydrolysis of Miscanthus sinensis to Monosaccharides. Bioscience, Biotechnology, and Biochemistry. 2008;72(3):805-10.

357. Du R, Huang R, Su R, Zhang M, Wang M, Yang J, et al. Enzymatic hydrolysis of lignocellulose: SEC-MALLS analysis and reaction mechanism. RSC Advances. 2013;3(6):1871-7.

358. Bernardez TD, Lyford K, Hogsett DA, Lynd LR. Adsorption of *Clostridium thermocellum* cellulases onto pretreated mixed hardwood, avicel, and lignin. Biotechnology and Bioengineering. 1993;42(7):899-907.

359. Eudes A, George A, Mukerjee P, Kim JS, Pollet B, Benke PI, et al. Biosynthesis and incorporation of side-chain-truncated lignin monomers to reduce lignin polymerization and enhance saccharification. Plant Biotechnology Journal. 2012;10(5):609-20.

360. Cai Y, Zhang K, Kim H, Hou G, Zhang X, Yang H, et al. Enhancing digestibility and ethanol yield of *Populus* wood via expression of an engineered monolignol 4-O-methyltransferase. Nature Communications. 2016;7:11989.

361. Yelle DJ, Kaparaju P, Hunt CG, Hirth K, Kim H, Ralph J, et al. Two-Dimensional NMR Evidence for Cleavage of Lignin and Xylan Substituents in Wheat Straw Through Hydrothermal Pretreatment and Enzymatic Hydrolysis. BioEnergy Research. 2013;6(1):211-21.

362. Achyuthan KE, Achyuthan AM, Adams PD, Dirk SM, Harper JC, Simmons BA, et al. Supramolecular Self-Assembled Chaos: Polyphenolic Lignin's Barrier to Cost-Effective Lignocellulosic Biofuels. Molecules. 2010;15(12):8641.

363. Basen M, Rhaesa AM, Kataeva I, Prybol CJ, Scott IM, Poole FL, et al. Degradation of high loads of crystalline cellulose and of unpretreated plant biomass by the thermophilic bacterium Caldicellulosiruptor bescii. Bioresource Technology. 2014;152:384-92.

364. Fu C, Mielenz J, Xiao X, Ge Y, Hamilton CY, Rodriguez M. Genetic manipulation of lignin reduces recalcitrance and improves ethanol production from switchgrass. Proc Natl Acad Sci U S A. 2011;108.

365. Yee KL, Rodriguez M, Tschaplinski TJ, Engle NL, Martin MZ, Fu C, et al. Evaluation of the bioconversion of genetically modified switchgrass using simultaneous saccharification and fermentation and a consolidated bioprocessing approach. Biotechnol Biofuels. 2012;5.

366. Lynd LR, Weimer PJ, Van Zyl WH, Pretorius IS. Microbial cellulose utilization: Fundamentals and biotechnology. Microbiol Mol Biol Rev. 2002;66.

367. Papanek B, Biswas R, Rydzak T, Guss AM. Elimination of metabolic pathways to all traditional fermentation products increases ethanol yields in *Clostridium thermocellum*. Metabolic Engineering. 2015;32:49-54.

368. Porth I, El-Kassaby YA. Using *Populus* as a lignocellulosic feedstock for bioethanol. Biotechnology Journal. 2015;10(4):510-24.

369. Cheng J, Yu Y, Zhu M. Enhanced biodegradation of sugarcane bagasse by *Clostridium thermocellum* with surfactant addition. Green Chemistry. 2014;16(5):2689-95.

370. Yu Z, Gwak K-S, Treasure T, Jameel H, Chang H-m, Park S. Effect of Lignin Chemistry on the Enzymatic Hydrolysis of Woody Biomass. ChemSusChem. 2014;7(7):1942-50.

371. Santos RB, Capanema EA, Balakshin MY, Chang H-m, Jameel H. Lignin Structural Variation in Hardwood Species. Journal of Agricultural and Food Chemistry. 2012;60(19):4923-30.

372. Kishimoto T, Chiba W, Saito K, Fukushima K, Uraki Y, Ubukata M. Influence of Syringyl to Guaiacyl Ratio on the Structure of Natural and Synthetic Lignins. Journal of Agricultural and Food Chemistry. 2010;58(2):895-901.

373. Jung HG, Smith RR, Endres CS. Cell wall composition and degradability of stem tissue from lucerne divergently selected for lignin and in vitro dry-matter disappearance. Grass and Forage Science. 1994;49(3):295-304.

374. Van Acker R, Leplé J-C, Aerts D, Storme V, Goeminne G, Ivens B, et al. Improved saccharification and ethanol yield from field-grown transgenic poplar deficient in cinnamoyl-CoA reductase. Proceedings of the National Academy of Sciences. 2014;111(2):845-50.

375. Chen Y, Stipanovic AJ, Winter WT, Wilson DB, Kim YJ. Effect of digestion by pure cellulases on crystallinity and average chain length for bacterial and microcrystalline celluloses. Cellulose. 2007;14.

376. Grabber JH, Ralph J, Hatfield RD, Quideau S. p-Hydroxyphenyl, Guaiacyl, and Syringyl Lignins Have Similar Inhibitory Effects on Wall Degradability. Journal of Agricultural and Food Chemistry. 1997;45(7):2530-2.

377. Li X, Ximenes E, Kim Y, Slininger M, Meilan R, Ladisch M, et al. Lignin monomer composition affects Arabidopsis cell-wall degradability after liquid hot water pretreatment. Biotechnology for Biofuels. 2010;3(1):27.

378. Skyba O, Douglas CJ, Mansfield SD. Syringyl-rich lignin renders poplars more resistant to degradation by wood decay fungi. Appl Environ Microbiol. 2013;79.

379. Huntley SK, Ellis D, Gilbert M, Chapple C, Mansfield SD. Significant Increases in Pulping Efficiency in C4H-F5H-Transformed Poplars: Improved Chemical Savings and Reduced Environmental Toxins. Journal of Agricultural and Food Chemistry. 2003;51(21):6178-83.

380. Hallac BB, Sannigrahi P, Pu Y, Ray M, Murphy RJ, Ragauskas AJ. Effect of ethanol organosolv pre-treatment on enzymatic hydrolysis of Buddleja davidii stem biomass. Ind Eng Chem Res. 2010;49.

381. Dehghani M, Karimi K, Sadeghi M. Pretreatment of Rice Straw for the Improvement of Biogas Production. Energy & Fuels. 2015;29(6):3770-5.

382. Inglesby MK, Zeronian SH. Direct dyes as molecular sensors to characterize cellulose substrates. Cellulose. 2002;9(1):19-29.

383. Chandra RP, Saddler JN. Use of the Simons' Staining Technique to Assess Cellulose Accessibility in Pretreated Substrates. Industrial Biotechnology. 2012;8(4):230-7.

384. Lu Y, Zhang Y-HP, Lynd LR. Enzyme–microbe synergy during cellulose hydrolysis by *Clostridium thermocellum*. Proceedings of the National Academy of Sciences. 2006;103(44):16165-9.

385. Islam R, Cicek N, Sparling R, Levin D. Influence of initial cellulose concentration on the carbon flow distribution during batch fermentation by *Clostridium thermocellum* ATCC 27405. Applied Microbiology and Biotechnology. 2008;82(1):141.

386. Linville JL, Rodriguez M, Jr., Land M, Syed MH, Engle NL, Tschaplinski TJ, et al. Industrial Robustness: Understanding the Mechanism of Tolerance for the *Populus* Hydrolysate-Tolerant Mutant Strain of *Clostridium thermocellum*. PLOS ONE. 2013;8(10):e78829.

387. Mori S, Barth HG. Size Exclusion Chromatography: Springer Berlin Heidelberg; 1999.

388. Wagner A, Tobimatsu Y, Phillips L, Flint H, Geddes B, Lu F, et al. Syringyl lignin production in conifers: Proof of concept in a Pine tracheary element system. Proceedings of the National Academy of Sciences. 2015;112(19):6218-23.

389. Esteghlalian AR, Bilodeau M, Mansfield SD, Saddler JN. Do Enzymatic Hydrolyzability and Simons' Stain Reflect the Changes in the Accessibility of Lignocellulosic Substrates to Cellulase Enzymes? Biotechnology Progress. 2001;17(6):1049-54.

390. Kostylev M, Wilson D. Synergistic interactions in cellulose hydrolysis. Biofuels. 2012;3(1):61-70.

391. Gupta RB, Demirbas A. Gasoline, Diesel, and Ethanol Biofuels from Grasses and Plants: Cambridge University Press; 2010.

392. Meng X, Wells T, Sun Q, Huang F, Ragauskas A. Insights into the effect of dilute acid, hot water or alkaline pretreatment on the cellulose accessible surface area and the overall porosity of *Populus*. Green Chemistry. 2015;17(8):4239-46.

393. Kumar L, Arantes V, Chandra R, Saddler J. The lignin present in steam pretreated softwood binds enzymes and limits cellulose accessibility. Bioresour Technol. 2012;103.

394. Chandra RP, Chu Q, Hu J, Zhong N, Lin M, Lee J-S, et al. The influence of lignin on steam pretreatment and mechanical pulping of poplar to achieve high sugar recovery and ease of enzymatic hydrolysis. Bioresource Technology. 2016;199:135-41.

395. Yu X, Atalla RH. A staining technique for evaluating the pore structure variations of microcrystalline cellulose powders. Powder Technology. 1998;98(2):135-8.

396. Arantes V, Saddler JN. Cellulose accessibility limits the effectiveness of minimum cellulase loading on the efficient hydrolysis of pretreated lignocellulosic substrates. Biotechnology for Biofuels. 2011;4(1):1-17.

397. Ding SY, Liu Y-S, Zeng Y, Himmel ME, Baker JO, Bayer EA. How does plant cell wall nanoscale architecture correlate with enzymatic digestibility? Science. 2012;338.

398. Plötze M, Niemz P. Porosity and pore size distribution of different wood types as determined by mercury intrusion porosimetry. European Journal of Wood and Wood Products. 2011;69(4):649-57.

399. Usta I. Comparative Study of Wood Density by Specific Amount of Void Volume (Porosity). Turkish Journal of Agriculture & Forestry. 2003;27(1):1.

400. Ozdemir T, Temiz A, Aydin I. Effect of Wood Preservatives on Surface Properties of Coated Wood. Advances in Materials Science and Engineering. 2015;2015:6.

401. Muchero W, Guo J, DiFazio SP, Chen J-G, Ranjan P, Slavov GT, et al. High-resolution genetic mapping of allelic variants associated with cell wall chemistry in *Populus*. BMC Genomics. 2015;16(1):24.

402. Chave J. Measuring wood density for tropical forest trees: A field manual for the CTFS sites Wood density measurement protocol 2005.

403. Sluiter A, Hames B, Ruiz R, Scarlata C, Sluiter J, Templeton D. Determination of sugars, byproducts, and degradation products in liquid fraction process samples laboratory analytical procedure. Golden, CO: National Renewable Energy Laboratory, Institutre MR; 2006 January 2008. Report No.: NREL/TP-510-42623.

404. Chandra R, Ewanick S, Hsieh C, Saddler JN. The characterization of pretreated lignocellulosic substrates prior to enzymatic hydrolysis, part 1: a modified Simons' staining technique. Biotechnol Prog. 2008;24.

405. Gurau L, Mansfield-Williams H, Irle M. The Influence of Wood Anatomy on Evaluating the Roughness of Sanded Solid Wood. Journal of the Institute of Wood Science. 2005;17(2):65-74.

406. Shmulsky R, Jones PD. Forest Products and Wood Science: Wiley; 2011.

407. Sun Q, Foston M, Meng X, Sawada D, Pingali SV, O'Neill HM, et al. Effect of lignin content on changes occurring in poplar cellulose ultrastructure during dilute acid pretreatment. Biotechnology for Biofuels. 2014;7(1):150.

408. Meng X, Foston M, Leisen J, DeMartini J, Wyman CE, Ragauskas AJ. Determination of porosity of lignocellulosic biomass before and after pretreatment by using Simons' stain and NMR techniques. Bioresource Technology. 2013;144:467-76.

409. Meng X, Sun Q, Kosa M, Huang F, Pu Y, Ragauskas AJ. Physicochemical Structural Changes of Poplar and Switchgrass during Biomass Pretreatment and Enzymatic Hydrolysis. ACS Sustainable Chemistry & Engineering. 2016;4(9):4563-72.

410. Karimi K, Taherzadeh MJ. A critical review of analytical methods in pretreatment of lignocelluloses: Composition, imaging, and crystallinity. Bioresource Technology. 2016;200:1008-18.

411. Ding J, Huang X, Zhang L, Zhao N, Yang D, Zhang K. Tolerance and stress response to ethanol in the yeast Saccharomyces cerevisiae. Applied Microbiology and Biotechnology. 2009;85(2):253.

412. Mathew AS, Wang J, Luo J, Yau S-T. Enhanced ethanol production via electrostatically accelerated fermentation of glucose using Saccharomyces cerevisiae. Scientific Reports. 2015;5:15713.

413. Grabber JH, Mertens DR, Kim H, Funk C, Lu F, Ralph J. Cell wall fermentation kinetics are impacted more by lignin content and ferulate cross-linking than by lignin composition. Journal of the Science of Food and Agriculture. 2009;89(1):122-9.

414. Studer MH, DeMartini JD, Davis MF, Sykes RW, Davison B, Keller M, et al. Lignin content in natural *Populus* variants affects sugar release. Proc Natl Acad Sci U S A. 2011;108.

415. Shao X, Jin M, Guseva A, Liu C, Balan V, Hogsett D, et al. Conversion of Avicel and AFEX pretreated corn stover by *Clostridium thermocellum* and simultaneous saccharification and fermentation: insights into microbial conversion of pretreated cellulosic biomass. Bioresourc Technol. 2011;102.

416. Lynd LR, Laser MS, Brandsby D, Dale BE, Davison B, Hamilton R, et al. How biotech can transform biofuels. Nat Biotechnol. 2008;26.

417. Schuster BG, Chinn MS. Consolidated Bioprocessing of Lignocellulosic Feedstocks for Ethanol Fuel Production. BioEnergy Research. 2013;6(2):416-35.

418. Lynd LR, Zyl WHv, McBride JE, Laser M. Consolidated bioprocessing of cellulosic biomass: an update. Current Opinion in Biotechnology. 2005;16(5):577-83.

419. Klein-Marcuschamer D, Oleskowicz-Popiel P, Simmons BA, Blanch HW. The challenge of enzyme cost in the production of lignocellulosic biofuels. Biotechnol Bioeng. 2012;109.

420. Gefen G, Anbar M, Morag E, Lamed R, Bayer EA. Enhanced cellulose degradation by targeted integration of a cohesin-fused β-glucosidase into the *Clostridium thermocellum* cellulosome. Proceedings of the National Academy of Sciences of the United States of America. 2012;109(26):10298-303.

421. Chakraborty S, Fernandes VO, Dias FMV, Prates JAM, Ferreira LMA, Fontes CMGA, et al. Role of Pectinolytic Enzymes Identified in *Clostridium thermocellum* Cellulosome. PLOS ONE. 2015;10(2):e0116787.

422. Zverlov VV, Fuchs K-P, Schwarz WH. Chi18A, the Endochitinase in the Cellulosome of the Thermophilic, Cellulolytic Bacterium *Clostridium thermocellum*. Applied and Environmental Microbiology. 2002;68(6):3176-9.

423. Henrissat B, Claeyssens M, Tomme P, Lemesle L, Mornon JP. Cellulase families revealed by hydrophobic cluster analysi. Gene. 1989;81(1):83-95.

424. Swamy MV, Ram MS, Seenayya G. β-Amylase from *Clostridium thermocellum* SS8 - a thermophilic, anaerobic, cellulolytic bacterium. Letters in Applied Microbiology. 1994;18(6):301-4.

425. Tyurin AA, Sadovskaya NS, Nikiforova KR, Mustafaev ON, Komakhin RA, Fadeev VS, et al. *Clostridium thermocellum* thermostable lichenase with circular

permutations and modifications in the N-terminal region retains its activity and thermostability. Biochimica et Biophysica Acta (BBA) - Proteins and Proteomics. 2015;1854(1):10-9.

426. Halstead JR, Vercoe PE, Gilbert HJ, Davidson K, Hazlewood GP. A family 26 mannanase produced by *Clostridium thermocellum* as a component of the cellulosome contains a domain which is conserved in mannanases from anaerobic fungi. Microbiology. 1999;145(11):3101-8.

427. Yoo CG, Pu Y, Li M, Ragauskas AJ. Elucidating Structural Characteristics of Biomass using Solution-State 2 D NMR with a Mixture of Deuterated Dimethylsulfoxide and Hexamethylphosphoramide. ChemSusChem. 2016;9(10):1090-5.

428. Kline LM, Hayes DG, Womac AR, Labbe N. Simplified Determination of Lignin Content in Hard and Soft Woods via UV-Spectrophotometric Analysis of Biomass Dissolved in Ionic Liquids. BioResources. 2010;5(3):1366-83.

429. Liu Y, Hu T, Wu Z, Zeng G, Huang D, Shen Y, et al. Study on biodegradation process of lignin by FTIR and DSC. Environmental Science and Pollution Research. 2014;21(24):14004-13.

430. Zeng J, Singh D, Laskar DD, Chen S. Degradation of native wheat straw lignin by *Streptomyces* viridosporus T7A. International Journal of Environmental Science and Technology. 2013;10(1):165-74.

431. Ma J, Zhang K, Liao H, Hector SB, Shi X, Li J, et al. Genomic and secretomic insight into lignocellulolytic system of an endophytic bacterium Pantoea ananatis Sd-1. Biotechnology for Biofuels. 2016;9(1):25.

432. Picart P, Müller C, Mottweiler J, Wiermans L, Bolm C, Domínguez de María P, et al. From Gene Towards Selective Biomass Valorization: Bacterial β-Etherases with Catalytic Activity on Lignin-Like Polymers. ChemSusChem. 2014;7(11):3164-71.

433. Sonoki T, Iimura Y, Masai E, Kajita S, Katayama Y. Specific degradation ofβ-aryl ether linkage in synthetic lignin (dehydrogenative polymerizate) by bacterial enzymes ofSphingomonas paucimobilis SYK-6 produced in recombinant*Escherichia coli*. Journal of Wood Science. 2002;48(5):429.

434. Camarero S, Galletti GC, Martínez AT. Preferential degradation of phenolic lignin units by two white rot fungi. Applied and Environmental Microbiology. 1994;60(12):4509-16.

435. Pedulli GF, Lucarini M, Pedrielli P. Bond Dissociation Energies of Phenolic and Amine Antioxidants. In: Minisci F, editor. Free Radicals in Biology and Environment. 3. Free Radicals in Biology and Environment: Springer Netherlands; 2013. p. 500.

436. Sáez-Jiménez V, Baratto MC, Pogni R, Rencoret J, Gutiérrez A, Santos JI, et al. Demonstration of Lignin-to-Peroxidase Direct Electron Transfer: A Transient-State

Kinetics, Directed Mutagenesis, EPR, and NMR StudyA Journal of Biological Chemistry. 2015;290(38):23201-13.

437. Harvey PJ, Schoemaker HE, Bowen RM, Palmer JM. Single-electron transfer processes and the reaction mechanism of enzymic degradation of lignin. FEBS Letters. 1985;183(1):13-6.

438. Ragauskas AJ, Beckham GT, Biddy MJ, Chandra R, Chen F, Davis MF, et al. Lignin Valorization: Improving Lignin Processing in the Biorefinery. Science. 2014;344(6185).

439. Li C, Zhao X, Wang A, Huber GW, Zhang T. Catalytic Transformation of Lignin for the Production of Chemicals and Fuels. Chemical Reviews. 2015;115(21):11559-624.

440. Bugg TDH, Rahmanpour R. Enzymatic conversion of lignin into renewable chemicals. Current Opinion in Chemical Biology. 2015;29:10-7.

441. Wei Z, Zeng G, Huang F, Kosa M, Huang D, Ragauskas AJ. Bioconversion of oxygen-pretreated Kraft lignin to microbial lipid with oleaginous Rhodococcus opacus DSM 1069. Green Chemistry. 2015;17(5):2784-9.

442. Salvachua D, Karp EM, Nimlos CT, Vardon DR, Beckham GT. Towards lignin consolidated bioprocessing: simultaneous lignin depolymerization and product generation by bacteria. Green Chemistry. 2015;17(11):4951-67.

443. Mu W, Ben H, Ragauskas A, Deng Y. Lignin Pyrolysis Components and Upgrading—Technology Review. BioEnergy Research. 2013;6(4):1183-204.

444. Rinaldi R, Jastrzebski R, Clough MT, Ralph J, Kennema M, Bruijnincx PCA, et al. Paving the Way for Lignin Valorisation: Recent Advances in Bioengineering, Biorefining and Catalysis. Angewandte Chemie International Edition. 2016;55(29):8164-215.

445. Choi YS, Singh R, Zhang J, Balasubramanian G, Sturgeon MR, Katahira R, et al. Pyrolysis reaction networks for lignin model compounds: unraveling thermal deconstruction of [small beta]-O-4 and [small alpha]-O-4 compounds. Green Chemistry. 2016;18(6):1762-73.

446. Chu S, Subrahmanyam AV, Huber GW. The pyrolysis chemistry of a [small beta]-O-4 type oligomeric lignin model compound. Green Chemistry. 2013;15(1):125-36.

447. Zhang J-j, Jiang X-y, Ye X-n, Chen L, Lu Q, Wang X-h, et al. Pyrolysis mechanism of a β-O-4 type lignin dimer model compound. Journal of Thermal Analysis and Calorimetry. 2016;123(1):501-10.

448. Huang J, Liu C, Wu D, Tong H, Ren L. Density functional theory studies on pyrolysis mechanism of β-O-4 type lignin dimer model compound. Journal of Analytical and Applied Pyrolysis. 2014;109:98-108.

449. Strassberger Z, Alberts AH, Louwerse MJ, Tanase S, Rothenberg G. Catalytic cleavage of lignin β-O-4 link mimics using copper on alumina and magnesia–alumina. Green Chemistry. 2013;15(3):768-74.

450. Reiter J, Strittmatter H, Wiemann LO, Schieder D, Sieber V. Enzymatic cleavage of lignin [small beta]-O-4 aryl ether bonds via net internal hydrogen transfer. Green Chemistry. 2013;15(5):1373-81.

451. Wang J, Liu L, Wilson AK. Oxidative Cleavage of the β-O-4 Linkage of Lignin by Transition Metals: Catalytic Properties and the Performance of Density Functionals. The Journal of Physical Chemistry A. 2016;120(5):737-46.

452. Jia S, Cox BJ, Guo X, Zhang ZC, Ekerdt JG. Hydrolytic Cleavage of β-O-4 Ether Bonds of Lignin Model Compounds in an Ionic Liquid with Metal Chlorides. Industrial & Engineering Chemistry Research. 2011;50(2):849-55.

453. Zhang J, Liu Y, Chiba S, Loh T-P. Chemical conversion of β-O-4 lignin linkage models through Cu-catalyzed aerobic amide bond formation. Chemical Communications. 2013;49(97):11439-41.

454. Sun Q, Khunsupat R, Akato K, Tao J, Labbe N, Gallego NC, et al. A study of poplar organosolv lignin after melt rheology treatment as carbon fiber precursors. Green Chemistry. 2016;18(18):5015-24.

455. Biswas R, Prabhu S, Lynd LR, Guss AM. Increase in Ethanol Yield via Elimination of Lactate Production in an Ethanol-Tolerant Mutant of *Clostridium thermocellum*. PLOS ONE. 2014;9(2):e86389.

456. Argyros DA, Tripathi SA, Barrett TF, Rogers SR, Feinberg LF, Olson DG, et al. High ethanol titers from cellulose by using metabolically engineered thermophilic, anaerobic microbes. Appl Environ Microbiol. 2010;77.

457. Deng Y, Olson DG, Zhou J, Herring CD, Shaw AJ, Lynd LR. Redirecting carbon flux through exogenous pyruvate kinase to achieve high ethanol yields in *Clostridium thermocellum*. Metab Eng. 2013;15.